College of Health Sciences

School of Pharmacy

Department of Pharmaceutical Chemistry and Pharmacognosy

Aminoalkyl and Oxazine of 2-Naphthol Derivatives: Synthesis, *In vitro* Antimicrobial and *In Silico* Studies

By: Gizachew Motbaynor

February, 2024

Addis Ababa, Ethiopia

Addis Ababa University

College of Health Sciences

School of Pharmacy

Department of Pharmaceutical Chemistry and Pharmacognosy

Aminoalkyl and Oxazine of 2-Naphthol Derivatives: Synthesis, *In vitro* Antimicrobial and *In Silico* Studies

A Thesis Submitted to the Department of Pharmaceutical Chemistry and Pharmacognosy Presented in Partial Fulfillment of the Requirements for the Master of Science Degree in Medicinal Chemistry

By: Gizachew Motbaynor (B. Pharm.)

Advisors:

Dr. Daniel Bisrat (Ph.D.)

Professor Kaleab Asres (Ph. D.)

February, 2024

Addis Ababa, Ethiopia

Addis Ababa University

School of Graduate Studies

This is to certify that the thesis prepared by Gizachew Motbaynor, entitled: **"Aminoalkyl and Oxazine of 2-Naphthol Derivatives: Synthesis, *In vitro* Antimicrobial and *In Silico* Studies"** and submitted in partial fulfillment of the requirements for the Degree of Master of Science in Medicinal Chemistry complies with the regulations of the university and meets the accepted standards with respect to originality and quality.

Signed by the Examining Committee:

External examiner: Dr. Solomon Mequanente Signature _____Date _____

Internal examiner: Alemu Tadesse (Asst. professor) Signature_____ Date_____

Advisor: Dr. Daniel Bisrat Signature_____ Date _____

Advisor: Prof. Kaleab Asres Signature_____ Date _____

_____

Head of Department

ABSTRACT

Aminoalkyl and Oxazine of 2-Naphthol Derivatives: Synthesis, *In vitro* Antimicrobial and *In Silico* Studies

Gizachew Motbaynor

Addis Ababa University, 2024

Despite remarkable advancements in the past decade, infectious diseases continue to pose a significant threat, affecting millions and burdening global public health systems and economies. Currently, there is growing interest in 2-naphthol derivatives, particularly 1-aminoalkyl-2-naphthol derivatives, owing to their biological activities and their potential application in synthesizing other significant bioactive molecules. Therefore, in this study, two compounds were synthesized from a 2-naphthol framework. The synthesized compounds were purified through column chromatography, and their chemical structures were identified using ^{1}H and ^{13}C, DEPT-90, and DEPT-135 NMR spectral data, as 1-(phenyl(*ortho*-tolylamino)methyl)naphthalene-2-ol (**37**) and 2-benzyl-2,3-dihydro-1H-naphtho[1,2-e][1,3]oxazine (**39**). The potential antimicrobial activity of the synthesized compounds was evaluated by the disk diffusion and broth dilution method. At the same time, molecular docking and ADMET studies were conducted to investigate their possible mechanism of action and drug-like properties.

From our findings, both synthesized compounds exhibited promising antibacterial activity against most tested bacterial strains at 200 µg/ml, showing zones of inhibitions (ZOIs) ranging from 6.0 mm to 15.5 mm. The positive standard ciprofloxacin demonstrated ZOIs between 11.5 mm and 20.5 mm. Compound 37 exhibited greater susceptibility against *E. coli* with a MIC value of 25 µg/ml followed by *V. cholera* (MIC) at 50 µg/ml.

In contrast, Gram-positive bacteria such as *Bacillus pumilus* and *B. subtilis* demonstrated the lowest sensitivity to compounds (**37)** and (**39**), displaying a ZOI value of 6.0 mm at 200 µg/ml. Both compounds 37 and 39 also displayed antifungal activity against most tested fungal species. In molecular docking analysis, compounds (**37)** and (**39)** demonstrated significant binding energy within the binding pocket of *E. coli DNA gyrase* B, yielding docking scores of -8.092 and -7.754 kcal/mol, respectively. Similarly, with *C. albicans* lanosterol 4α-demethylase, they displayed docking scores of -7.792 and -8.995 kcal/mol, respectively. Following the ADMET prediction analysis, both synthesized compounds exhibit favorable pharmacokinetics and drug-like characteristics, making them suitable for oral administration. In addition to the *in vitro* bioassay activity test, molecular docking results and ADMET predictions collectively convey the promising antimicrobial properties of both synthesized compounds. These findings imply that conducting further synthesis and evaluation of 2-naphthol derivatives could be beneficial in the ongoing efforts to develop antimicrobial drugs for combating infectious diseases and microbial resistance.

Keywords: *antimicrobial, antibacterial, antifungal, Mannich base, 2-naphthol, oxazine, aminoalkyl, in silico study, DNA gyrase B, molecular docking, ADMET*

ACKNOWLEDGMENT

First and foremost, I would like to thank Almighty God for his mercy in giving me strength and patience to complete the study.

I express my deepest gratitude to Dr. Daniel Bisrat, my advisor, for his invaluable guidance throughout this project. Special thanks to Professor Kaleab Asres for his support in the antimicrobial activity work. I extend my sincere appreciation to Prof. Mazumder from the Department of Pharmaceutical Technology at Noida Institute of Engineering and Technology in India for overseeing the antimicrobial activity.

I would also like to acknowledge Addis Ababa University for granting the research budget, and Bahir Dar University for sponsoring my MSc study. I am also very grateful for the BASIL project for covering some of my research expenses. A heartfelt thank you to all my friends for their unwavering support.

TABLE OF CONTENTS

ABSTRACT iv

ACKNOWLEDGMENT vi

LIST OF FIGURES xi

LIST OF SCHEMES xii

LIST OF TABLES xiii

LIST OF ABBREVIATIONS AND ACRONYMS xiv

1. INTRODUCTION 1

1.1 Infectious Disease 1

1.1.1 Overviews of Infectious Disease 1

1.1.2 Bacterial Infection 1

1.1.3 Fungal Infection 2

1.2 Statement of the Problem 3

1.3 Objective of the Study 4

1.3.1 General Objective 4

1.3.2 Specific Objectives 4

1.4 Significance of the Study 5

2. LITERATURE REVIEW 6

2.1 The Aminoalkyl Base and Mannich Reaction 6

2.2 Antimicrobial Activity of 2- naphthol Derivatives 8

2.3 Potential Antimicrobial Targets 13

3. MATERIALS AND METHODS 15

3.1 Materials 15

3.1.1 Chemicals and Reagents 15

3.1.2 Instruments 15

3.1.3 Test Micro-organisms 16

3.1.3.1 Bacterial Strains 16

3.1.3.2 Fungal Strains 17

3.2 Methods 17

3.2.1 Synthesis of 2-naphthol Derivatives 17

3.2.1.1 Synthesis of Aminoalkyl Derivative (37) 17

3.2.1.2 Synthesis of 1,3-oxazine derivative of 2-naphthol (39) 17

3.2.2 Structural Elucidation 18

3.2.3 *In vitro* Antimicrobial Activity Assay 19

3.2.3.1 Preparation of Inoculum and Standardization 19

3.2.3.2 Determination of Zones of Inhibition 20

3.2.3.3 Determination of Minimum Inhibitory Concentrations (MICs) 20

3.2.4 *In silico* Studies of the Synthesized Compounds 21

3.2.4.1 Molecular Docking Study 21

3.2.4.1.1 Protein Preparation 22

3.2.4.1.2 Ligand Preparation 22

3.2.4.1.3 Receptor Grid Generation 22

3.2.4.1.4 Glide Extra Precision (XP) Ligand Docking 23

3.2.4.2 Pharmacokinetics and Drug-likeness Properties 23

4. RESULT AND DISCUSSION 24

4.1 Synthesis of 2-naphthol Derivatives 24

4.1.1 Synthesis of Aminoalkyl Derivative of 2-naphthol (37) 24

4.1.2 Synthesis of 1,3-oxazine Derivative of 2-naphthol (39) 25

4.2 Structural Elucidation 26

4.2.1 Structural Elucidation 1-(phenyl(*o*-tolylamino)methyl)naphthalene-2-ol (37) 26

4.2.2 Structural Elucidation of 2-benzyl-2,3-dihydro-1H-naphtho[1,2-e][1,3]oxazine (39) 28

4.3 Antimicrobial Activity 30

4.3.1 Antibacterial Activity 30

4.3.2 Antifungal Activity 32

4.4 *In silico* Studies of the Synthesized Compounds 33

4.4.1 Molecular Docking Study 33

4.4.2 ADMET Predictions of the Synthesized Compounds 38

5. CONCLUSION 42

6. RECOMMENDATIONS 43

7. REFERENCES 44

8. Appendices 56

8.1 TLC chromatogram of synthesized compounds 56

8.2 ^{1}H and ^{13}C NMR spectra of synthesized compounds 57

8.2.1 ^{1}H, ^{13}C, DEPT-135, and DEPT-90 NMR spectra of compound 37..... 57

8.2.2 ^{1}H, ^{13}C, DEPT-135 and DEPT-90 NMR spectra of compound 39..... 60

8.3 Molecular Docking Results of Ciprofloxacin and Voriconazole 64

LIST OF FIGURES

Figure 1: Betti base 6

Figure 2: Clinically used Mannich bases 8

Figure 3: FDA-approved 2-naphthol and naphthol-based drugs 10

Figure 4: 2- naphthol containing antimicrobial agents 12

Figure 5: Compounds acting on *E. coli* DNA gyrase B and *C. albicans* lanosterol 14α-demethylase 14

Figure 6: (A): 3D model, (B): 3D model zoomed, and (C): 2D presentation of binding interaction of compound **3**7 with the residues of *E. coli* DNA gyrase B 35

Figure 7: (A): 3D model, (B): 3D zoomed model (C): 2D binding interactions of compound 39 against the residues of *E. coli* DNA gyrase B.....35

Figure 8: (A): 3D representation, (B): 3D zoomed view, (C): 2D model of compound 37 docking interactions against the residue of *C. albicans* lanosterol 14α-demethylase (5v5z).....37

Figure 9: (A): 3D model, (B): 3D zoomed view, (C): 2D model of compound 39 docking interactions against the residue of *C. albicans* lanosterol 14α-demethylase (5v5z).....37

LIST OF SCHEMES

Scheme 1: Reaction of iminium with carbonyl aromatic compounds 7

Scheme 2: General synthesis of compounds **37** and **39** 18

Scheme 3: Flowchart of a target-based molecular docking procedure and analysis 23

Scheme 4: The proposed reaction mechanism for the synthesis of 1-(phenyl(ortho-tolylamino) methyl) naphthalene-2-ol (**37**) 25

Scheme 5: The proposed reaction mechanism for the synthesis of 2-benzyl-2,3-dihydro-1H-naphtho[1,2-e] [1,3]oxazine (**39**) 26

LIST OF TABLES

Table 1: ^{1}H and ^{13}C NMR data of compound 37 27

Table 2**:** ^{1}H and ^{13}C NMR data of compound (39) 29

Table 3**:** ZoIs and MICs of the synthesized compounds against 26 bacterial strains. 31

Table 4**:** ZOIs and MICs of the synthesized compounds against four fungal species 32

Table 5: Docking score, hydrogen bond, and hydrophobic interactions of compounds **37** and **39** against the binding site of DNA gyrase B (4z2e) and 14α-demethylase (5v5z).....34

Table 6: ADMET data of the synthesized compounds.....39

LIST OF ABBREVIATIONS AND ACRONYMS

^{13}CNMR	Carbon-13 Nuclear Magnetic Resonance
^{1}HNMR	Hydrogen Nuclear Magnetic Resonance
ADMET	Absorption Distribution Metabolism Elimination Toxicity
AIDS	Acquired Immune Deficiency Syndrome
AMR	Antimicrobial Resistance
ATCC	American Type Culture Collection
BBB	Blood-Brain Barrier
CDC	Center for Disease Control
CLSI	Clinical and Laboratory Standards Institute
d	doublet
dd	doublet of doublet
DEPT	Distortionless Enhancement by Polarization Transfer
DMSO-D6	Dimethylsulfoxide
EAS	Electrophilic Aromatic Substitution
HIV	Human Immunodeficiency Virus
Hz	herz
IC	Invasive Candidiasis
IFI	Invasive Fungal Infection
J	Coupling constant
m	multiplate
MDR	Multi-drug Resistance
MHB	Mueller Hinton Broth

MIC	Minimum Inhibitory Concentration
mm	millimeter
NCTC	National Collection Type Culture
OPLS-4	Optimized Potential for Liquid Simulation
PDB	Protein Data Bank
ppm	parts per million
RMSD	Root Mean Square Deviation
s	singlet
SBD	Sabouraud Dextrose Broth
SBDD	Structure-Based Drug Design
t	triplet
TLC	Thin Layer Chromatography
TMS	Trimethyl silyl
USA	United States of America
UV	Ultra-Violet
WHO	World Health Organization

1. INTRODUCTION

1.1 Infectious Disease

1.1.1 Overviews of Infectious Disease

Infectious diseases, caused by pathogens like bacteria, viruses, parasites, or fungi present a significant global threat, affecting public health and economies (J. M. van Seventer and N. S. Hochberg, 2017). Despite advancements, diseases like lower respiratory tract infections, HIV/AIDS, tuberculosis, diarrheal diseases, and malaria persist as leading causes of death worldwide, with a pronounced impact in developing countries (I. Abubakar *et al.*, 2015, S. Janowska *et al.*, 2023, I. N. Okeke *et al.*, 2005). In Ethiopia, these diseases contribute significantly to premature deaths (A. Misganaw *et al.*, 2017).

The emergence of antibiotic resistance adds urgency to the situation, with multidrug-resistant pathogens posing a severe global health risk (N. Gohil *et al.*, 2018). The World Health Organization (WHO) predicts a dire scenario, estimating 10 million annual deaths by 2050 due to antibiotic resistance (WHO, 2019). Currently, there is a critical shortage of new microbials, necessitating the discovery of novel antimicrobial agents to combat multidrug resistance.

1.1.2 Bacterial Infection

Bacterial infections are acknowledged as one of the significant global health challenges. A recent study under the title “Global Mortality Associated Bacterial Pathogens” reported an estimated 13.7 million infection-related deaths in 2019, with 7.7 million attributed to specific bacterial pathogens. Sepsis accounted for 56.2% of these deaths. Five major pathogens, including *Staphylococcus aureus* and *Escherichia coli*, were responsible for 54.9% of bacterial-related deaths. Mortality rates associated with these microbes were outrageous in sub-Saharan Africa (K. S. Ikuta *et al.*, 2022).

Antibiotics, crucial for treating bacterial infections, face challenges due to antimicrobial resistance (AMR). AMR, accelerated by improper antibiotic use (S. Mladenovic-Antic *et al.*, 2016), poses a substantial threat to global healthcare systems (P. Dadgostar, 2019, T. Mestrovic *et al.*, 2022). In 2019, an estimated 4.95 million deaths were attributed to bacterial AMR, including 1.27 million deaths directly attributable to drug resistance, emphasizing the urgent need for global action. Regionally, the highest and lowest mortality rates across all age groups were observed in Western Sub-Saharan Africa and Australasia, respectively. Among other things, the infectious syndrome of the lower respiratory tract was the most distressing (C. J. Murray *et al.*, 2022).

1.1.3 Fungal Infection

Despite their considerable impact on human health, fungal diseases are often overlooked as significant pathogens by the public and health authorities (M. L. Rodrigues and J. D. Nosanchuk, 2020). Life-threatening invasive fungal infections, are prevalent among immunocompromised individuals (G. D. Brown *et al.*, 2012, D. S. Perlin *et al.*, 2015), with conditions like asthma (W. W. Hope *et al.*, 2005), AIDS (B. J. Park *et al.*, 2009), bloodstream infections (H. Wisplinghoff *et al.*, 2004, H. Wisplinghoff *et al.*, 2014), neoplastic diseases, and corticosteroid therapies (S. S. Gonçalves *et al.*, 2016), contribute significantly to global morbidity and mortality.

Based on recent statistics, an estimated 3 million and 1.9 million people globally suffer from chronic and acute severe fungal infections, respectively, each year (F. Bongomin *et al.*, 2017). Approximately more than 1.5 million annual deaths globally are attributed to various fungal species, impacting over a billion people (E. Rayens and K. A. Norris, 2022). Chronic pulmonary aspergillosis and invasive candidiasis, caused by *Aspergillus fumigatus* and *Candida albicans*, respectively, represent major cases (F. Bongomin *et al.*, 2017).

Antifungal classes, like azoles, polyenes, echinocandins, and flucytosine, are commonly used but their misuse contributes to the emergence of drug-resistant pathogens, posing a global threat to public health and agriculture (L. E. Cowen *et al.*, 2015, C. Tratrat, 2020). Azole resistance particularly in *Candida* and *Aspergillu*s species, has been observed, emphasizing the urgent need for new antifungal drugs (S. J. Howard and M. C. Arendrup, 2011, M. A. Pfaller, 2012, D. S. Perlin *et al.*, 2017). Candidemia, especially from *Candida glabrata*, is increasingly resistant to azoles and echinocandins (M. A. Pfaller, 2012), while Asper*gillus fumigatus*, responsible for 80% of invasive infections, shows azole resistance (S. J. Howard and M. C. Arendrup, 2011). This highlights the pressing need for novel antifungal discoveries.

1.2 Statement of the Problem

Current antimicrobial agents are becoming less effective due to the rise of new microbial resistance mechanisms, leading to the spread of multidrug-resistant bacteria, or ‘’superbugs” (WHO, 2021). The development of resistance to new drugs is often a big issue. In addition, some existing drugs for infectious diseases have adverse side effects (S. Mohsen *et al.*, 2020), and affordability is a significant concern in developing countries, including Ethiopia.

To address these challenges, it is crucial to develop new chemical compounds with unique structures and mechanisms of action that are safe, affordable, and effective against disease-causing microbes. Our objective was to synthesize lead compounds from the 2-naphthol scaffold, aiming for reduced toxicity and enhanced antimicrobial effects.

1.3 Objective of the Study

1.3.1 General Objective

The general aim of this study was to synthesize, evaluate *in vitro* antimicrobial activity, and *in silico* study of aminoalkyl and oxazine 2-naphthol derivatives

1.3.2 Specific Objectives

- To synthesize aminoalkyl and oxazine 2-naphthol derivatives
- To characterize the chemistry of aminoalkyl and oxazine 2-naphthol derivatives
- To evaluate *in vitro* antibacterial activity of aminoalkyl and oxazine 2-naphthol derivatives
- To evaluate *in vitro* antifungal activity of aminoalkyl and oxazine 2-naphthol derivatives
- To conduct molecular docking of aminoalkyl and oxazine 2-naphthol derivatives
- To determine the drug-likeness of 2-*naphthol* derivatives

1.4 Significance of the Study

The emergence of new infectious diseases, coupled with a decline in new antibiotics and the continuous increase in antimicrobial resistance, underscores the need for the development of novel chemical entities. In drug discovery, design and synthesis of small molecules are an important and effective strategy for finding new drugs to combat microbial resistance. In this study, we synthesized two compounds (1-aminoalkyl and oxazine derivatives of 2-naphthol) through a Mannich-type reaction. Both compounds exhibited promising antimicrobial activities against a broad spectrum of bacteria and fungi strains, highlighting the potential of 2-naphthol derivatives as an effective scaffold for treating bacterial infections. Moreover, both compounds displayed activities against multi-drug-resistant bacteria in which it contributes to the health system. We These finding also contribute valuable insights to a broader research network aimed at discovering new antimicrobials in the fight against antimicrobial resistance (AMR).

2. LITERATURE REVIEW

2.1 The Aminoalkyl Base and Mannich Reaction

In the early 20th century, laboratories conducted research on reactions involving ammonia or amines, formaldehyde, and enolizable carbonyl compounds. The synthesis of 1-(α-aminobenzyl)-2-naphthol, also known as Betti bases, was initially achieved in 1900 by combining aryl aldehydes, ammonia, and 2-naphthol (M. Betti, 1900, M. Betti, 2003, A. Olyaei and M. Sadeghpour, 2019).

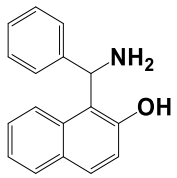

1

Figure 1: Betti base

In 1912, Mannich published a comprehensive work under the title "Mannich Aminoalkylations (Mannich Bases)", in response to the Betti investigation. The Mannich reaction involves the initial formation of an imine by combining two components, namely aldehyde and amine, as illustrated in Scheme 1. This imine further reacts with a carbonyl molecule to form an amino alkylation at alpha-carbon, or the imine can react with an aromatic compound via an electrophilic aromatic substitution (EAS) reaction (C. Cardellicchio *et al.*, 2010).

In Mannich-type reaction, it involves compounds with unenolizable aldehyde, and an amine in the presence of an acid catalyst, resulting in the formation of Mannich bases. This further undergoes EAS reaction with aromatic compounds, such as 2-naphthol, to form aminoalkyl derivatives (Scheme 1).

The structural heterogeneity of Mannich bases primarily arises from the different types of acidic hydrogen-containing substrates (ketones, carboxylic acids, phenols, and naphthol, among others) that can undergo aminomethylation (condensation).

Additionally, the variety of amine reagents used in the Mannich reaction contributes to this structural diversity (G. Roman, 2015, F. S. Tokalı *et al.*, 2022, K. G. Gamit and N. B. Patel, 2023). In this context, 2-naphthol, containing acidic hydrogen, is prone to the Mannich-type reaction, facilitating the synthesis of C-type Mannich bases. Studies have shown that one and two positions in the 2-naphthol ring are targets for various reactions, leading to the synthesis of biologically active compounds (R. R. Nagawade and D. B. Shinde, 2007). The Mannich reaction, along with etherification, is a suitable method for obtaining amino alkyl and 1,3- ozazine 2-naphthol derivatives with potential biological activity.

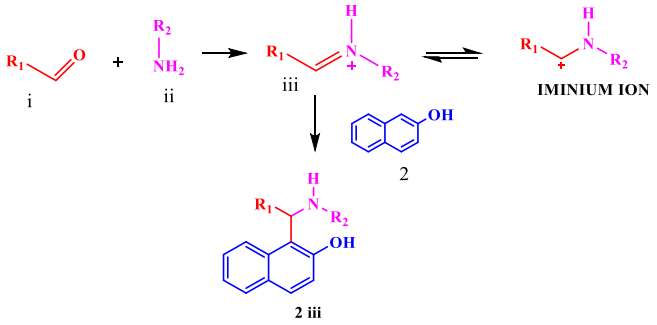

Scheme 1: Reaction of iminium with carbonyl aromatic compounds

Mannich bases play crucial roles in their application in pharmaceutical chemistry, particularly in optimizing and enhancing the pharmacokinetic properties of drugs within the human body. This is achieved by incorporating a polar or non-polar group into the structure, thereby improving the hydrophilic or lipophilic characteristics of the newly formed chemical entity (A. N. Saab *et al.*, 1990).

Additionally, Mannich bases serve as significant pharmacophores or bioactive lead molecules, leading to the synthesis of various potential active ingredients with high medicinal value that feature an aminoalkyl chain (S. Bala *et al.*, 2014). Clinical examples of Mannich bases with an aminoalkyl chain include fluoxetine (**3**), atropine (**4**), ranitidine (**5**), cocaine (**6**), trihexyphenidyl (**7**), procyclidine (**8**), biperiden (**9**), among others (see Figure 2). These compounds contribute to the development of pharmaceuticals with diverse therapeutic applications.

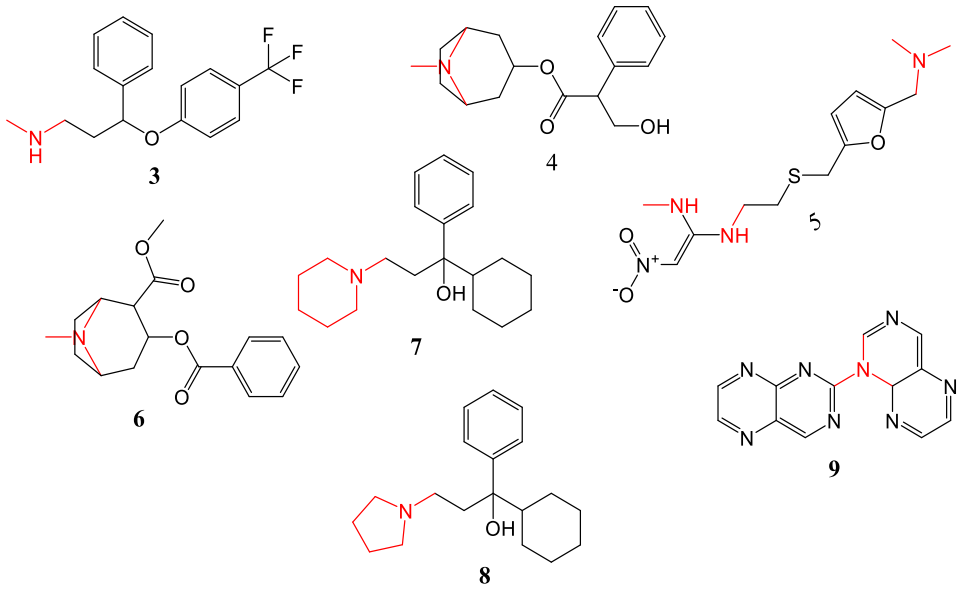

Figure 2: Clinically used Mannich bases

2.2 Antimicrobial Activity of 2- naphthol Derivatives

Naphthalene, a bicyclic aromatic hydrocarbon, is used as a versatile building block for synthesizing various scaffolds. Extensive research has explored its medicinal properties, including antimicrobial(Y. Rokade and R. Sayyed, 2009), antiviral (I. A. Ali *et al.*, 2005, N. S. Hamad *et al.*, 2010), antidiabetic (N. Mahindroo *et al.*, 2006), anticancer (I. A. Ali *et al.*, 2005), anti-inflammatory (W. V. Murray *et al.*, 1991), antihypertensive (K. Rahn *et al.*, 1974, K. L. Duchin *et al.*, 1980), anticonvulsant effects (R. V. Shingalapur *et al.*, 2010).

In particular, naphthalene-containing medications like bedaquiline, nafitifin, and terbinafine, among others, play a crucial role in managing microbial infections (G. Petranyi *et al.*, 1987). Furthermore, 2-naphthol, a hydroxy analog of naphthalene commonly used as a dye, exhibits excellent antimicrobial properties.

The FDA has approved several drugs containing 2-naphthol with diverse pharmacological activities (see Figure 3). Notable examples include nafcillin (**10**), an antibiotic belonging to the beta-lactam penicillin class, used for treating infections caused by gram-positive bacteria (F.-Y. Chang *et al.*, 2003). Rifampicin (**11**), another 2-naphthol-based drug, is employed as an antitubercular agent, often in combination with isoniazid, pyrazinamide, and ethambutol (A. Nusrath Unissa *et al.*, 2016). Tolnaftate (**12**), a synthetic anti-fungal with a thiocarbamate moiety, inhibits squalene epoxidase—an essential enzyme in ergosterol biosynthesis during the fungi life cycle (N. Ryder *et al.*, 1986).

FDA-approved 2-naphthol-based drugs extend to non-steroidal anti-inflammatory agents (NSAIDs). For instance, naproxen (**13**) and nabumetone (**14**) serve as examples of NSAIDs that inhibit the cyclooxygenase enzyme. In addressing central nervous system (CNS) diseases, FDA-approved drugs with naphthol scaffolds, such as duloxetine (**15**), are available. Additionally, propranolol (**16**), a naphthol-based cardiovascular drug, is utilized in the treatment of high blood pressure.

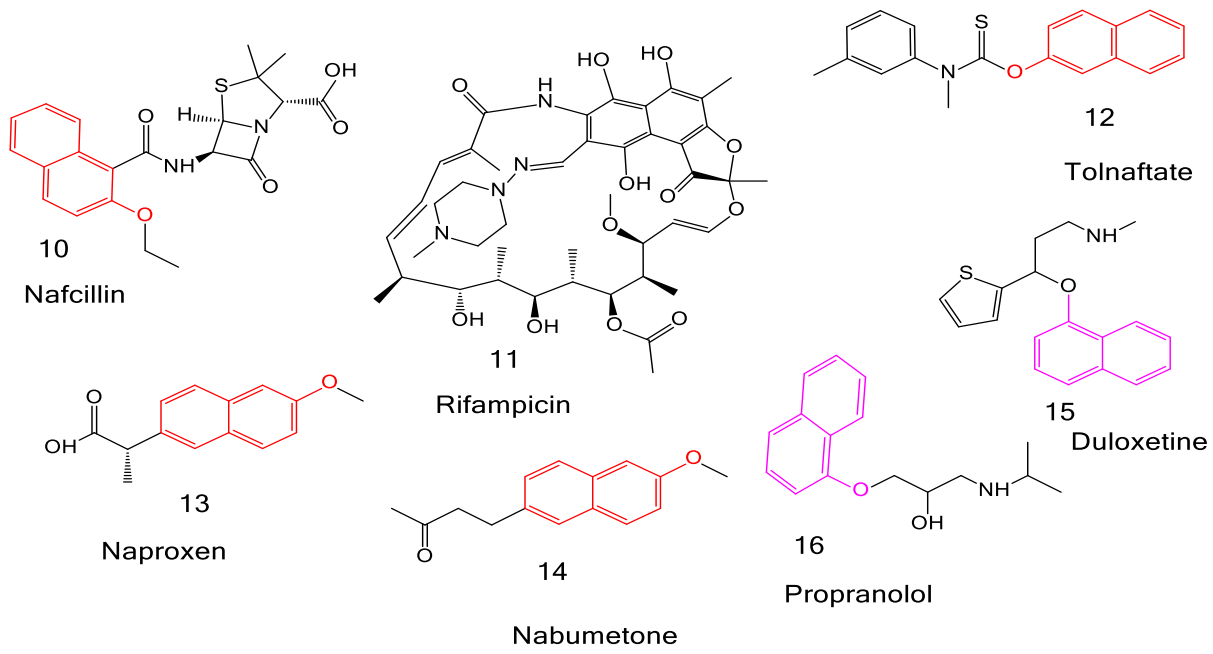

Figure 3: FDA-approved 2-naphthol and naphthol-based drugs

In search for effective antimicrobials to address the challenge of antimicrobial resistance, recent research has focused on synthesizing a novel series of 2-naphthol-based derivatives (**see Figure 4**). Jasim and Mustafa conducted a study synthesizing a series of 2-naphthol derivatives and assessing their antimicrobial activity. Among these, Compound (**17)** exhibited significant aerobic gram-negative bactericidal activity, with a minimum bactericidal concentration (MBC) of 2.35 µg/ml and a minimum inhibitory concentration (MIC) of 1.4 µg/ml. Notably, Compound (**18)** demonstrated the most effective fungicidal potential, with an MBC of 1.7 µg/ml and a MIC of 1.25 µg/ml (S. F. F. Jasim and Y. F. Mustafa, 2022).

In another study, R. Kumar et al. synthesized derivatives featuring 4-amino-3-hydroxy-naphthalene-1-sulfonic acid with a 2-naphthol scaffold, evaluating their antibacterial and antifungal activities. Compounds (**19)** and (**20)** emerged as potent antimicrobial agents against S. aureus, with MIC values of 1.22 µM/ml and 1.20 µM/ml, respectively.

Additionally, these compounds displayed high potency against gram-positive bacilli and certain fungal species tested (R. Kumar *et al.*, 2012).

Azetidinone derivatives linked to the 2-naphthol framework were synthesized and evaluated for their antimicrobial activity (Y. Rokade and N. Dongare, 2010). Among the compounds synthesized, compound (**21)** demonstrated activity against *E. coli*, S. aureus, *P. aeruginosa*, and *A. niger*. Şahin et al. synthesized new compounds derived from the 1 or 2-naphthol framework and assessed their antimicrobial activity against three bacterial species (S. aureus, E. coli, and P. aeruginosa) and three fungal species (C. albicans, C. krusei, and C. parapsilosis) using the micro broth dilution method. All synthesized compounds exhibited activity against the selected organisms, with MIC values ranging from 32 to 256 µg/ml. Compound **(23)** displayed significant activity (32 µg/ml) against all fungal species, while both compounds (**22)** and (**23)** showed moderate activity (64 µg/ml) against S. aureus (G. Şahin *et al.*, 2002).

5,6-Dimethoxynaphthalene-2-carboxylic acid derivatives (**25)** were synthesized and evaluated for their *in vitro* antibacterial activity against pathogenic bacteria, revealing inhibition zones ranging from 11 to 26 mm (S. Göksu *et al.*, 2005). Chopde et al. investigated the antibacterial activities of 2-naphthol-based compounds against nine bacterial strains, including *E. coli*, *B. subtilis*, *S. aureus*, and *Salmonella sp*. Compound (**26)** exhibited inhibition zones on agar plates (12.5, 22.1, and 31.3 mm) against *B. subtilis*, *E. coli*, and *Salmonella sp*., respectively (H. N. Chopde *et al.*, 2010).

K.M. Rathod evaluated azo-2-naphthol compounds (**27)** against five representative human pathogenic microorganisms and achieved growth inhibition of the tested bacterial strains of 15–20 mm (K. Rathod, 2011).

D. Azarifar et al. synthesized 3,5-dinaphthyl-substituted 2-pyrazoline derivatives and evaluated their antimicrobial activity against *Escherichia coli, Staphylococcus aureus, Klebsiella pneumoniae, Proteus mirabillis, Shigella dysentery, and Salmonella typhi.*

The naphthalene substituted with chlorine, hydroxy, and dimethylamino-$N(CH_3)_2$ and carboxamide-$CONH_2$ groups at the N-1 position of the 2-pyrazoline ring showed very good antimicrobial activity. Compound **(28a-28c)** was the most promising with MIC between 16 and 63 mM against various test organisms. The MIC values of the compounds showed that the hydroxyl and chlorine groups on the naphthyl ring in position 3 contributed to a significant increase in antimicrobial activity (D. Azarifar and M. Shaebanzadeh, 2002).

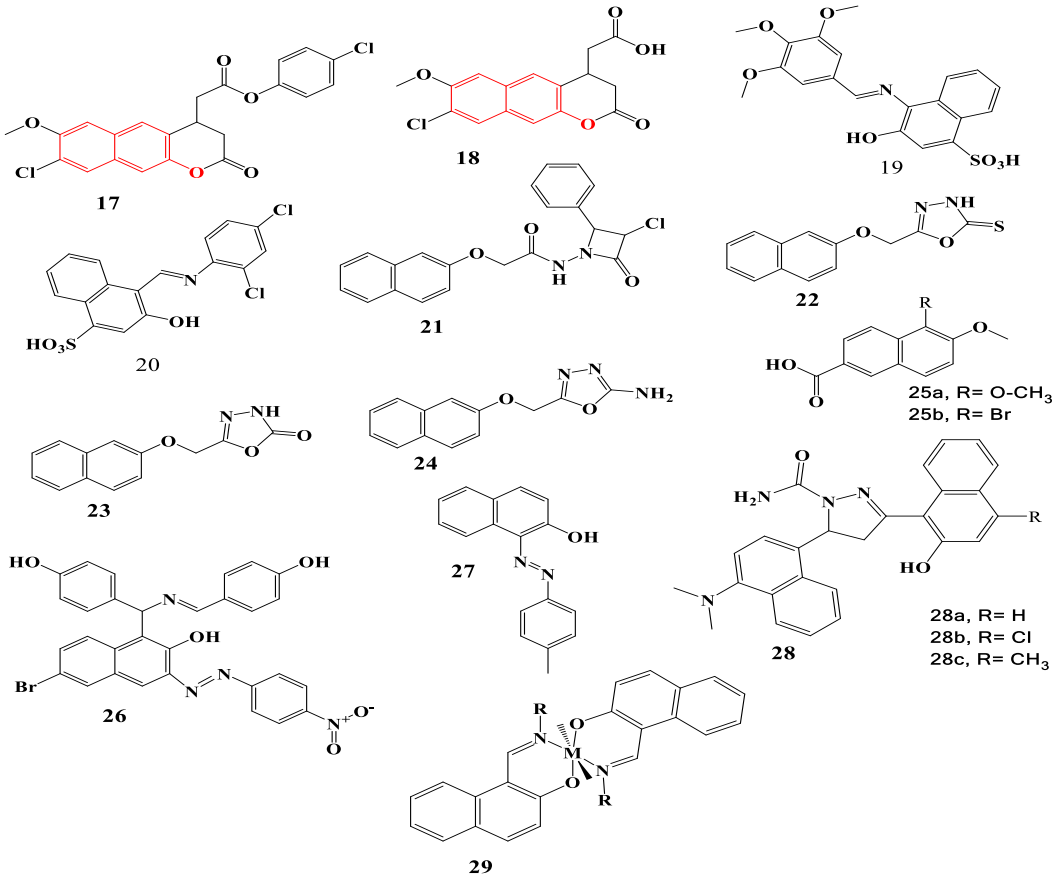

Figure 4: 2- naphthol containing antimicrobial agents

2.3 Potential Antimicrobial Targets

The search for new chemical substances to combat diseases is ongoing. When it comes to fighting diseases with drugs, the process involves identifying a target, typically a cellular component that induces cell death or halts growth when exposed to a drug (A. Maxwell, 1997). Antimicrobials, commonly utilized for treating microbial infections, operate by targeting specific structures or processes crucial for microbial growth or survival, without adversely affecting the host (A. Coates *et al.*, 2002, C. Walsh, 2000).

One well-known target in bacterial cell wall biosynthesis is Penicillin-binding proteins (PBPs), which serve as targets for β-lactams and glycopeptide antibiotics. PBPs, located on the outside of the cytoplasm, perform peptidoglycan transpeptidase and endopeptidase functions. They are present in nearly all gram-positive and gram-negative bacteria, although the number varies from species to species (P. Sarkar *et al.*, 2017, N. Georgopapadakou, 1993). In addition to PBPs, the bacterial protein synthesis pathway (G. Sanyal and P. Doig, 2012), bacterial DNA replication and repair (Sanyal and Doig, 2012), and folate biosynthesis pathway (E. D. Brown and G. D. Wright, 2005) are commonly used targets for antibacterial drug development.

Antibacterial chemotherapy primarily focuses on bacterial type II topoisomerases, namely DNA gyrase (GyrA2GyrB2) and the closely related Topo IV. Due to their high similarity, inhibitors designed for antibacterial topoisomerases typically target both enzymes (Y. Pommier *et al.*, 2010, G. Sanyal and P. Doig, 2012). DNA gyrase, a type II topoisomerase, introduces negative supercoils into DNA by utilizing ATP hydrolysis. While essential in all bacteria, it is absent in higher eukaryotes, making it an attractive target for antibacterial drug development (F. Collin *et al.*, 2011, A. Maxwell, 1997). Bacterial type II topoisomerases (DNA gyrase and Topo IV) are the targets of quinolones and aminocoumarin antibiotics (**Figure 5**) (Y. Pommier *et al.*, 2010).

Quinolones like ciprofloxacin (**30)** and aminocoumarin antibiotics (novobiocin **31** and clorobiocin **32**) target bacterial type II topoisomerases (DNA gyrase and Topo IV) (D. Lafitte *et al.*, 2002).

In contrast, antifungal drug discovery has a relatively small number of well-validated molecular targets. One of the most established pathways in antifungal therapy is the biosynthesis of the key fungal sterol ergosterol. Ergosterol biosynthesis is the target of clinically useful antifungals, including triazoles like fluconazole, which specifically target the product of the ERG11 gene, P450 lanosterol 14α-demethylase (E. D. Brown and G. D. Wright, 2005). Azoles (**Figure 5**) such as compounds (**33)** and (**34)** block sterol biosynthesis by inhibiting the fungal sterol 14α-demethylase enzyme, thereby blocking sterol biosynthesis (T. Y. Hargrove *et al.*, 2015).

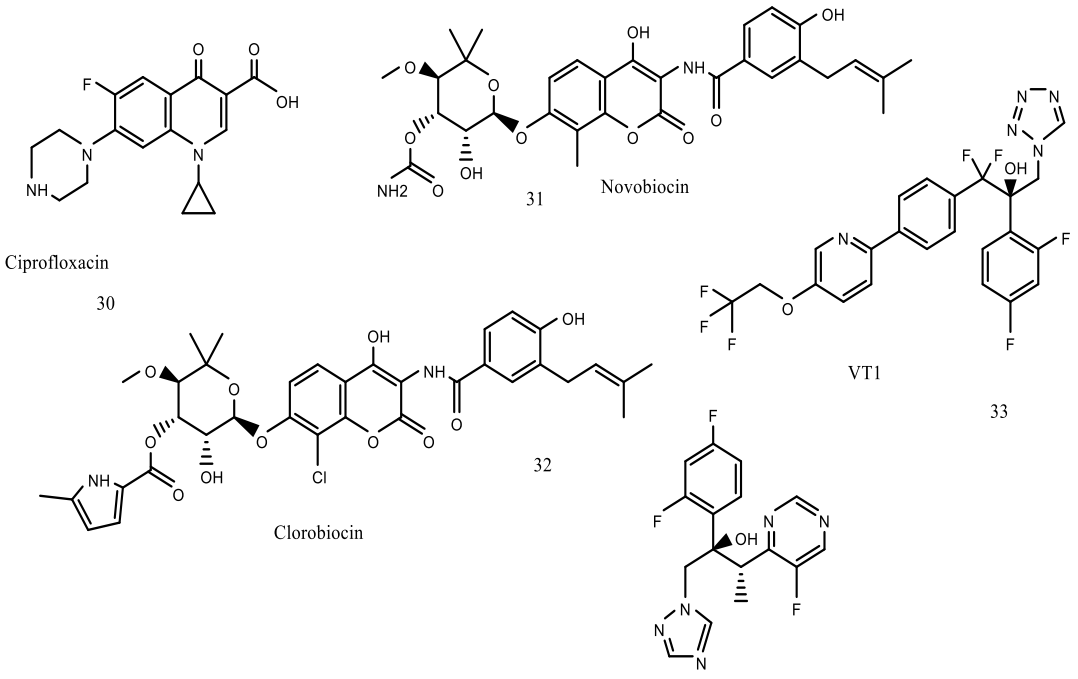

Figure 5: Compounds acting on *E. coli* DNA gyrase B and *C. albicans* lanosterol 14α-demethylase

3. MATERIALS AND METHODS

3.1 Materials

3.1.1 Chemicals and Reagents

The following chemicals, reagents, and solvents were used to perform the experiments. Benzylamine (99%), O-toluidine (2- methylaniline), 2-naphthol (LobaChem PV. LTD., Mumbai, India). Formaldehyde, $ZnCl_2$ (Sigma-Aldrich Co., Stein helm, Germany), ethanol, hexane, ethyl acetate, methanol, and chloroform (LobaChem PV. LTD., Mumbai, India) obtained from the Department of Pharmaceutical Chemistry, College of Health Science, Addis Ababa University were used for the synthesis, purification, and chromatogram of the compounds. Tetramethyl silane (TMS) and $CDCl_3$ were used as internal standard and solvent respectively in NMR spectroscopy. All the solvents, chemicals, and reagents were analytical grade. Nutrient Agar (NA), Mueller-Hinton Broth (MHB), Sabouraud Dextrose Agar (SDA) and Sabouraud Dextrose Broth (SDB) (HiMedia Laboratories Pvt. Ltd. India), (Sisco Research Laboratories Pvt. Ltd. India) were used for media preparation. Ciprofloxacin and Griseofulvin were used as a reference drug.

3.1.2 Instruments

Analytical TLC plates (60 F_{254}, 0.2 mm thick, Merck KGaA, Darmstadt, Germany) and columnar silica gel (60 F_{254}, 70–240 mesh, Merck KGaA, Darmstadt, Germany) were used for the analysis and purification of the compounds. A rotary evaporator (BUCHI Rotavapor™ R-300, Switzerland) was used to remove solvents. A UV-visible spectrophotometer (Evolution 60S) was used to visualize the TLC chromatogram. ^{1}H and ^{13}C NMR spectra were recorded at 400 MHz and 100 MHz, respectively, on a Bruker Avance DMX400 FT NMR spectrometer (Bruker, Billerica, Massachusetts, USA).

Incubator (Model 100-800 Memmert), Autoclave, Biosafety cabinet (Biostar Model 50/60), Vortex (Fisher brand), Water bath, Inoculation loops, Electric balance, Magnetic stirrer, Cavate, Test tube, Pipette tips, Pipette filler, Micropipette (10–200 µl), Microtiter plates, Capillary tube and a measuring cylinder were used for synthesis and antimicrobial test. Software tools such as Chem Office 2019 (ChemDraw version: 2019.1), MestrNova, and Schrödinger suite (version: 2023.1) were used for creating chemical sketches and preparing structural data files (SDF), reading NMR data, and docking, respectively.

3.1.3 Test Micro-organisms

3.1.3.1 Bacterial Strains

The *in vitro* antibacterial assays were carried out against the following Gram-positive bacterial strains (GPBSs): *Bacillus pumilus* 82, American type culture collection (ATCC 6633) strains of *B. subtilis,* and *Staphylococcus aureus* ML 267. Gram-negative bacterial strains used were: *Escherichia coli* 3:37C, *E. coli* 7360, *E. coli* 872, *E. coli* CD/99/1, *E. coli* K 88, *E. coli* T 37, *E. coli* ROW 7/12, *E. coli* 5933, *E. coli* HB101, *E. coli* 600, *Salmonella enterica* TD 01, *S. typhi* Ty2, *Shigella boydii* D13629, *S. dysentery* 8, *S. flexneri* Type 6, *S. soneii* 1, and NCTC strains of *Vibrio cholera (Vibrio cholerae* NCTC 4693, *V. cholerae* NCTC 5596, *V. cholerae* NCTC 10732, and *V. cholerae* NCTC 11501). In addition to this, *Pseudomonas aeruginosa* MDR 1*, *S. aureus* MDR 1*, and *S. aureus* MDR 2* resistant bacterial strains were employed. All the bacterial strains were procured from the Department of Technology, Jadavpur University; Central Drugs Laboratory, Kolkata and Institute of Microbial Technology, Chandigarh, India. The purity of the strains was checked according to the standard microbiological, cultural, and biochemical tests before sensitivity tests against the test sample.

3.1.3.2 Fungal Strains

Antifungal activity testing was carried out against the following fungal pathogens: *Aspergillus niger* ATCC 6275, *Candida albicans* ATCC 10231, *Penicillium funiclosum* NCTC 287and *P. notatum* ATCC 11625.

3.2 Methods

3.2.1 Synthesis of 2-naphthol Derivatives

Compound (**37)** and compound (**39)** were synthesized using the general one-pot three-component reaction principles outlined in Scheme 2, following the published method by (B. Priya *et al.*, 2016).

3.2.1.1 Synthesis of Aminoalkyl Derivative (37)

Compound **37** was synthesized by reacting benzaldehyde (2 mmol), 2-naphthol (2 mmol), and O-toluidine (2 mmol) in ethanol with a $ZnCl_2$ catalyst (10 mol%). Initially, benzaldehyde and $ZnCl_2$ were prepared in a 25 mL Erlenmeyer flask. O-toluidine was added to this mixture. Meanwhile, 2-naphthol was prepared in ethanol in a separate flask. The benzaldehyde-$ZnCl_2$-O-toluidine solution was then gradually added dropwise to the 2-naphthol solution. The reaction mixture was refluxed at 120 °C with continuous stirring for 10 hours. TLC was used to monitor the reaction progress, with a mobile phase of hexane: ethyl acetate (5:1). After completion, the mixture was cooled to room temperature and partitioned with distilled water and ethyl acetate (3 x 20 ml). The ethyl acetate fraction was purified using silica gel column chromatography, eluting with a hexane: ethyl acetate ratio of 1:1, resulting in a white crystal substance (compound **37**).

3.2.1.2 Synthesis of 1,3-oxazine derivative of 2-naphthol (39)

In a 25 mL Erlenmeyer flask, 10 mol% of $ZnCl_2$ was initially added to 37% aqueous formaldehyde (10 mmol). Benzylamine (5 mmol) was gradually added to the formaldehyde-$ZnCl_2$ solution with continuous stirring.

Simultaneously, a solution of 2-naphthol (5 mmol) in EtOH was prepared in a separate flask. The formaldehyde-benzylamine solution was then gradually added to the 2-naphthol solution. The reaction mixture was then refluxed at 120 °C for 7 hrs with continuous stirring. The reaction progress was monitored by TLC using a solvent system of hexane-EtOAc (5:1). After completion, the reaction mixture was cooled to room temp, and subjected to extraction with distilled water (3 x 20 ml) and EtOAc, respectively. The EtOAc layer was subjected to silica gel column chromatography, yielding two fractions (Fr) by elution with hexane (Fr. 1) and hexane-EtOAc (2:1; Fr. 2). After removing the solvent from Fr. 2, a white solid crystal was obtained, and identified as the 1,3-oxazine derivative of 2-naphthol (compound **39**).

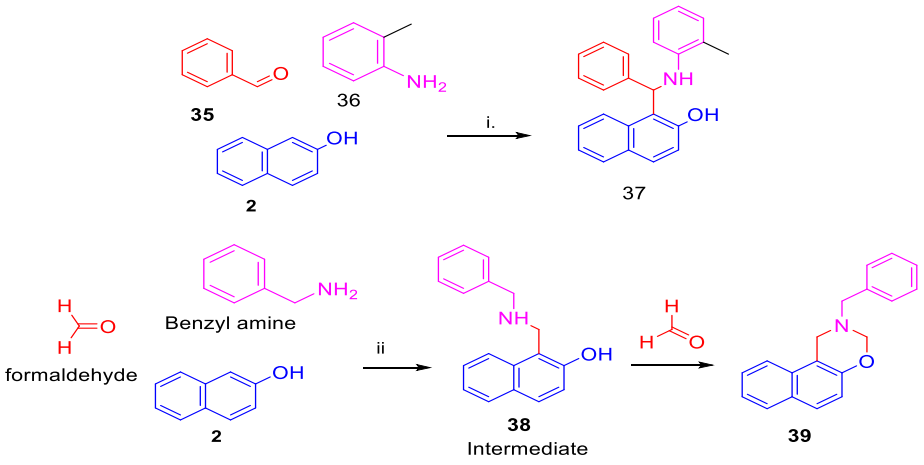

Reagents and conditions: (i). EtOH, $ZnCl_2$, 120 °C, 10 hr.; (ii). EtOH, $ZnCl_2$, 120 °C, 7 hr.

Scheme 2: General synthesis of compounds **(37)** and **(39)**

3.2.2 Structural Elucidation

The structures of the compound were determined using ^{1}H and ^{13}C nuclear magnetic resonance (NMR) at 400 MHz and 100 MHz, respectively, recorded at room temperature in $CDCl_3$.Scanning ranges were 0-12 ppm for ^{1}H NMR and 0-220 ppm for ^{13}C NMR.

Tetramethylsilane (TMS) served as an internal standard. Results were reported in δ (ppm) for chemical shifts and Hz for coupling constants (J). ^{1}H NMR signal multiplicities were denoted as singlet (s), doublet (d), doublet of doublets (dd), triplet (t), or multiple (m).

3.2.3 *In vitro* Antimicrobial Activity Assay

3.2.3.1 Preparation of Inoculum and Standardization

All culture media used were prepared according to the manufacturer's instructions. The media was sterilized at 121 °C for 15 minutes in an autoclave and allowed to cool to 50 – 45 °C in a water bath. Subsequently, 20 ml of the medium was poured into 100 mm diameter Petri dishes and allowed to solidify under aseptic conditions in the level II biosafety cabinet. All selected strains were sub-cultured on Petri dishes containing nutrients and Sabouraud agar media specific for bacteria and fungi, respectively. The antimicrobial experiment was conducted according to the Clinical and Laboratory Standards Institute (CLSI) guideline (M. P. Weinstein and J. S. Lewis, 2020). For antimicrobial experiments, 4–5 bacterial/fungal colonies for each organism tested were inoculated using an inoculating loop in Petri dishes containing agar medium. Each bacterial and fungal test organism was incubated at 37 °C for 24 hours and at 25 °C for 3 days, respectively. Standardization was carried out by taking 3-5 inoculums from a fresh pure culture of the test organism and preparing a suspension with Mueller-Hinton broth (for bacteria) and Sabroud dextrose broth for fungi. The bacterial/fungal suspension were vortexed to achieve uniform distribution. The density of bacterial/fungal suspension was measured by spectrophotometer at 625 nm and a path length of 1 cm until the obtained absorbance value was 0.08 to 0.1, which is equivalent to $1x10^{8}$ colony forming units (CFU)/ml bacteria and $1\text{-}5x10^{6}$ spores/ml fungi. The standardized suspension was further diluted 1:100 in Müller-Hinton broth to yield a colony suspension containing 1×10^{6} CFU/ml bacteria.

Final suspensions of 5×10^5 CFU/ml were used for broth dilutions. Similarly, for fungi, 1-5 x 10^6 spore or vegetative cells/ml were further diluted 1:10 in Sabouraud dextrose broth to give a colony suspension of 1-5 x 10^5 CFU/ml.

3.2.3.2 Determination of Zones of Inhibition

The *in vitro* antibacterial susceptibility test was carried out using the disc diffusion method based on the CLSI protocol (CLSI, 2012) by determining zones of inhibition produced by the test samples and comparing them with the standard drug. Two sets of dilutions of 200 µg/ml, a test sample, and ciprofloxacin dissolved in 1% DMSO were prepared in sterile McCartney bottles. Bacteria cell suspensions were adjusted to 1×10^8 bacterial/ml inoculum. Each final suspension of 5×10^5 CFU/ml bacteria was inoculated on Mueller-Hinton agar plates, and the plates were then allowed to dry for 5 minutes. Sterile filter paper discs (Whatman no. 1) of 6-mm diameter was impregnated in a stock solution (200 µg/ml) of test samples and placed on the surface of inoculated Mueller-Hinton agar plates, marked as quadrant at the back of the Petri dishes. A ciprofloxacin 200 µg disk was used as the positive control, and a 1% DMSO-soaked filter paper disk was used as the negative control. The Plates were incubated for 24 h at 37°C. After incubation, the zones of inhibition were recorded as the diameter of the growth-free zones measured in mm. The antifungal potential of the test sample at (1500 µg/ml) was screened by disc diffusion method (as described for the determination of antibacterial activity) against the fungal pathogens on Saborauds dextrose media. The Petri dishes were incubated at room temperature for 3 days and the diameter of the zone of inhibition was measured in mm. Griseofulvin was used as a reference standard.

3.2.3.3 Determination of Minimum Inhibitory Concentrations (MICs)

The MICs of the samples were determined using the broth microdilution method described by (A. Schumacher *et al.*, 2018).

Nutrient agar and Saboraud's dextrose agar were used for bacterial and fungal growth, respectively. In addition, Muller-Hinton broth (MHB) and Saborauds dextrose broth (SDB) were used for suspension. Serial dilutions of test compounds were carried out to obtain concentrations ranging from 3.125 µg/ml to 800 µg/ml and 50 to 2000 µg/ml in the 96 well plates containing 100 µl Muller-Hinton broth (MHB) and Saborauds dextrose broth for antibacterial and antifungal activity tests, respectively by dissolving the test samples in 1% DMSO. Wells were inoculated with a diluted bacterial and fungal suspension standardized to final concentration loads of 5 x 10^5 CFU/ml and 0.5-2.5 $\times 10^4$ CFU/ml for bacteria and fungi, respectively. Then, bacterial strains were incubated at 37 °C for 24 hours and 3 days for fungus. A well plate containing nutrient broth only and nutrients with microbes was incubated at the same temperature and time, serving as sterility and growth control respectively. Then a color-giving agent, 40 μL of [3-(4,5-dimethylthiazol-2-yl)-2,5-diphenyltetrazolium bromide] was added into the well plates and incubated at 37 °C for bacteria and 25 °C for fungi for 30 min. The test experiments were prepared in triplicates. The lowest concentrations at which disappearing of purple color was recorded as the MIC value of the synthesized compounds

3.2.4 *In silico* Studies of the Synthesized Compounds

3.2.4.1 Molecular Docking Study

Molecular docking analysis was conducted to assess how the synthesized compounds bind within the active sites of the target protein, utilizing the Glide module (Schrodinger Suites 2023.1), following the methodology outlined in the publication by (P. Sp *et al.*, 2022). Molecular docking comprises four key processes: Protein Preparation, Ligand Preparation, Receptor Grid Generation, and Ligand Docking (**Scheme 3**).

3.2.4.1.1 Protein Preparation

The target proteins (DNA gyrase B, PDB code: 4Z2E, and lanosterol 14α-demethylase, PDB code: 5V5Z) were retrieved in PDB format from the protein database (www.rcsb.org). The proteins were prepared and refined using the Protein Preparation Wizard module in Maestro's Schrödinger Suite. This involved adding hydrogen to heavy atoms, correcting missing side chains, assigning bonding orders, and addressing ionization and tautomer states. Water molecules were removed, and atom-confined energy minimization was conducted using the optimized potential for liquid simulation (OPLS_4) force fields. The energy minimization process concluded when the root mean square deviation (RMSD) of the heavy atoms exceeded 0.3 Å (standard)(F. Sapundzhi *et al.*, 2023, M. Mechelke and M. Habeck, 2010).

3.2.4.1.2 Ligand Preparation

All synthesized compounds were drawn using ChemDraw 2019 version 1 in structural data format (SDF). Subsequently, the ligands were prepared using the Ligprep wizard in Maestro, a component of the Schrödinger Suite. The process included 2D-to-3D conversion, tautomeric state generation, and adjustment of ring configurations at a physiological pH of 7.0 +/- 2.0, accomplished through Epik2.2. Additionally, energy minimization was conducted using the OPLS-4 force field, resulting in the generation of two and three potential stereoisomers for compounds **(37)** and **(39)**, respectively.

3.2.4.1.3 Receptor Grid Generation

The docking pocket was established through a grid array using the Glide protocol for generating the receptor grids. The grid boxes were computed in x, y and z coordinates within a specified region centering on the co-crystallized ligand, with the docked ligand restricted to a length of 6.0 Å (T. Qidwai, 2016).

3.2.4.1.4 Glide Extra Precision (XP) Ligand Docking

Molecular docking analysis was performed by utilizing standard parameters, specifically the Glide protocol, employing an extra-precision (XP) docking module. The final score was determined by assessing the placement of the docked ligand within the receptor's active site. The interpretation of docking results took into account factors such as the docking score, the count of hydrogen bonds, and pi interactions. Ligands with lowest docking score was considered favorable.

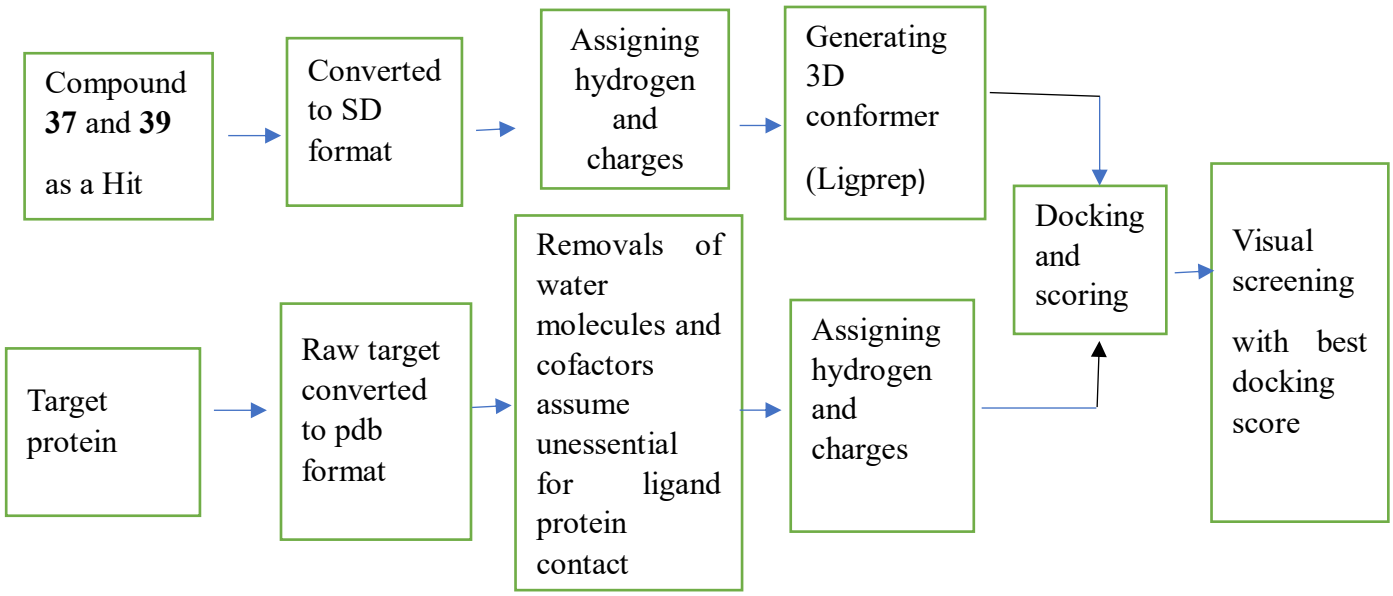

Scheme 3: Flowchart of a target-based molecular docking procedure and analysis

3.2.4.2 Pharmacokinetics and Drug-likeness Properties

The molecular structures of compounds **(37)** and **(39)** were examined using the Qikprop within Schrödinger Suite 2023 version 1 to assess whether each synthesized compound adheres to Lipinski's rule of five. ADMET descriptor algorithms of the Qikprop prediction protocol were employed to analyze the pharmacokinetic properties of the synthesized compounds. The outcome of these analyses offers insights into the drug-likeness and oral bioavailability of the synthesized compounds.

4. RESULT AND DISCUSSION

4.1 Synthesis of 2-naphthol Derivatives

The growing interest in 1-aminoalkyl-2-naphthol derivatives is attributed to their diverse biological activities and their role in preparing other bioactive compounds, including aminoalkyl naphthols and oxazines. Specifically, the synthesis involves a one-pot multicomponent Mannich-type reaction.

4.1.1 Synthesis of Aminoalkyl Derivative of 2-naphthol (37)

Compound **37** was synthesized through a Mannich-type reaction in a one-pot condensation involving 2-naphthol, benzaldehyde, and O-toluidine in the presence of a Lewis acid ($ZnCl_2$) catalyst. The reaction mechanism is comprised of multiple steps.

Step 1: The carbonyl oxygen of benzaldehyde undergoes an acid-base reaction with the Lewis acid $ZnCl_2$. This forms a strong coordination bond, enhancing the electrophilicity of the carbonyl carbon and activating the carbonyl carbon for increased reactivity in chemical reactions.

Step 2: Imine formation through a nucleophilic addition reaction where O-toluidine reacts with the carbonyl group of benzaldehyde.

Step 3: The electrophilic aromatic substitution reaction involves 2-naphthol reacting with an imine to produce the 1-aminoalkyl derivative of 2-naphthol (the reaction mechanism is depicted in Scheme 4)

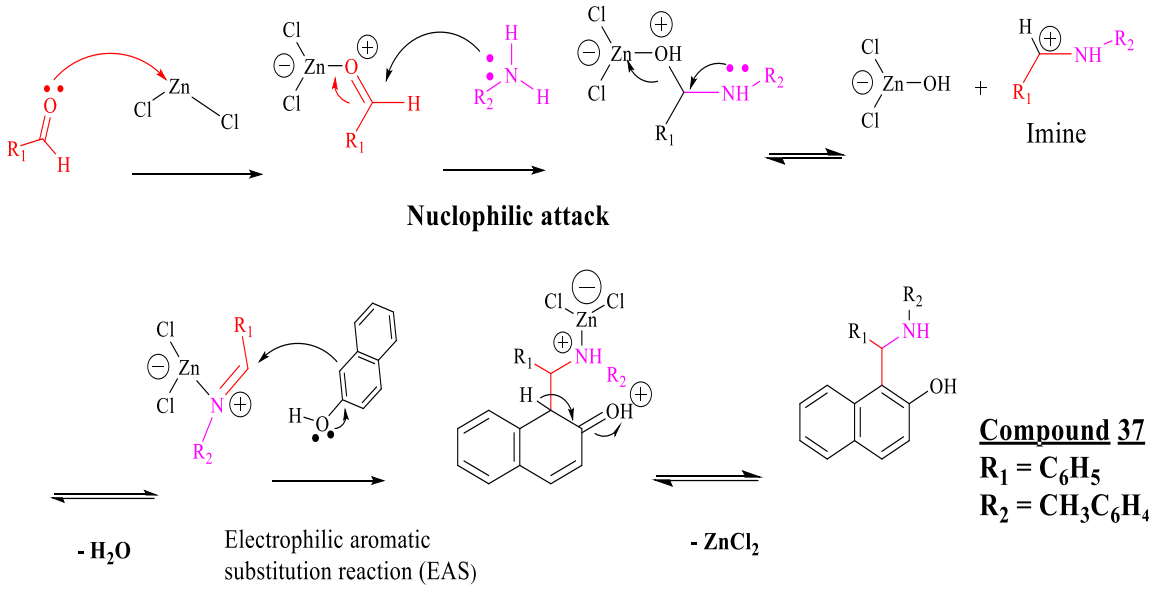

Scheme 4: The proposed reaction mechanism for the synthesis of 1-(phenyl(ortho-tolylamino) methyl) naphthalene-2-ol (**37**)

4.1.2 Synthesis of 1,3-oxazine Derivative of 2-naphthol (39)

Compound 39 was synthesized through a one-pot condensation reaction that involved 2-naphthol (5 mmol), formaldehyde (10 mmol), and benzylamine (5 mmol) in the presence of a $ZnCl_2$ catalyst. The synthesis process followed a mechanism similar to that described for compound (**37**). Subsequently, the intermediate aminoalkyl-2-naphthol derivative (**38**) was subjected to heating with an excess of formaldehyde in absolute ethanol, leading to ring closure and the formation of 1,3-oxazine derivatives of 2-naphthol.

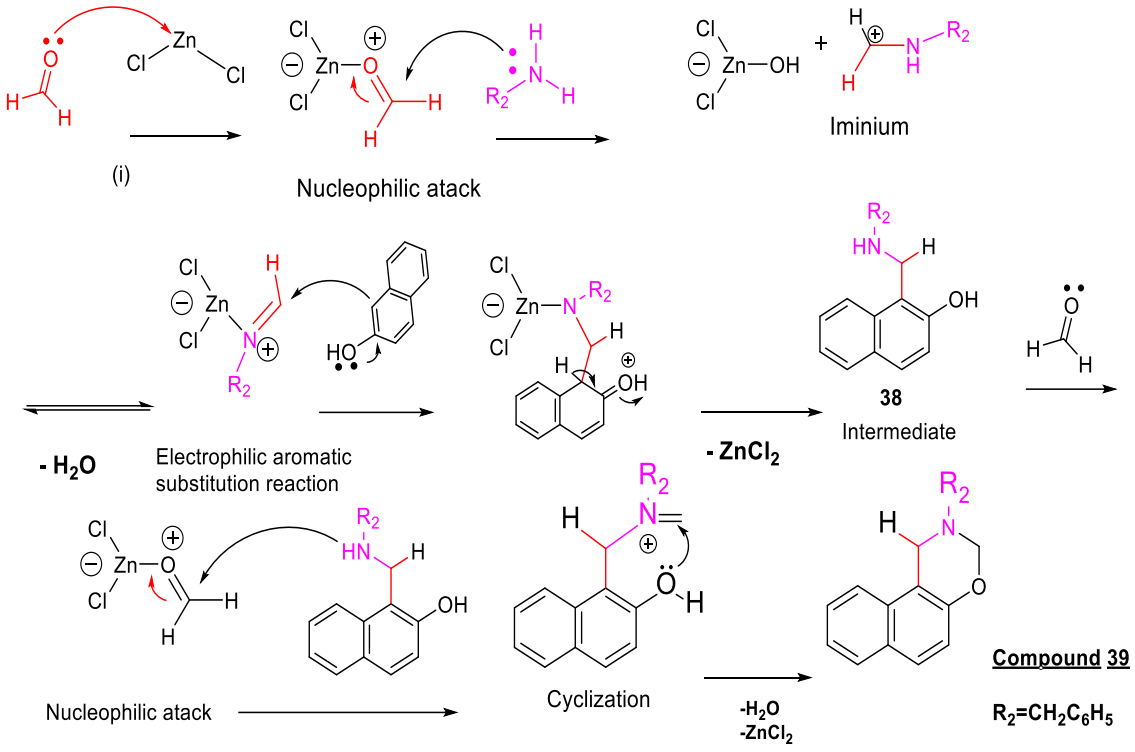

Scheme 5: The proposed reaction mechanism for the synthesis of 2-benzyl-2,3-dihydro-1H-naphtho[1,2-e] [1,3]oxazine (**39**)

4.2 Structural Elucidation

The structural elucidation of the synthesized compounds (**37**) and (**39**) was achieved by utilizing ^{1}H, ^{13}C, DEPT-90, and DEPT-135 NMR spectral data.

4.2.1 Structural Elucidation 1-(phenyl(*o*-tolylamino)methyl)naphthalene-2-ol (37)

Compound 37 was successfully synthesized via a three-component condensation reaction of benzaldehyde, O-toluidine, and 2-naphthol in the presence of a $ZnCl_2$ catalyst, yielding white crystals (0.88 mmol, 44.3% w/w). The compound exhibited an Rf value of 0.5 on TLC when hexane/EtOAc (1:1) was used as the mobile phase.

The ^{1}H-NMR spectrum of compound 37 revealed a broad singlet signal at δ11.41, indicative of a chelated aromatic hydroxyl (1H, brs, Ar-OH).

Additionally, a singlet at δ4.07 (s, 1H, Ar2-CN) suggested the presence of a benzylic methine, confirming the formation of an alkylamino group. This was further supported by a signal at δ62.32 in the ^{13}C-NMR spectrum. In the ^{1}H-NMR spectrum, a singlet signal resonating at δ6.25 was indicative of the existence of a secondary amine group (1H, R_2 NH), supporting the formation of a secondary alkylamino group. The presence of a monosubstituted benzyl group originating from benzaldehyde was also noted.

The structural analysis of compound (**37)** was also consistent with the ^{13}C-NMR, DEPT-90, and DEPT-135 spectral data, indicating the presence of 24 carbon atoms, including sixteen methines (one sp^3 and fifteen sp^2 methines), one methyl carbon, and seven quaternary carbons. The chemical shifts of all protons and carbons in the ^{1}H and ^{13}C-NMR spectra of compound 37 are summarized in Table 1.

Table 1: ^{1}H and ^{13}C NMR data of compound 37

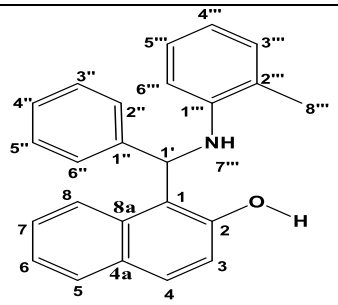

Compound 37

Position	^{13}C NMR δC (ppm)	^{1}H NMR δH (ppm)
1, 2, 4a, 8a, 1", 1'"	113.85, 156.36, 130.46, 131.67, 141.27, 144.91	
3	114.49	7.15 (d, J = 8.7 Hz, 1H, C-H 3)
4	129.26	7.87 – 7.73 (3H, m, C-H 4, 5, 8)
5	130.12	
6	123.01	

7	127.71	7.54 – 7.47 (2H, m, C-H 6, 7)
8	125.09	
2-OH	-------	11.41 (1H, brs, Ar-OH)
1'	62.32	4.07 (s, 1H, Ar2-NH)
7'''-NH	------	6.25 (s, 1H, C-NH -Ar)
2 '''	121.51	
3 '''	129.19	7.15 (d, J = 8.7 Hz, 1H, C-H 3''')
4'''	121.65	6.88 (td, 1H, J = 7.4, 1.2 Hz, C-H 4''')
5'''	128.74	6.98 (1H, td, J = 7.7, 1.7 Hz, C-H 5''')
6'''	120.13	6.72 (1H, dd, J = 8.1, 1.3 Hz, C-H 6''')
2'', 3'', 4'', 5'', 6''	128.16, 129.61, 126.98, 129.61, 128.16	7.46 – 7.28 (m, 5H, C-H 2'', 3'', 4'', 5'', 6'')
8'''	18.00	2.24 (3H, s, Ar-CH_3)

Ar = aromatic, ppm = parts per million, s = singlet, d = doublet, t = triplet

4.2.2 Structural Elucidation of 2-benzyl-2,3-dihydro-1H-naphtho[1,2-e][1,3]oxazine (39)

Compound 39 was obtained in the form of white crystals (3.52 mmol, 70.5% w/w yield), and its Rf value on TLC using hexane/EtOAc (2:1) as the mobile phase was 0.6. The ^{1}H-NMR spectrum of compound 39 revealed two important methylene signals at δ4.97 (s, 2H, O–CH_2 –N, C-H 3) and δ4.34 (s, 2H, -Ar–CH_2 –N, C-H 1), confirming the formation of a tri-substituted 1,3-oxazine group. This was further supported by signals at δ82.21 and δ47.42 in the ^{13}C-NMR spectrum. Additionally, benzyl methylene adjacent to the amine group was suggested by a singlet signal at δ4.00 (s, 2H, -Ar-CH_2 -N, H-**7'**). The presence of a mono-substituted benzyl group originating from benzylamine was also observed.

In the ^{13}C-NMR spectrum together with DEPT-90 and DEPT-135, compound 39 displayed nineteen signals corresponding to nineteen carbon atoms, including eleven sp^2 methines, three sp^3 methylene carbons, and five quaternary carbon atoms. The complete assignment of all protons and carbons can be found in Table 2.

Table 2**:** ^{1}H and ^{13}C NMR data of compound (39)

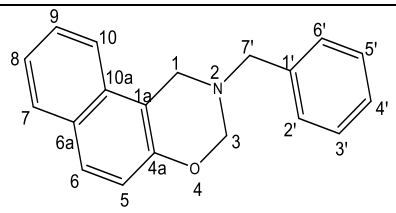

Compound 39

Position	^{13}C NMR δC (ppm)	^{1}H NMR δH (ppm)
1	47.42	4.34 (s, 2H, -Ar-CH_2-N)
1a	111.84	
3	82.21	4.97 (s, 2H, O-CH_2-N)
4a	151.90	
5	118.4	7.69 (d, *J* = 8.9 Hz, 1H, 5)
6	128.18	7.11 (dd, *J* = 8.9, 0.9 Hz, 1H, 6)
6a	132.09	
7	128.78	7.55 (dt, *J* = 8.4, 1.1 Hz, 1H, 7)
8	123.62	7.50 – 7.28 (m, 2H, 8, 9)
9	126.63	
10	121.24	7.80 (dd, *J* = 8.9, 1.3 1H, 10)
10a	129.14	
1'	138.42	
2' and 6'	129.14	7.50 – 7.28 (m, 5H, 2'-6')
3' and 5'	128.64	
4'	127.56	
7'	56.25	4.00 (s, 2H, -Ar-CH_2-N)

Ar= aromatic, s = singlet, d = doublet, t = triplet, m = multiplet

4.3 Antimicrobial Activity

4.3.1 Antibacterial Activity

Using disk diffusion and broth dilution methods, we assessed the *in vitro* antibacterial activity of 1-(phenyl(o-tolylamino)methyl)naphthalene-2-ol (**37**) and 2-benzyl-2,3-dihydro-1H-naphtho[1,2-e][1,3]oxazine (**39**) as described (R. M. Humphries *et al.*, 2018).

Table 3 presents the ZOI and MIC values for compounds (**37**) and (**39)** against three Gram-positive bacteria (*B. pumilus*, *B. subtilis*, and *S. aureus*) and twenty Gram-negative bacteria, including ten strains of *E. coli*, two strains of *Salmonella*, four strains of *Shigella*, four strains of *V. cholera*, and three multi-drug resistant strains.

Our findings revealed that both compounds exhibited comparable but variable inhibitory activities against most tested bacterial strains, with MIC values ranging from 25 µg/ml to 200 µg/ml. The overall inhibitory effectiveness of compounds (**37)** and (**39)** against the tested Gram-negative bacteria is particularly notable, with compound (**37)** demonstrating the lowest MIC value of 25 µg/ml against most tested strains of *E. coli*

Despite the extra lipopolysaccharide layer forming a hydrophobic permeability barrier in Gram-negative bacteria, which typically contributes to antibiotic resistance, both compounds (**37)** and (**39)** showed strong antibacterial activity against Gram-negative bacteria like *E. coli* and *V. cholera*, with a MIC value of 25-50 µg/ml. And, their activity against *Salmonella* and *Shigella* species was relatively weak, with MICs ranging from 100-200 µg/ml. However, Gram-positive *Bacilli* (*B. pumilus* and *B. subtilis*) displayed high resistance to both compounds, evident by a zone of inhibition (ZOI) of 6.0 mm at a concentration of 200 µg/ml. Furthermore, compound (**37)** exhibited inhibitory activity against drug-resistant *S. aureus* (*S. aureus MDR 1** and *S. aureus MDR 2*)* in a pattern similar to that of susceptible strains.

In conclusion, these findings suggest that both compounds **(37)** and **(39)** could possess the potential to combat diseases caused by Gram-negative bacteria as well as multi-drug resistance bacterial strains.

Table 3**:** ZoIs and MICs of the synthesized compounds against 26 bacterial strains.

Bacterial strains	ZoI (200 µg/ml) [a]			MIC (µg/ml) [b]	
	Compound			Compound	
	37	39	Cipr	37	39
Bacillus pumilus 82	6.0	6.0	19.0	ND	ND
B. subtilis ATCC 6633	6.0	6.0	18.0	ND	ND
Escherichia coli 3:37C	15.5	14.5	16.5	25	50
E. coli 872	14.5	14.0	16.0	25	50
E. coli CD/99/1	14.5	14.0	17.0	25	50
E. coli K88	15.0	13.5	17.0	25	50
E. coli LT37	14.5	13.5	16.0	25	50
E. coli NCTC 5933	14.0	13.0	16.0	25	50
E. coli NCTC 7360	14.5	13.5	17.0	25	50
E. coli ROW 7/12	15.0	14.0	16.5	25	50
E. coli HB101	13.0	12.0	14.0	50	200
E. coli C600	12.5	11.5	13.5	50	200
Salmonella enterica TD 01	13.5	13.5	19.0	100	100
S. typhi Ty2	13.5	13.5	16.0	100	200
Shigella boydii D 13629	12.0	12.0	20.0	200	200
S. dysentery 8	11.5	11.5	20.0	200	200
S. flexneri Type 6	12.0	12.0	20.5	200	200
S. soneii 1	13.0	13.0	19.5	200	200
Staphylococcus aureus ML 267	13.5	13.5	18.0	50	50
Vibrio cholerae NCTC 10732	14.5	14.5	19.0	50	50
V. cholera NCTC 11501	14.5	14.5	18.5	50	50
V. cholerae NCTC 4693	14.0	14.0	17.5	50	50
V. cholerae NCTC 5596	14.5	14.5	18.5	50	50
*Pseudomonas aeruginosa MDR 1**	10.5	10.5	12.5	100	100
*S. aureus MDR 1**	10.5	10.0	11.5	50.0	200.0
*S. aureus MDR 2**	11.5	11.5	12.0	50.0	200.0

[a] Zones of inhibition measured including 6 mm diameter of the disc, b = triplicate, Cipro= Ciprofloxacin, ND= Not determined, MDR= multidrug resistance

4.3.2 Antifungal Activity

Table 4 presents the results of antifungal activity studies for compounds **(37)** and **(39)** against four fungal species (*A. niger*, *C. albicans*, *P. funiculosum*, and *P. notatum*).

Our study revealed a notable sensitivity of the tested fungal species to both compounds, with MIC values ranging from 800 to 1500 µg/ml. Among the tested fungal species, *C. albicans, A. niger, and P. notatum* demonstrated similar susceptibility to both compounds **(37)** and **(39)**, exhibiting a ZOI of 13.0 mm, 12.0 mm, and 12.5 mm, respectively, and a consistent MIC of 800 µg/ml each. However, *P. funiculosum* displayed weaker sensitivity (MIC = 1500 µg/ml) compared to the other tested fungal species. The standard drug griseofulvin demonstrated comparable ZOIs to the synthesized compound at 1500 µg/ml. Both compounds **(37)** and **(39)** have the potential to address diseases caused by *C. albicans* and *A. niger*, the main species responsible for invasive oral or vaginal candidiasis, and aspergillosis (F. Bongomin *et al.*, 2017), respectively.

Table 4**:** ZOIs and MICs of the synthesized compounds against four fungal species

Fungal strains	ZoI (1500 µg/ml) [a]			(MIC µg/ml) [b]	
	Compound			Compound	
	37	39	Gris	37	39
Aspergillus niger ATCC 6275	13.0	13.0	14.0	800	800
Candida albicans ATCC 10231	12.0	12.0	15.0	800	800
Penicillium funiculosum NCTC 287	10.0	11.0	13.0	1500	1500
P. notatum ATCC 11625	12.5	12.5	13.0	800	800

[a] Zones of inhibition measured including 6 mm diameter of the disc; b = triplicate, Gris = Griseofulvin

4.4 *In silico* Studies of the Synthesized Compounds

4.4.1 Molecular Docking Study

In pharmaceutical research, the utilization of structure-based drug design through molecular docking stands as an advanced and crucial technique. Molecular docking is a process that attempts to define the native position, orientation, and conformation of the ligand molecule within the active site of the target molecule using computer-based programs. These programs typically work by calculating energy grids and flexibly generating ligand binding "poses" (J. De Ruyck *et al.*, 2016).

This approach, as outlined by Shoichet et al., focuses on accurately predicting the binding interactions between receptor and ligand molecules objectively to identify potential lead compounds (B. K. Shoichet *et al.*, 2002).

In this study, our specific choice of *E. coli* DNA gyrase B (PDB: 4z2e) and *C. albicans* lanosterol 14α-demethylase (PDB: 5v5z) as a potential target for molecular docking was based on an assessment of the structural features of the synthesized compounds and preliminary docking analysis. Similarly, the well-known inhibitors ciprofloxacin and voriconazole were docked to validate the docking protocol against DNA gyrase B of *E. coli* and lanosterol 14α-demethylase of *C. albicans* respectively. The docking scores for the synthesized compounds and the standards are presented in Table 5, where a more negative score indicates a stronger binding between the ligand and its target.

DNA gyrase B enzyme plays a crucial role in introducing negative supercoils and relieving topological strain in an ATP-dependent manner during DNA replication (K. Drlica and X. Zhao, 1997). Interestingly, compounds (**37)** and (**39)** demonstrated effective docking score with *E. coli* DNA gyrase B (PDB: 4z2e) with docking scores of -8.092 and -7.754 kcal/mol, respectively.

In comparison, ciprofloxacin exhibited a docking score of -13.37 kcal/mol. The corresponding results are graphically depicted in Figures 6 and 7 and summarized in Table 5.

Table 5: Docking score, hydrogen bond, and hydrophobic interactions of compounds (**37)** and (**39)** against the binding site of DNA gyrase B (4z2e) and 14α-demethylase (5v5z)

PDB code	Compound	DS kcal/mol	Interacting residue of the target		
			RIHB	Residue	Types of interaction
4z2e	37	-8.092	DA; H_2	DG; H_1, DT; E_{15}, DA; F_5 (2x)	4 PPI
	39	-7.754	----------	Glu 475[b], DA; F_5[a], DG; H_1 ,	Sb[a], PcI[b], 2 PPI[c]
	Ciprofloxacin	-13.37		GLU 475[a], Mg; H_{102}[a], DA; F_4[b], DG;H_1[b]	4 Sb[a], 4 PPI[c]
5v5z	37	-7.792	-------	Hydrophobic interaction	……..
	39	-8.995	SER 378	TYR 118[c], HIE 377[b], PHE[b] 380	1PPI[c], 2PcI[b]
	Voriconazole	-8.476	SER 378	TYR 118, HIE 377	2PPI[c]

DS Dockin Score = RIHB = Residue involved in a hydrogen bond, [a]Salt bridge, [b]Pi cation interaction, [c]Pi pi interaction

It is evident that compound (**37)** demonstrated best docking score (-8.092 kcal/mol) at the binding site of *E. coli* DNA gyrase B. Figure 6 illustrates the 2D and 3D interaction between compound (**37)** and various residue *E. coli* DNA gyrase B. Compound 39 also displayed strong binding interactions with various residues of DNA gyrase B with docking score of (-7.754 kcal/mol), forming salt bridges with GLU 475 and participating in π-to-π interactions (Figure 7). Notably, both synthesized compounds displayed a strong binding affinity with *E. coli* DNA gyrase B, comparable to ciprofloxacin. The 2D and 3D interaction between ciprofloxacin and *E. coli* DNA gyrase B is depicted in Appendix 8.3.

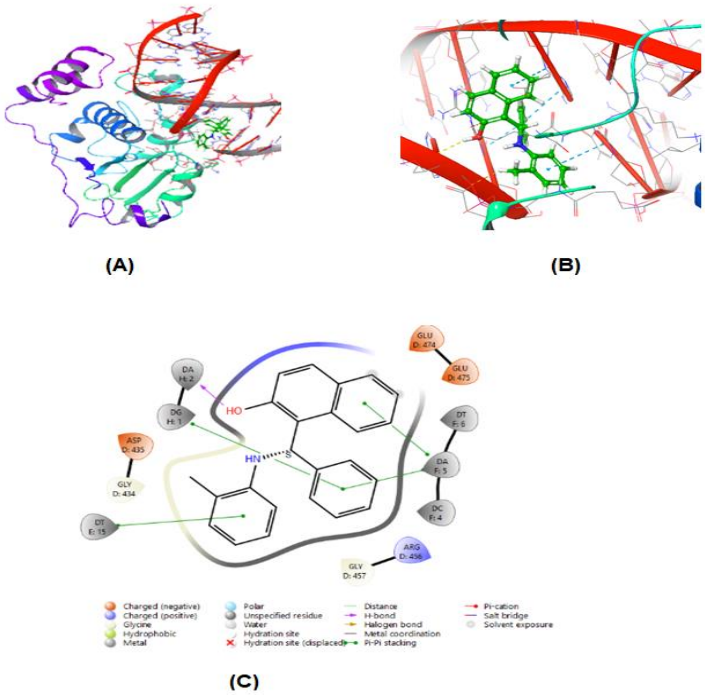

Figure 6: (A): 3D model, (B): 3D model zoomed, and (C): 2D presentation of binding interaction of compound **3**7 with the residues of *E. coli* DNA gyrase B

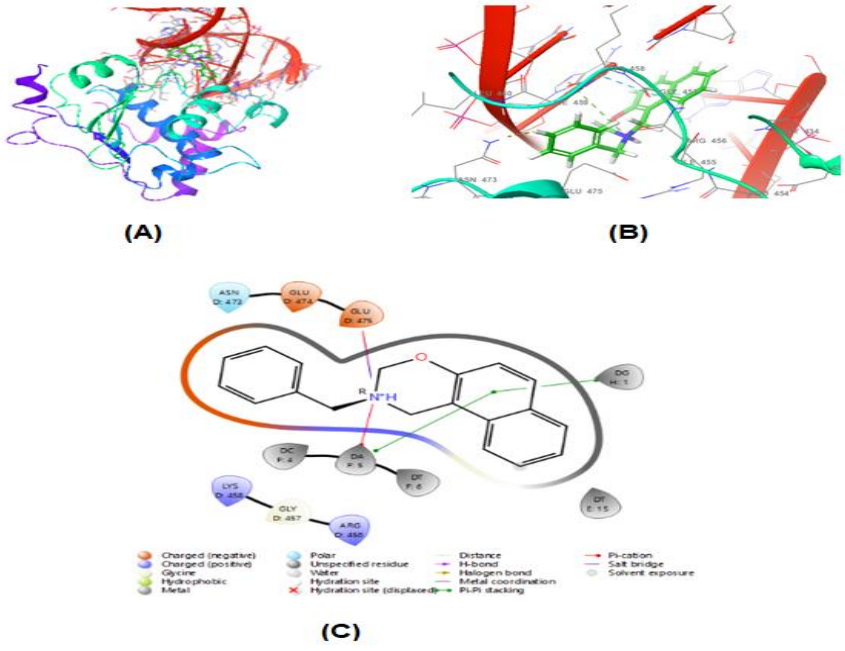

Figure 7: (A): 3D model, (B): 3D zoomed model (C): 2D binding interactions of compound 39 against the residues of *E. coli* DNA gyrase B

The fungal lanosterol 14α-demethylase (PDB: 5v5z) was selected as a prospective target for molecular docking involving compounds (**37)** and (**39)**, based on preliminary docking tests. Both compounds were subjected to docking in the active site of *C. albicans* 14α-demethylase and compared against clinical standards voriconazole. The findings are presented in Table 5 and depicted in Figures 8 and 9.

Interestingly, compound (**39)** demonstrated strong binding affinity to *C. albicans* 14α-demethylase, with a molecular docking score of -8.995 kcal/mol, surpassing the interaction observed with the reference molecule, voriconazole (-8.476 kcal/mol). Compound (**39)** formed a hydrogen bond with the SER 378 amino residue of *C. albicans* 14α-demethylase (Figure 9). On the other hand, compound 37 exhibited a docking score of -7.792 kcal/mol, primarily engaging in hydrophobic interactions within the binding pockets of *C. albicans* Lanosterol 14α-demethylase (Figure 8).

Overall, the molecular docking results from this study suggest that the aminoalkyl and oxazine derivatives 2- naphthol (compound **37** and **39**) observed as an inhibitor of *E. coli* DNA gyrase B and *C. albicans* Lanosterol 14α-demethylase potentially serve as lead molecules for further optimization and could be considered as candidates for further exploration as antimicrobial agents.

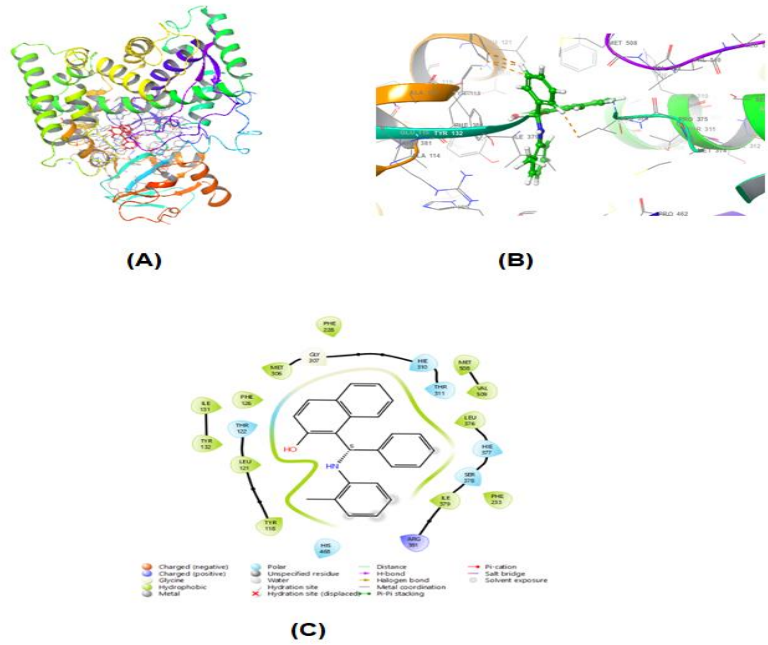

Figure 8: (A): 3D representation, (B): 3D zoomed view, (C): 2D model of compound 37 docking interactions against the residue of *C. albicans* lanosterol 14α-demethylase (5v5z)

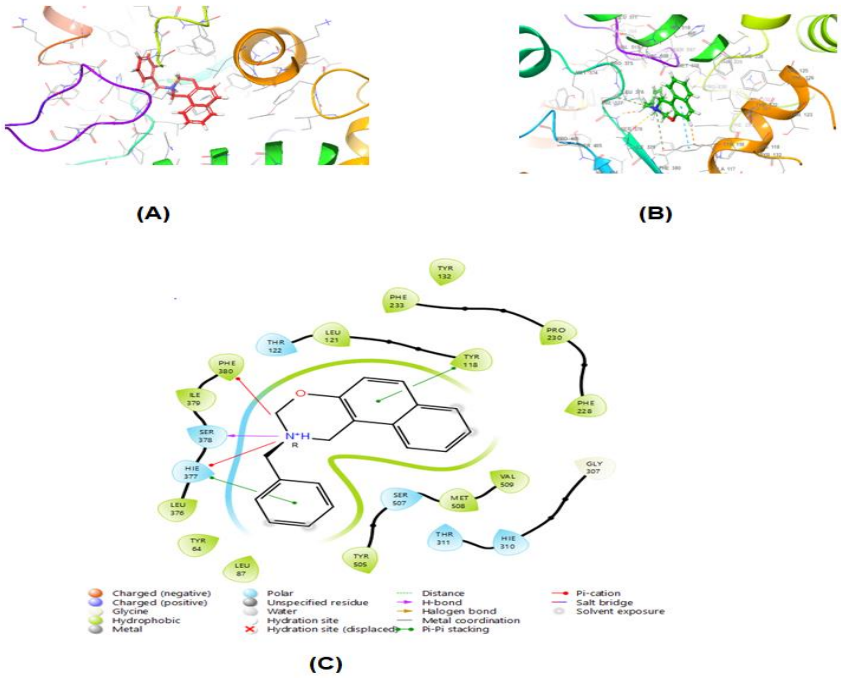

Figure 9: (A): 3D model, (B): 3D zoomed view, (C): 2D model of compound 39 docking interactions against the residue of *C. albicans* lanosterol 14α-demethylase (5v5z)

4.4.2 ADMET Predictions of the Synthesized Compounds

Utilization of virtual screening software for predicting pharmacokinetic and physicochemical characteristics is very crucial for the design and optimization of bioactive compounds (T. Qidwai, 2016). The QikProp software, a component of the Schrodinger module, was employed to predict the pharmacokinetic and physicochemical characteristics of compounds (**37)** and (**39**) within the biological system. Similarly, the well-known standard drugs (ciprofloxacin and voriconazole) were utilized for validation purposes. Drug-likeness and oral bioavailability of the compounds were predicted and compared following Lipinski's rule of five (C. A. Lipinski *et al.*, 1997).

The ADMET analysis revealed that 2-benzyl-2,3-dihydro-1H-naphtho[1,2-e][1,3]oxazine (**39**) complies with all parameters of Lipinski's rule. However, 1-(phenyl(*o*-tolylamino) methyl) naphthalene-2-ol (**37**) violates Lipinski's rule due to the partitioning of octanol to water (logP) falling above the normal range (Table 6).

The pharmacokinetic (ADMET) properties of compounds (**37)** and (**39)** were predicted against various parameters, including apparent Caco-2 permeability (colon carcinoma cell), the rule of 5 (number of Lipinski rule violations), blood-brain barrier permeability, water solubility (QPlogS), and QplogHERG (IC_{50} prediction for blocking HERGK+ - human ether-a-go-go gene). The summary of these predictions is presented in Table 6.

Both compounds fell within the recommended range for most parameters, except for the IC_{50} for blocking HERG-K+ channels (QPlogHERG), which was below -5 for both the synthesized compounds. Notably, Table 6 indicates that both compounds (**37)** and (**39)** exhibit excellent absorption in human intestinal tissue, enhanced permeability in Caco2 cell lines, and a high likelihood of crossing the blood-brain barrier.

Table 6: ADMET data of the synthesized compounds

S. N	Descriptors	Predicted values		Reference		Recommended value
		37	39	Cpr	Vori	
1.	Molecular weight	339.436	275.349	331.346	349.315	<500
2.	HB donor	2.000	0.000	1.000	1.000	≤ 5
3.	HB acceptor	2.000	2.750	6.000	6.250	≤ 10
4.	PlogP o/w	5.479*	3.788,	0.280	3.000	≤ 5
5.	PlogS (Aquas solubility)	-5.333	-3.074,	-3.790	-3.705	-6.5/ 0.5
6.	logKhsa (albumin binding)	0.855	0.410	0.043	-0.117	-1.5/1.5
7.	%HOA	100	100	48.000	100	>80 %[a], < 25%[b]
8.	PlogHERG	-6.313*	-6.418*	-3.407	-5.000	> -5
9.	PlogBB, brain/blood	0.103	0.830	-0.722	-0.402	-3/1.2
10	QPPCaco-2	2403	6774	12	1229	<25%[a] ,>500%[b]

PlogBB = brain/blood partition coefficient, %HOA = percent of human oral absorption, Cpr = Ciprofloxacin, Vori = Voriconazole, *Indicates deviation from recommended value, a = poor, b = good

The rapidly increasing resistance of microorganisms, both bacteria, and fungi, to available treatments is a global medical challenge of high priority (WHO, 2021). The emergence of multidrug-resistant organisms, notably *S. aureus,* and *E. coli*, is a pressing issue demanding attention. Addressing this challenge requires the development of antimicrobials with distinct modes of action to counteract multidrug resistance. Research has indicated that positions one and two in the 2-naphthol heterocyclic ring are crucial targets for various reactions, leading to the synthesis of biologically active compounds. In response, we designed and synthesized aminoalkyl and 1,3-oxazine 2-naphthol derivatives with potential biological activity.

In our study, the synthesized compounds **(37)** and **(39)** exhibited promising antimicrobial activities against several tested bacterial and fungal strains.

Our findings align with previous reports on molecules (**22-24**) derived from 2-naphthol scaffolds, showing strong antimicrobial activity (MIC=32-256 µg/ml) (G. Şahin *et al.*, 2002).

Additionally, a study by Jasim and Mustafa highlighted the significant efficacy of 2-naphthol derivatives, specifically compound (**17)**, against *E. coli*, *S. typhi*, and *S. dysentery*, with MIC values of (1.4, 1.95, and 1.85 µg/ml), respectively (S. F. F. Jasim and Y. F. Mustafa, 2022). Despite the additional lipopolysaccharide layer forming a hydrophobic permeability barrier in Gram-negative bacteria such as *E. coli* and *V. cholera*, which typically restricts the diffusion of antibiotics (A. H. Delcour, 2009), it is interesting that both *E. coli* and *V. cholera* exhibited susceptibility to compounds (**37)** and (**39)**, with a MIC value of (25-50) µg/ml. This observation is in line with a prior study by Göksu et al., where 5,6-dimethoxynaphthalene-2-carboxylic acid **(25a)** and 5-bromo-6-methoxynaphthalene-2-carboxylic acid (**25b**) derived from the 2-naphthol scaffold demonstrated significant activity against Gram-negative bacterial strains (S. Göksu *et al.*, 2005). Furthermore, a notable finding in our study is that resistant strains including *S. aureus* exhibited susceptibility to compound (**37)** and *MDR Pseudomonas aeruginosa* to both the synthesized compounds. This suggests a significant potential for compounds (**37)** and (**39)** in combating multi-drug-resistant microbes.

In the molecular docking analysis, both synthesized compounds demonstrated strong binding affinity within the active site of the bacterial DNA gyrase B enzyme, a potential target for various antibacterial drugs. Similarly, both compounds exhibited favorable interactions within the active site of lanosterol 14α-demethylase in *C. albicans*. However, it is crucial to experimentally validate the strong binding nature of compounds (**37)** and (**39)**. Furthermore, in the ADMET analysis, both synthesized compounds displayed favorable pharmacokinetics and drug-like characteristics, suggesting their suitability for oral administration.

In summary, the results from the *in vitro* bioassay activity test, molecular docking analysis, and ADMET predictions collectively affirm the promising antimicrobial properties of both synthesized compounds. These findings highlight the potential benefits of further synthesis and evaluation of 2-naphthol derivatives in the ongoing efforts to develop antimicrobial drugs for combating infectious diseases and microbial resistance.

5. CONCLUSION

Antimicrobial resistance, both bacteria and fungi, to available treatments is a global medical challenge of high priority. One effective strategy to address this challenge involves synthesizing compounds with antimicrobial properties. In this study, Aminoalkyl and Oxazine of 2-naphthol derivatives were successfully synthesized using a 2-naphthol framework through a Mannich-type condensation reaction. The synthesized compounds showed promising antibacterial and antifungal activity. The molecular docking result reveals that both the synthesized compounds displayed better interaction with the target protein. ADMET analysis indicates both compounds comply with most parameters of Lipinski's rule. Overall, aminoalkyl and oxazine derivatives of 2-naphthol hold great potential as lead compounds in the development of novel antimicrobial drugs to tackle the growing threat of infectious diseases and antimicrobial resistance. These results also suggest the need for further investigation to synthesize additional 2-naphthol derivatives to evaluate their antimicrobial potential.

6. RECOMMENDATIONS

Based on the present findings, the following recommendations are suggested:

- Acute toxicity studies need to be performed
- *In vivo* antimicrobial studies have to be carried out
- Binding nature (mechanism of actions) needs to be validated experimentally

7. REFERENCES

Abubakar, I., Tillmann, T. & Banerjee, A. 2015. Global, regional, and national age-sex specific all-cause and cause-specific mortality for 240 causes of death, 1990-2013: a systematic analysis for the Global Burden of Disease Study 2013. *Lancet,* **385 (**9963**):** 117-171.

Ali, I. A., Al-Masoudi, I. A., Saeed, B., Al-Masoudi, N. A. & La Colla, P. 2005. Amino acid derivatives, part 2: Synthesis, antiviral, and antitumor activity of simple protected amino acids functionalized at N-terminus with naphthalene side chain. *Heteroatom Chemistry,* **16 (**2**):** 148-155.

Azarifar, D. & Shaebanzadeh, M. 2002. Synthesis and characterization of new 3, 5-dinaphthyl substituted 2-pyrazolines and study of their antimicrobial activity. *Molecules,* **7 (**12**):** 885-895.

Bala, S., Sharma, N., Kajal, A. & Kamboj, S. 2014. Mannich bases: an important pharmacophore in present scenario. **2014:** 191072.

Betti, M. 1900. General condensation reaction between β-naphthol, aldehydes and amines. *Gazz. Chim. Ital,* **30:** 310-316.

Betti, M. 2003. β-Naphthol Phenylaminomethane: 2-Naphthol, 1-(α-aminobenzyl)-. *Organic Syntheses,* **9:** 60-60.

Bongomin, F., Gago, S., Oladele, R. O. & Denning, D. W. 2017. Global and Multi-National Prevalence of Fungal Diseases-Estimate Precision. *J Fungi (Basel),* **3 (**4**):**

Brown, E. D. & Wright, G. D. 2005. New targets and screening approaches in antimicrobial drug discovery. *Chemical reviews,* **105 (**2)**:** 759-774.

Brown, G. D., Denning, D. W., Gow, N. A., Levitz, S. M., Netea, M. G. & White, T. C. 2012. Hidden killers: human fungal infections. *Sci Transl Med,* **4 (**165)**:** 165rv113-165rv113.

Cardellicchio, C., Capozzi, M. A. M. & Naso, F. 2010. The Betti base: the awakening of a sleeping beauty. *Tetrahedron: Asymmetry,* **21 (**5)**:** 507-517.

Chang, F.-Y., Peacock Jr, J. E., Musher, D. M., Triplett, P., MacDonald, B. B., Mylotte, J. M., O'Donnell, A., Wagener, M. M. & Victor, L. Y. 2003. Staphylococcus aureus bacteremia: recurrence and the impact of antibiotic treatment in a prospective multicenter study. *Medicine,* **82 (**5)**:** 333-339.

Chopde, H. N., Meshram, J. S., Pagadala, R. & Mungole, A. J. 2010. Synthesis, characterization and antibacterial activity of some novel azo-azoimine dyes of 6-bromo-2-naphthol. *Int. J. Chem. Tech. Res,* **2 (**3)**:** 1823-1830.

CLSI (2012). Methods for dilution antimicrobial susceptibility tests for Bacteria that grow aerobically; aproved standard-Ninth Edition. CLSI document M07-A9.

Coates, A., Hu, Y., Bax, R. & Page, C. 2002. The future challenges facing the development of new antimicrobial drugs. *Nat Rev Drug Discov,* **1 (**11)**:** 895-910.

Collin, F., Karkare, S. & Maxwell, A. 2011. Exploiting bacterial DNA gyrase as a drug target: current state and perspectives. *Appl Microbiol Biotechnol,* **92 (**3)**:** 479-497.

Cowen, L. E., Sanglard, D., Howard, S. J., Rogers, P. D. & Perlin, D. S. 2015. Mechanisms of antifungal drug resistance. *Cold Spring Harbor perspectives in medicine,* **5 (**7**):**

Dadgostar, P. 2019. Antimicrobial Resistance: Implications and Costs. *Infection and Drug Resistance,* **12 (**null**):** 3903-3910.

De Ruyck, J., Brysbaert, G., Blossey, R. & Lensink, M. F. 2016. Molecular docking as a popular tool in drug design, an in silico travel. *Advances and Applications in Bioinformatics and Chemistry***:** 1-11.

Delcour, A. H. 2009. Outer membrane permeability and antibiotic resistance. *Biochim Biophys Acta,* **1794 (**5**):** 808-816.

Drlica, K. & Zhao, X. 1997. DNA gyrase, topoisomerase IV, and the 4-quinolones. *Microbiology and molecular biology reviews,* **61 (**3**):** 377-392.

Duchin, K. L., Vukovich, R. A., Dennick, L. G., Groel, J. T. & Willard, D. A. 1980. Effects of nadolol β-blockade on blood pressure in hypertension. *Clinical Pharmacology & Therapeutics,* **27 (**1**):** 57-63.

Gamit, K. G. & Patel, N. B. 2023. Synthesis and in Vitro Biological Activity Study of Novel Phenol Mannich Base Analogs Containing Spiroheterocycle as Core Compound. *European Journal of Advanced Chemistry Research,* **4 (**3**):** 60-65.

Georgopapadakou, N. 1993. Penicillin-binding proteins and bacterial resistance to beta-lactams. *Antimicrob Agents Chemother,* **37 (**10**):** 2045-2053.

Gohil, N., Ramírez-García, R., Panchasara, H., Patel, S., Bhattacharjee, G. & Singh, V. 2018. Book review: quorum sensing vs. quorum quenching: a battle with no end in sight. Frontiers Media SA.

Göksu, S., UĞUZ, M. T., Özdemir, H. & Seçen, H. 2005. A concise synthesis and the antibacterial activity of 5, 6-dimethoxynaphthalene-2-carboxylic acid. *Turkish Journal of Chemistry,* **29 (**2)**:** 199-205.

Gonçalves, S. S., Souza, A. C. R., Chowdhary, A., Meis, J. F. & Colombo, A. L. 2016. Epidemiology and molecular mechanisms of antifungal resistance in Candida and Aspergillus. *Mycoses,* **59 (**4)**:** 198-219.

Hamad, N. S., Al-Haidery, N. H., Al-Masoudi, I. A., Sabri, M., Sabri, L. & Al-Masoudi, N. A. 2010. Amino acid derivatives, part 4: synthesis and anti-HIV activity of new naphthalene derivatives. *Archiv der Pharmazie,* **343 (**7)**:** 397-403.

Hargrove, T. Y., Wawrzak, Z., Lamb, D. C., Guengerich, F. P. & Lepesheva, G. I. 2015. Structure-Functional Characterization of Cytochrome P450 Sterol 14alpha-Demethylase (CYP51B) from Aspergillus fumigatus and Molecular Basis for the Development of Antifungal Drugs. *J Biol Chem,* **290 (**39)**:** 23916-23934.

Hope, W. W., Walsh, T. J. & Denning, D. W. 2005. The invasive and saprophytic syndromes due to Aspergillus spp. *Medical Mycology,* **43 (**Supplement_1)**:** S207-S238.

Howard, S. J. & Arendrup, M. C. 2011. Acquired antifungal drug resistance in Aspergillus fumigatus: epidemiology and detection. *Medical Mycology,* **49 (**Supplement_1)**:** S90-S95.

Humphries, R. M., Ambler, J., Mitchell, S. L., Castanheira, M., Dingle, T., Hindler, J. A., Koeth, L. & Sei, K. 2018. CLSI Methods Development and Standardization Working Group Best Practices for Evaluation of Antimicrobial Susceptibility Tests. *Journal of Clinical Microbiology,* **56 (**4**):** 10.1128/jcm.01934-01917.

Ikuta, K. S., Swetschinski, L. R., Aguilar, G. R., Sharara, F., Mestrovic, T., Gray, A. P., Weaver, N. D., Wool, E. E., Han, C. & Hayoon, A. G. 2022. Global mortality associated with 33 bacterial pathogens in 2019: a systematic analysis for the Global Burden of Disease Study 2019. *The Lancet,* **400 (**10369**):** 2221-2248.

Janowska, S., Andrzejczuk, S., Gawryś, P. & Wujec, M. 2023. Synthesis and Antimicrobial Activity of New Mannich Bases with Piperazine Moiety. *Molecules* [Online], 28.

Jasim, S. F. F. & Mustafa, Y. F. 2022. Synthesis, ADME Study, and Antimicrobial Evaluation of Novel Naphthalene-Based Derivatives. *Journal of Medicinal and Chemical Sciences,* **5 (**5**):** 793-807.

Kumar, R., Kumar, P., Kumar, M. & Narasimhan, B. 2012. Synthesis, anti-microbial evaluation, and QSAR studies of 4-amino-3-hydroxy-naphthalene-1-sulfonic acid derivatives. *Medicinal Chemistry Research,* **21:** 4301-4310.

Lafitte, D., Lamour, V., Tsvetkov, P. O., Makarov, A. A., Klich, M., Deprez, P., Moras, D., Briand, C. & Gilli, R. 2002. DNA gyrase interaction with coumarin-based inhibitors: the role of the hydroxybenzoate isopentenyl moiety and the 5 '-methyl group of the noviose. *Biochemistry,* **41 (**23**):** 7217-7223.

Lipinski, C. A., Lombardo, F., Dominy, B. W. & Feeney, P. J. 1997. Experimental and computational approaches to estimate solubility and permeability in drug discovery and development settings. *Advanced Drug Delivery Reviews,* **23 (**1**):** 3-25.

Mahindroo, N., Wang, C.-C., Liao, C.-C., Huang, C.-F., Lu, I.-L., Lien, T.-W., Peng, Y.-H., Huang, W.-J., Lin, Y.-T. & Hsu, M.-C. 2006. Indol-1-yl acetic acids as peroxisome proliferator-activated receptor agonists: design, synthesis, structural biology, and molecular docking studies. *J Med Chem,* **49 (**3**):** 1212-1216.

Maxwell, A. 1997. DNA gyrase as a drug target. *Trends in microbiology,* **5 (**3**):** 102-109.

Mechelke, M. & Habeck, M. 2010. Robust probabilistic superposition and comparison of protein structures. *BMC Bioinformatics,* **11 (**1**):** 363.

Mestrovic, T., Aguilar, G. R., Swetschinski, L. R., Ikuta, K. S., Gray, A. P., Weaver, N. D., Han, C., Wool, E. E., Hayoon, A. G. & Hay, S. I. 2022. The burden of bacterial antimicrobial resistance in the WHO European region in 2019: A cross-country systematic analysis. *The Lancet Public Health,* **7 (**11**):** e897-e913.

Misganaw, A., Haregu, T. N., Deribe, K., Tessema, G. A., Deribew, A., Melaku, Y. A., Amare, A. T., Abera, S. F., Gedefaw, M., Dessalegn, M., Lakew, Y., Bekele, T., Mohammed, M., Yirsaw, B. D., Damtew, S. A., Krohn, K. J., Achoki, T., Blore, J., Assefa, Y. & Naghavi, M. 2017. National mortality burden due to communicable, non-communicable, and other diseases in Ethiopia, 1990-2015: findings from the Global Burden of Disease Study 2015. *Popul Health Metr,* **15:** 29.

Mladenovic-Antic, S., Kocic, B., Velickovic-Radovanovic, R., Dinic, M., Petrovic, J., Randjelovic, G. & Mitic, R. 2016. Correlation between antimicrobial consumption and antimicrobial resistance of Pseudomonas aeruginosa in a hospital setting: a 10-year study. *Journal of clinical pharmacy and therapeutics,* **41 (**5)**:** 532-537.

Mohsen, S., Dickinson, J. A. & Somayaji, R. 2020. Update on the adverse effects of antimicrobial therapies in community practice. *Canadian Family Physician,* **66 (**9)**:** 651-659.

Murray, C. J., Ikuta, K. S., Sharara, F., Swetschinski, L., Aguilar, G. R., Gray, A., Han, C., Bisignano, C., Rao, P. & Wool, E. 2022. Global burden of bacterial antimicrobial resistance in 2019: a systematic analysis. *The Lancet,* **399 (**10325)**:** 629-655.

Murray, W. V., Wachter, M. P., Kasper, A. M., Argentieri, D. C., Capetola, R. J. & Ritchie, D. M. 1991. Novel 6-oxo-6-naphthylhexanoic acid derivatives with anti-inflammatory and 5-lipoxygenase inhibitory activity. *Eur J Med Chem,* **26 (**2)**:** 159-166.

Nagawade, R. R. & Shinde, D. B. 2007. Synthesis of amidoalkyl naphthols by an iodine-catalyzed multicomponent reaction of β-naphthol. *Mendeleev Communications,* **17 (**5)**:** 299-300.

Nusrath Unissa, A., Hanna, L. E. & Swaminathan, S. 2016. A Note on Derivatives of Isoniazid, Rifampicin, and Pyrazinamide Showing Activity Against Resistant Mycobacterium tuberculosis. *Chem Biol Drug Des,* **87 (**4)**:** 537-550.

Okeke, I. N., Laxminarayan, R., Bhutta, Z. A., Duse, A. G., Jenkins, P., O'Brien, T. F., Pablos-Mendez, A. & Klugman, K. P. 2005. Antimicrobial resistance in developing countries. Part I: recent trends and current status. *Lancet Infect Dis,* **5 (**8)**:** 481-493.

Olyaei, A. & Sadeghpour, M. 2019. Recent advances in the synthesis and synthetic applications of Betti base (aminoalkylnaphthol) and bis-Betti base derivatives. *RSC Advances,* **9 (**32**):** 18467-18497.

Park, B. J., Wannemuehler, K. A., Marston, B. J., Govender, N., Pappas, P. G. & Chiller, T. M. 2009. Estimation of the current global burden of cryptococcal meningitis among persons living with HIV/AIDS. *Aids,* **23 (**4**):** 525-530.

Perlin, D. S., Rautemaa-Richardson, R. & Alastruey-Izquierdo, A. 2017. The global problem of antifungal resistance: prevalence, mechanisms, and management. *The Lancet Infectious Diseases,* **17 (**12**):** e383-e392.

Perlin, D. S., Shor, E. & Zhao, Y. 2015. Update on Antifungal Drug Resistance. *Curr Clin Microbiol Rep,* **2 (**2**):** 84-95.

Petranyi, G., Meingassner, J. G. & Mieth, H. 1987. Antifungal activity of the allylamine derivative terbinafine in vitro. *Antimicrob Agents Chemother,* **31 (**9**):** 1365-1368.

Pfaller, M. A. 2012. Antifungal drug resistance: mechanisms, epidemiology, and consequences for treatment. *The American journal of medicine,* **125 (**1**):** S3-S13.

Pommier, Y., Leo, E., Zhang, H. & Marchand, C. 2010. DNA topoisomerases and their poisoning by anticancer and antibacterial drugs. *Chem Biol,* **17 (**5**):** 421-433.

Priya, B., Cherkadu, V., Kalavagunta, P., Ravirala, N. & Shivananju, N. 2016. Zinc Chloride Catalyzed, Dipolar Aprotic Solvent-Mediated, One-Pot Synthesis of 2-[(Benzo[d]thiazol-2-ylamino)(phenyl)methyl]phenols. *Synlett,* **27 (**20**):** 2795-2798.

Qidwai, T. 2016. QSAR modeling, docking and ADMET studies for exploration of potential anti-malarial compounds against Plasmodium falciparum. *In Silico Pharmacol,* **5 (**1)**:** 6.

Rahn, K., Hawlina, A., Kersting, F. & Planz, G. 1974. Studies on the antihypertensive action of the optical isomers of propranolol in man. *Naunyn-Schmiedeberg's archives of pharmacology,* **286:** 319-323.

Rathod, K. 2011. Synthesis and antimicrobial activity of azo compounds containing resorcinol moiety. *Asian Journal of Research in Chemistry,* **4 (**5)**:** 734-736.

Rayens, E. & Norris, K. A. 2022. Prevalence and Healthcare Burden of Fungal Infections in the United States, 2018. *Open Forum Infectious Diseases,* **9 (**1)**:**

Rodrigues, M. L. & Nosanchuk, J. D. 2020. Fungal diseases as neglected pathogens: A wake-up call to public health officials. *PLoS Negl Trop Dis,* **14 (**2)**:** e0007964.

Rokade, Y. & Dongare, N. 2010. Synthesis and antimicrobial activity of some azetidinone derivatives with the β-naphthol. *Rasayan J. Chem,* **3 (**4)**:** 641.

Rokade, Y. & Sayyed, R. 2009. Naphthalene derivatives: A new range of antimicrobials with high therapeutic value. *Rasayan J. Chem,* **2 (**4)**:** 972-980.

Roman, G. 2015. Mannich bases in medicinal chemistry and drug design. *Eur J Med Chem,* **89:** 743-816.

Ryder, N., Frank, I. & Dupont, M. 1986. Ergosterol biosynthesis inhibition by the thiocarbamate antifungal agents tolnaftate and tolciclate. *Antimicrob Agents Chemother,* **29 (**5)**:** 858-860.

Saab, A. N., Sloan, K. B., Beall, H. D. & Villanueva, R. 1990. Effect of Aminomethyl (N-Mannich Base) Derivatization on the Ability of S6Acetyloxymethyl-S-Mercaptopurine Prodrug to Deliver 6-Mercaptopurine through Hairless Mouse Skin. *Journal of Pharmaceutical Sciences,* **79 (**12)**:** 1099-1104.

Şahin, G., Palaska, E., Ekizoğlu, M. & Özalp, M. 2002. Synthesis and antimicrobial activity of some 1, 3, 4-oxadiazole derivatives. *Il Farmaco,* **57 (**7)**:** 539-542.

Sanyal, G. & Doig, P. 2012. Bacterial DNA replication enzymes as targets for antibacterial drug discovery. *Expert Opin Drug Discov,* **7 (**4)**:** 327-339.

Sapundzhi, F., Popstoilov, M. & Lazarova, M. RMSD Calculations for Comparing Protein Three-Dimensional Structures. *In:* Georgiev, I., Datcheva, M., Georgiev, K. & Nikolov, G., eds. Numerical Methods and Applications, 2023// 2023 Cham. Springer Nature Switzerland, 279-288.

Sarkar, P., Yarlagadda, V., Ghosh, C. & Haldar, J. 2017. A review on cell wall synthesis inhibitors with an emphasis on glycopeptide antibiotics. *Medchemcomm,* **8 (**3)**:** 516-533.

Schumacher, A., Vranken, T., Malhotra, A., Arts, J. & Habibovic, P. 2018. In vitro antimicrobial susceptibility testing methods: agar dilution to 3D tissue-engineered models. *European Journal of Clinical Microbiology & Infectious Diseases,* **37:** 187-208.

Shingalapur, R. V., Hosamani, K. M., Keri, R. S. & Hugar, M. H. 2010. Derivatives of benzimidazole pharmacophore: Synthesis, anticonvulsant, antidiabetic and DNA cleavage studies. *Eur J Med Chem,* **45 (**5)**:** 1753-1759.

Shoichet, B. K., McGovern, S. L., Wei, B. & Irwin, J. J. 2002. Lead discovery using molecular docking. *Current Opinion in Chemical Biology,* **6 (**4)**:** 439-446.

Sp, P., R, A. S. K. & Ks, J. 2022. Insights from the molecular docking analysis of compounds from Vitex negundoi with targets from Klebsiella pneumoniai causing urinary tract infection. *Bioinformation,* **18 (**11)**:** 1062-1068.

Tokalı, F. S., Taslimi, P., Demircioğlu, İ. H., Şendil, K., Tuzun, B. & Gülçin, İ. 2022. Novel phenolic Mannich base derivatives: synthesis, bioactivity, molecular docking, and ADME-Tox Studies. *Journal of the Iranian Chemical Society,* **19 (**2)**:** 563-577.

Tratrat, C. 2020. 1, 2, 4-Triazole: A privileged scaffold for the development of potent antifungal agents-a brief review. *Curr Top Med Chem,* **20 (**24)**:** 2235-2258.

van Seventer, J. M. & Hochberg, N. S. 2017. Principles of Infectious Diseases: Transmission, Diagnosis, Prevention, and Control. *International encyclopedia of public health***:** 22-39.

Walsh, C. 2000. Molecular mechanisms that confer antibacterial drug resistance. *Nature,* **406 (**6797)**:** 775-781.

Weinstein, M. P. & Lewis, J. S. 2020. The Clinical and Laboratory Standards Institute Subcommittee on Antimicrobial Susceptibility Testing: Background, Organization, Functions, and Processes. *Journal of Clinical Microbiology,* **58 (**3)**:** 10.1128/jcm.01864-01819.

WHO (2019). New report calls for urgent action to avert antimicrobial resistance crisis. New York, WHO.

WHO (2021). Global antimicrobial resistance and use surveillance system (GLASS) report 2021. Geneva, WHO.

Wisplinghoff, H., Bischoff, T., Tallent, S. M., Seifert, H., Wenzel, R. P. & Edmond, M. B. 2004. Nosocomial Bloodstream Infections in US Hospitals: Analysis of 24,179 Cases from a Prospective Nationwide Surveillance Study. *Clinical Infectious Diseases,* **39 (**3)**:** 309-317.

Wisplinghoff, H., Ebbers, J., Geurtz, L., Stefanik, D., Major, Y., Edmond, M. B., Wenzel, R. P. & Seifert, H. 2014. Nosocomial bloodstream infections due to Candida spp. in the USA: species distribution, clinical features and antifungal susceptibilities. *International journal of antimicrobial agents,* **43 (**1)**:** 78-81.

8. Appendices

8.1 TLC chromatogram of synthesized compounds

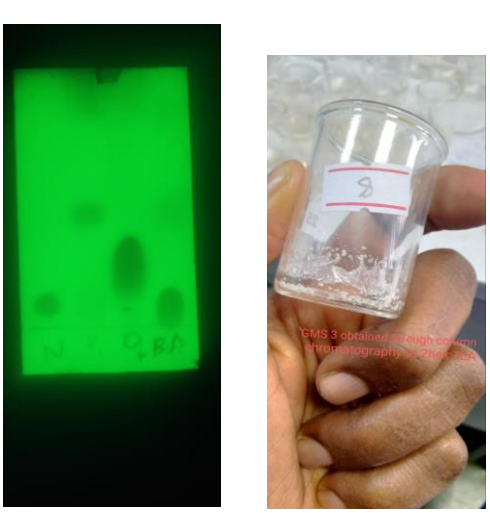

(A).

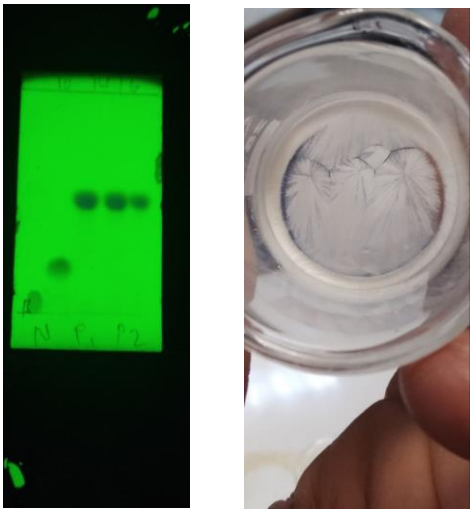

(B).

(A) Normal phase TLC chromatogram of and a white crystal of compound 37compared with 2-Naphthol (N), benzaldehyde (BA), and O-toluidine (OT) under UV 254 nm light source with the solvent system hexane/ethyl acetate (1:1), (B). Normal phase TLC chromatogram and a white crystal of compound 39 compared with 2-Naphthol (N) and benzylamine (B) under UV -254 nm light source with the solvent system hexane/ethyl acetate (2:1)

8.2 ^{1}H and ^{13}C NMR spectra of synthesized compounds

8.2.1 ^{1}H, ^{13}C, DEPT-135, and DEPT-90 NMR spectra of compound 37

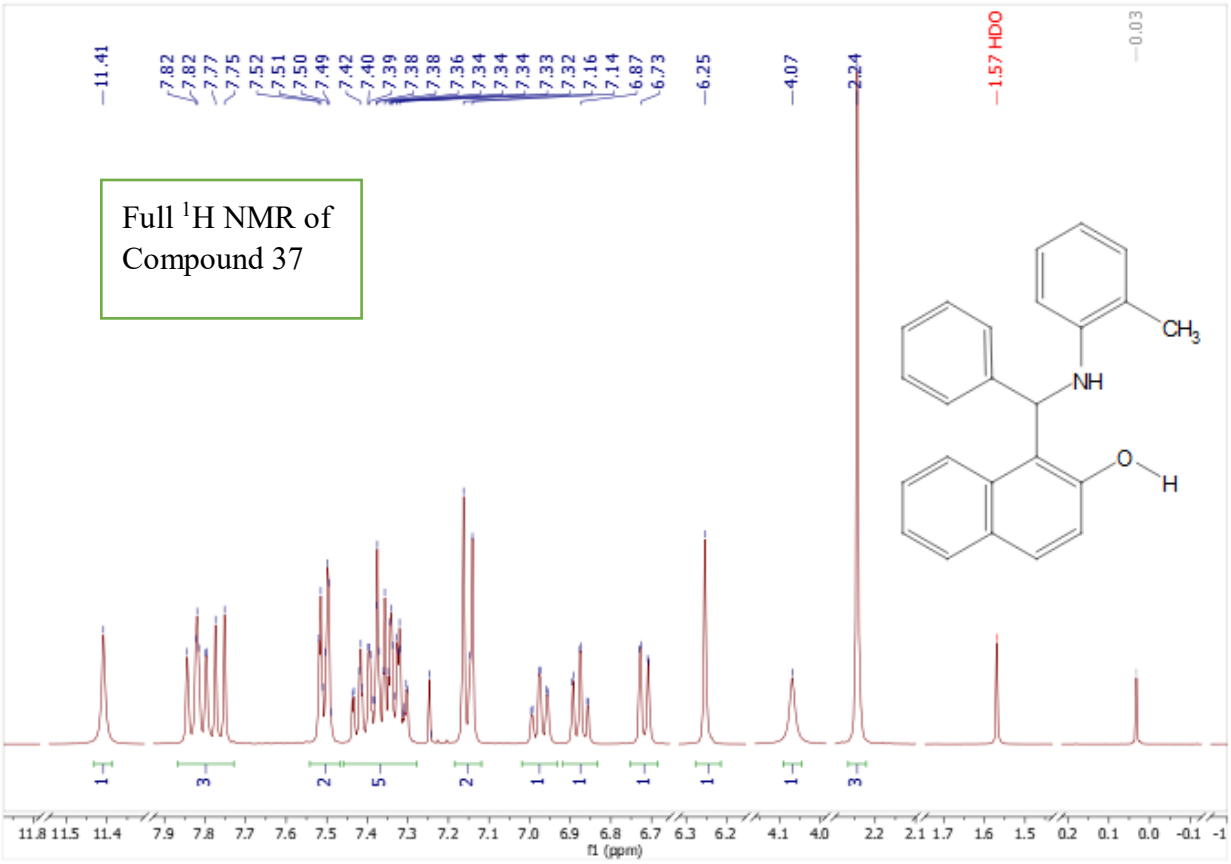

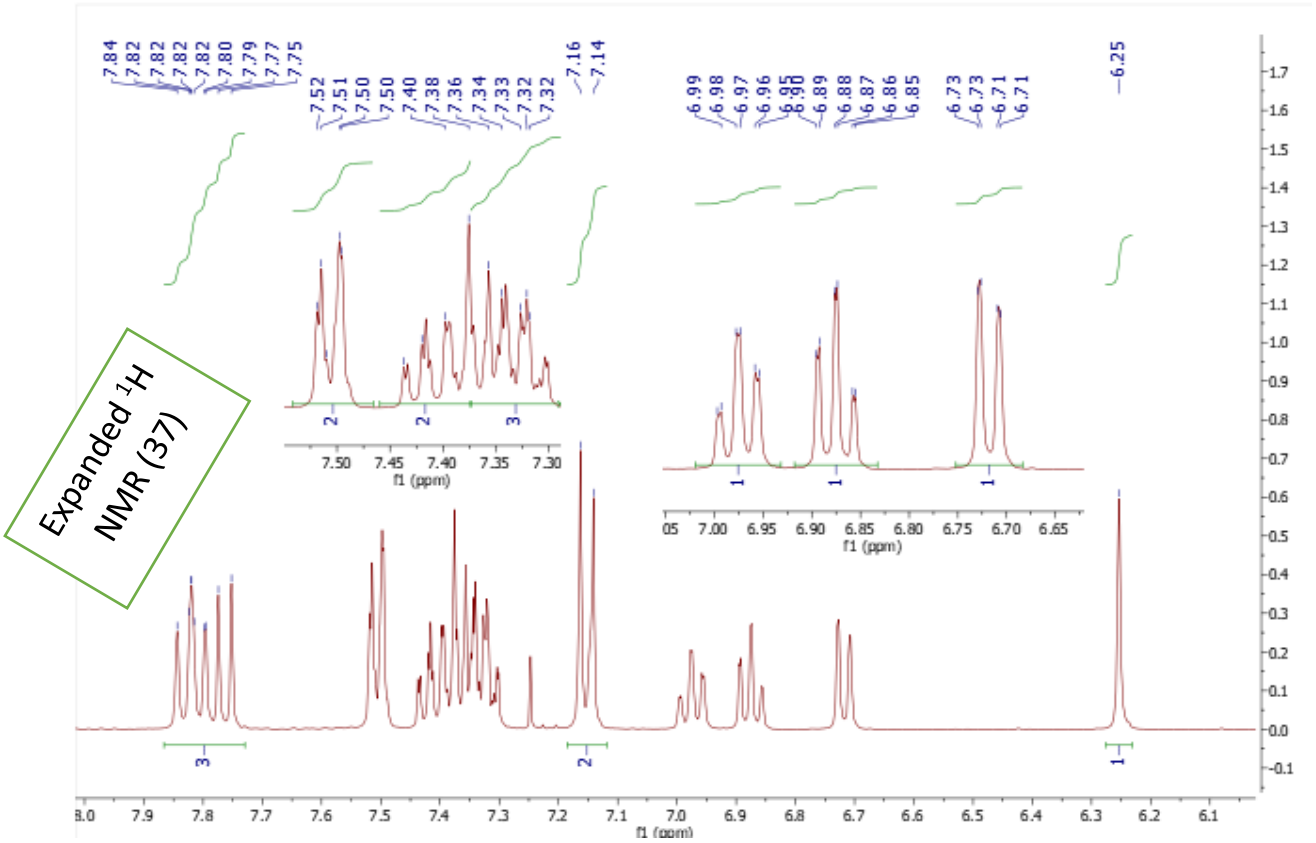
Expanded ^{1}H NMR (37)
f1 (ppm)

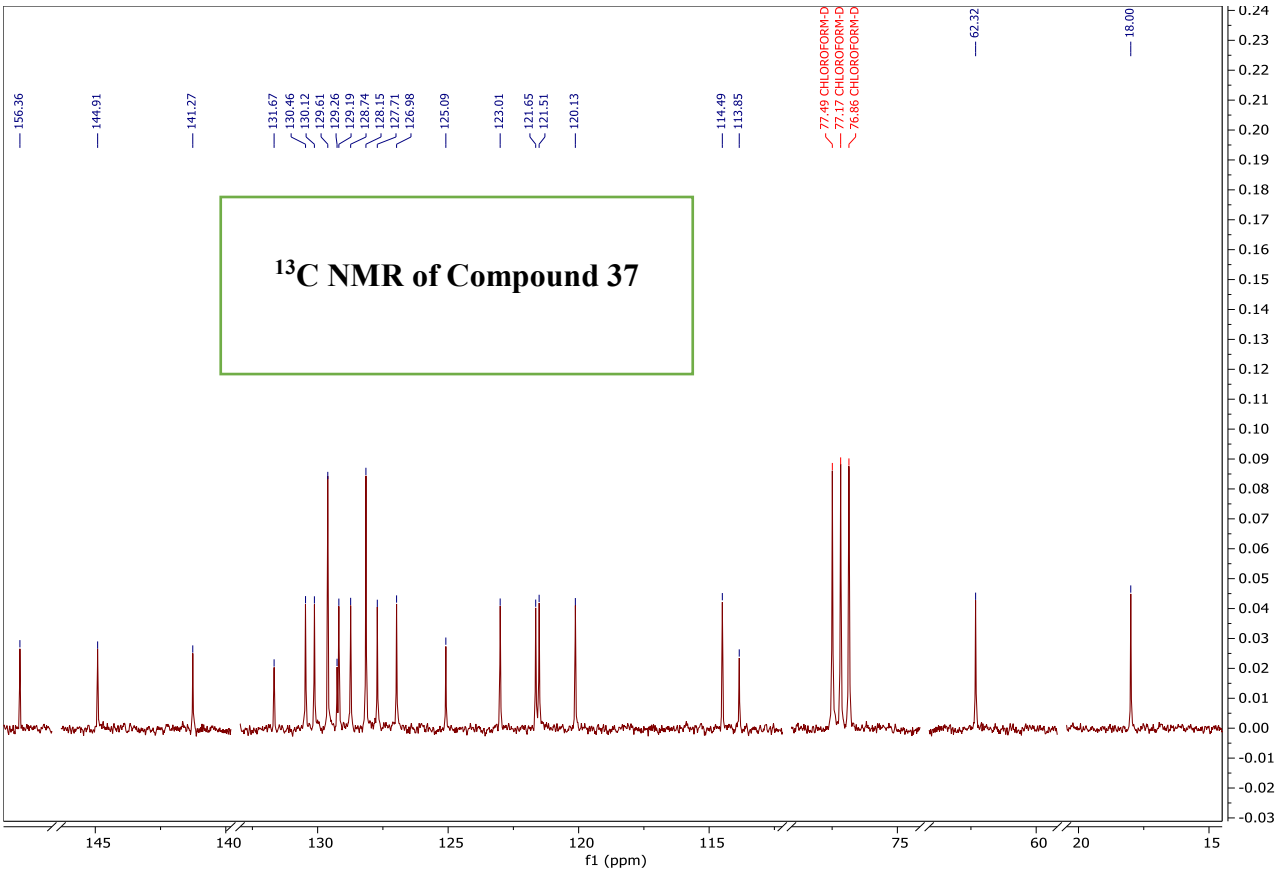

^{13}C NMR of Compound 37

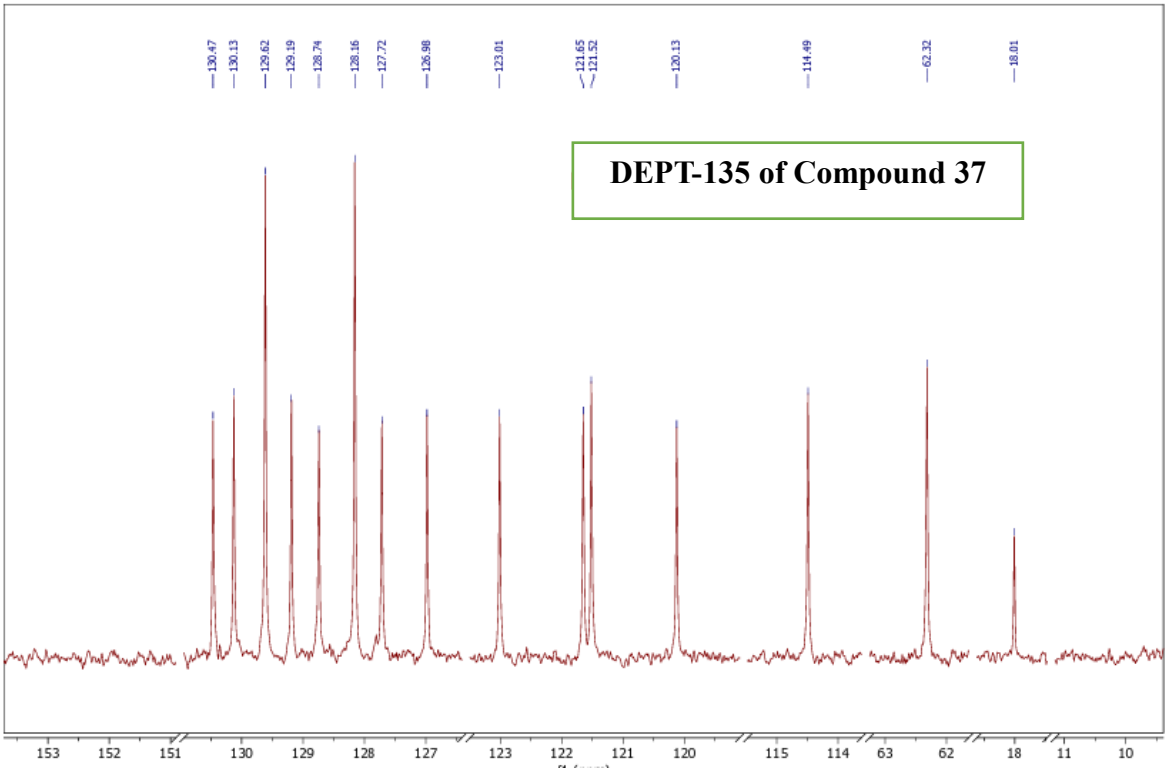

DEPT-135 of Compound 37

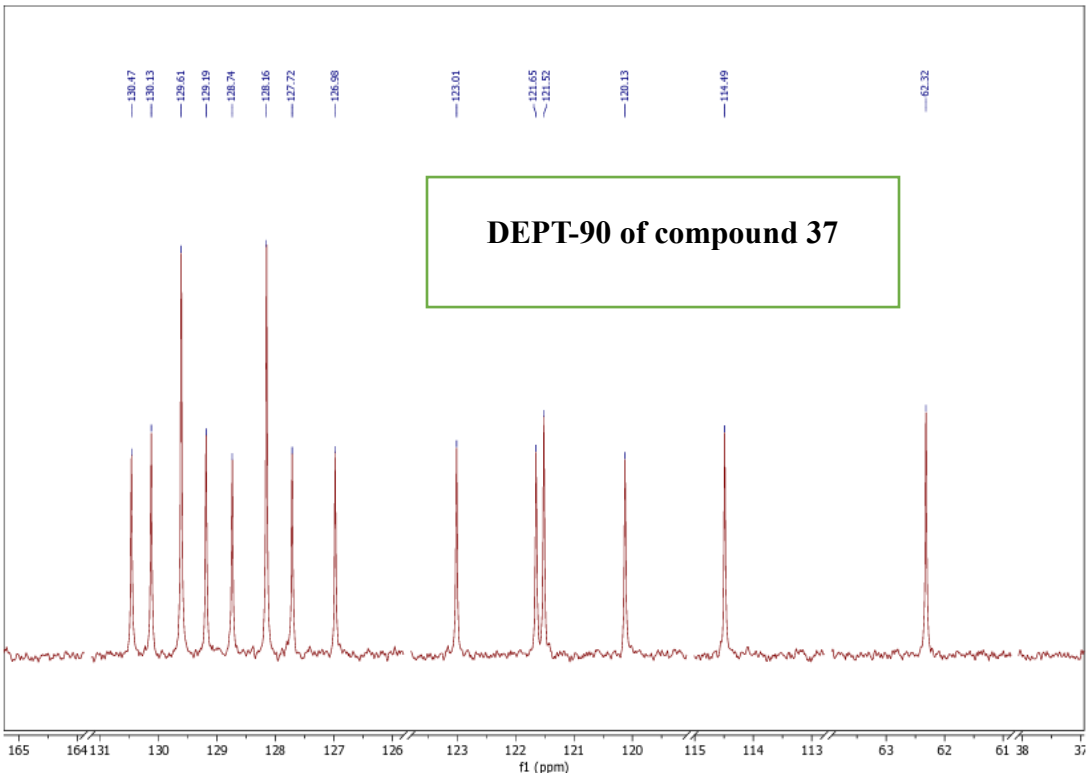

8.2.2 ^{1}H, ^{13}C, DEPT-135 and DEPT-90 NMR spectra of compound 39

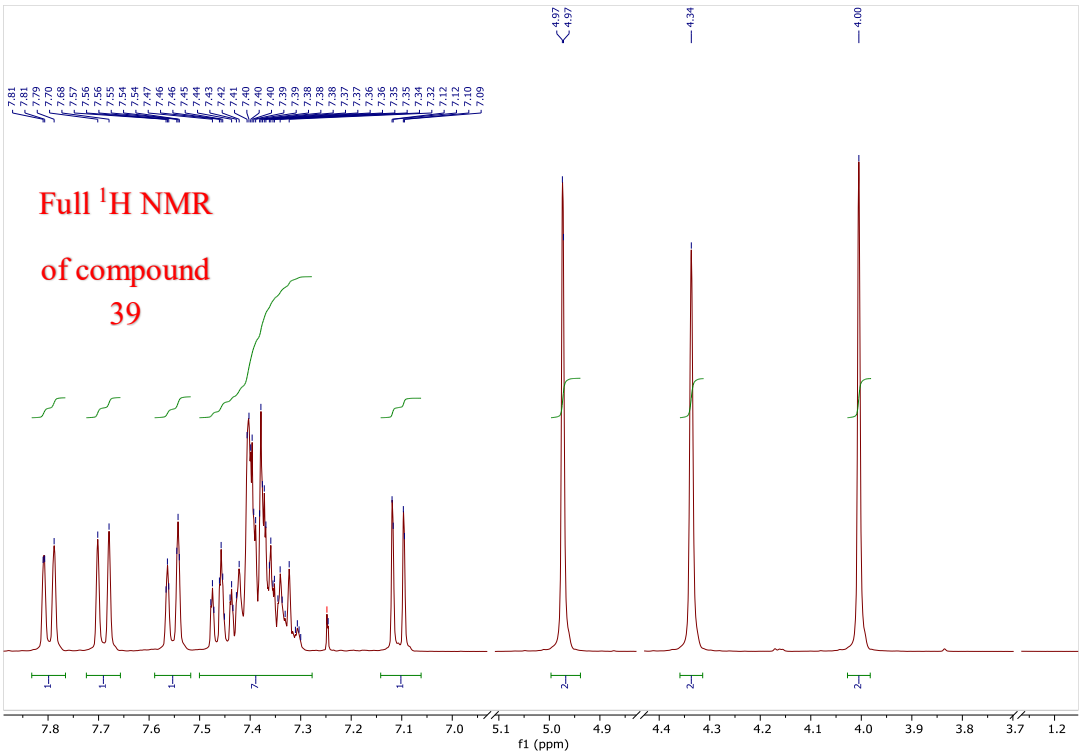

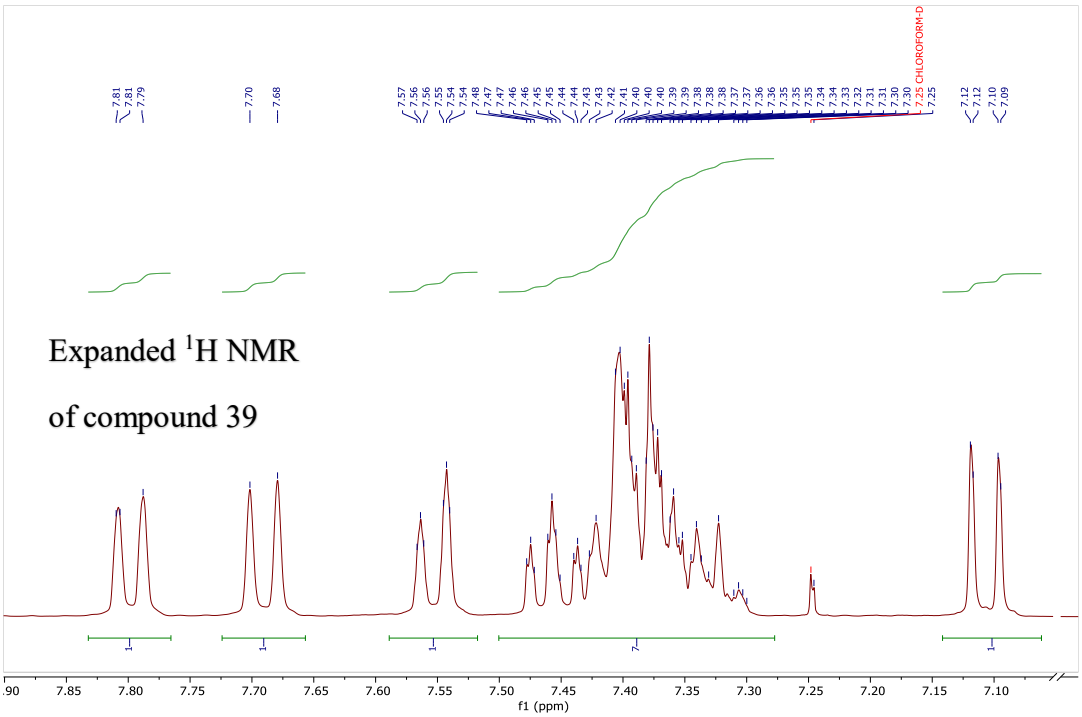
Expanded ^{1}H NMR
of compound 39
f1 (ppm)

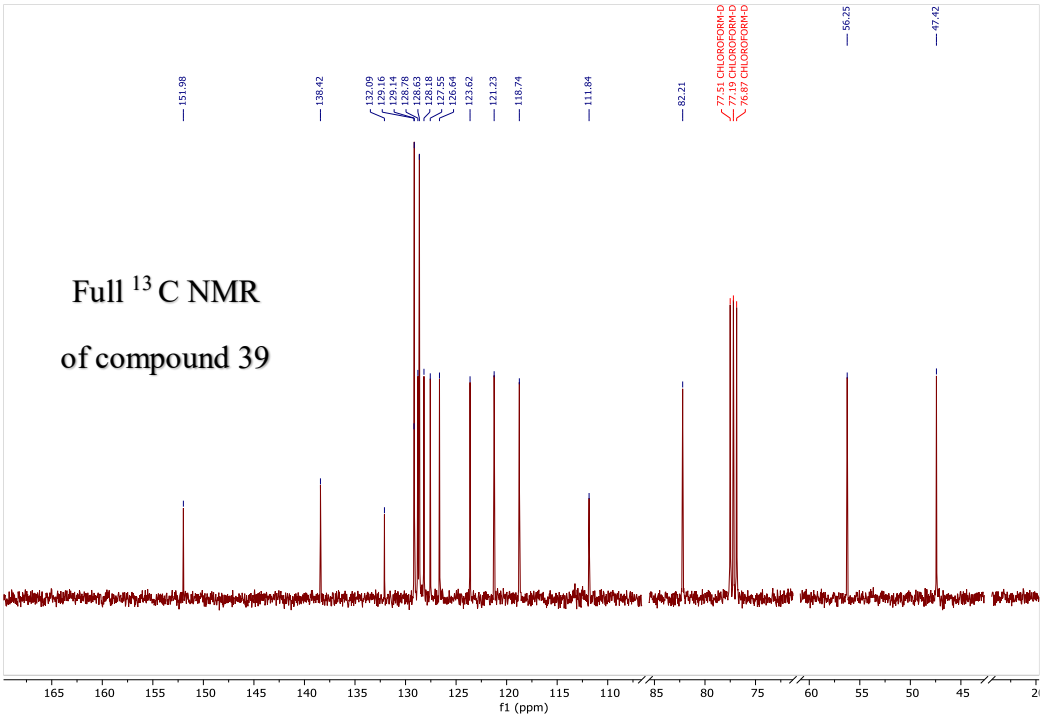
Full ^{13}C NMR
of compound 39
f1 (ppm)

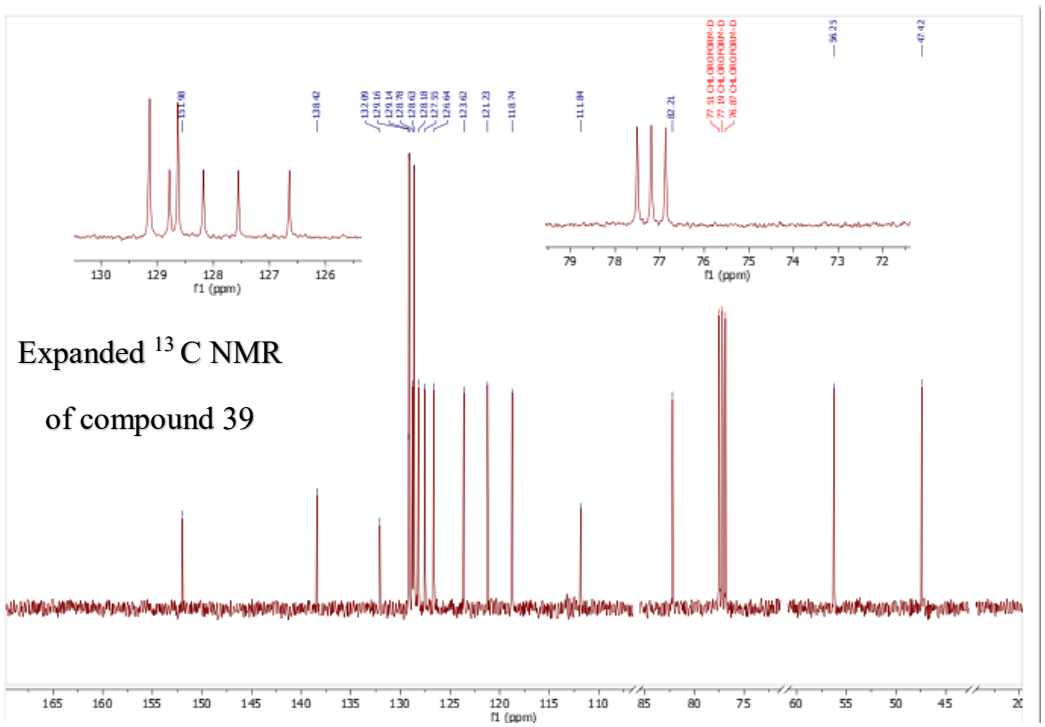
Expanded ^{13}C NMR
of compound 39
f1 (ppm)

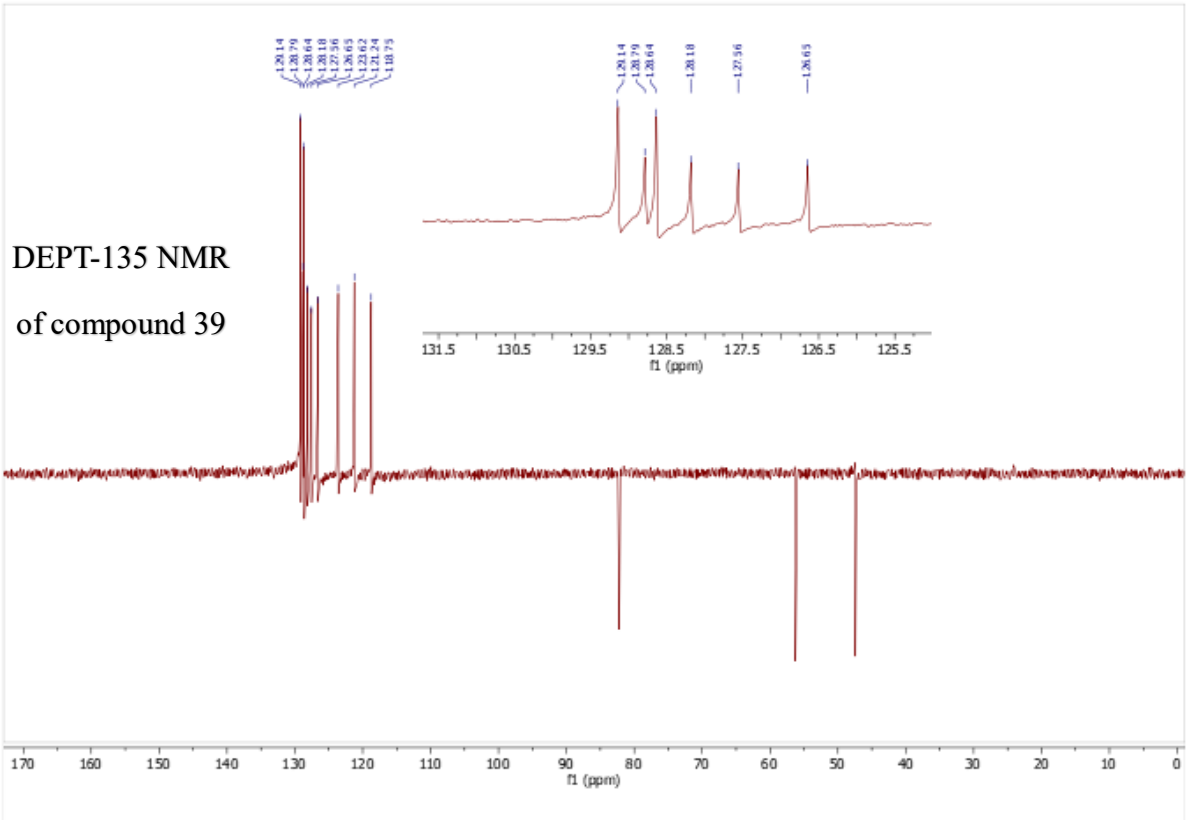
DEPT-135 NMR
of compound 39
f1 (ppm)

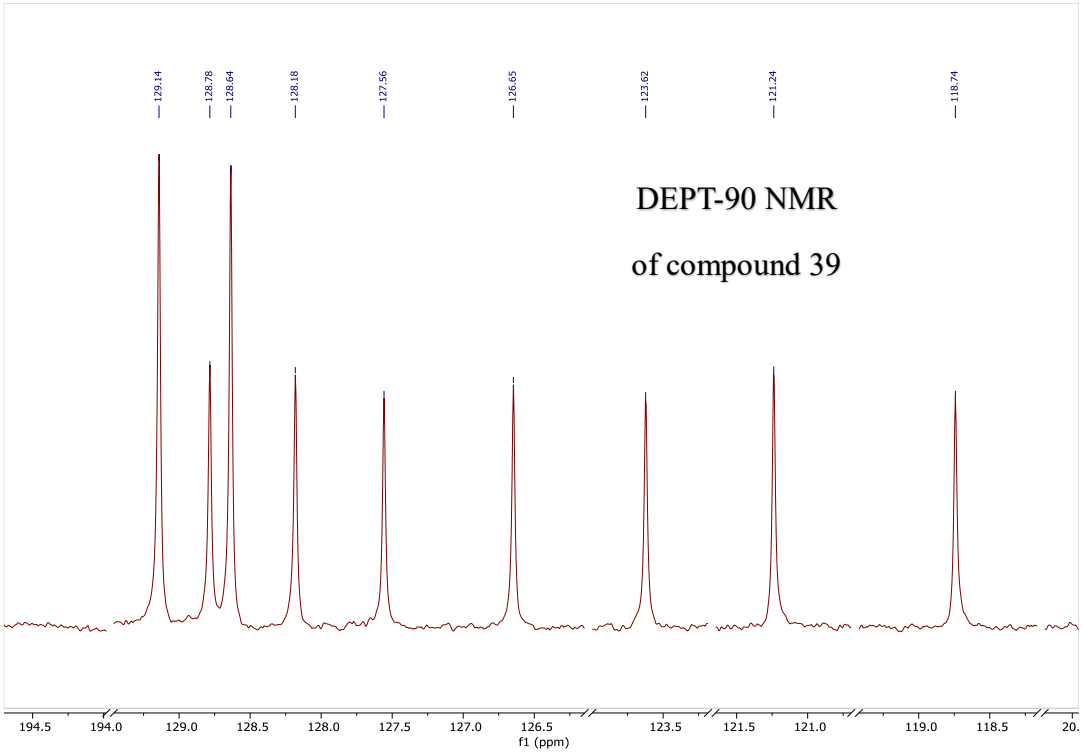
129.14
128.78
128.64
128.18
127.56
126.65
123.62
121.24
118.74
DEPT-90 NMR
of compound 39
194.5
194.0
129.0
128.5
128.0
127.5
127.0
126.5
123.5
121.5
121.0
119.0
118.5
f1 (ppm)

8.3 Molecular Docking Results of Ciprofloxacin and Voriconazole

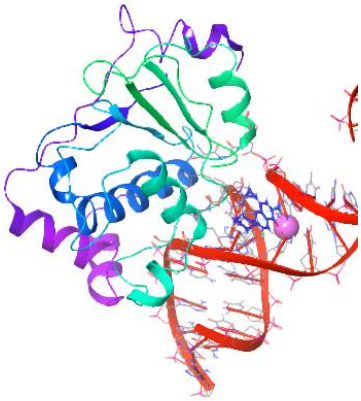

A. 3D visualization

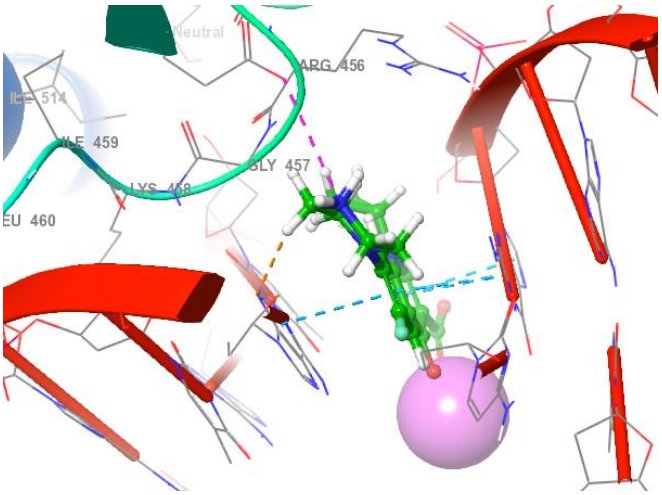

B. 3D zoomed visualization

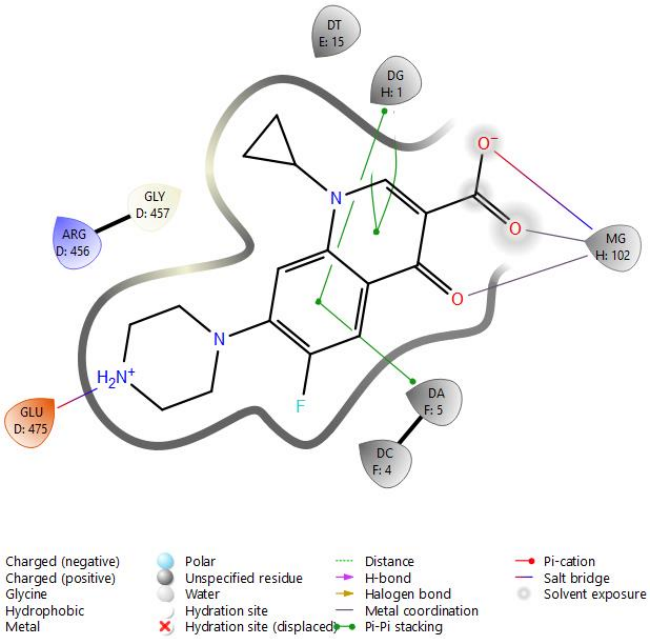

C. 2D visualization

A. 3D visualization, B: 3D zoomed visualization C. 2D visualization of the molecular docking interaction of ciprofloxacin against *E. coli* DNA Gyrase B (4z2e)

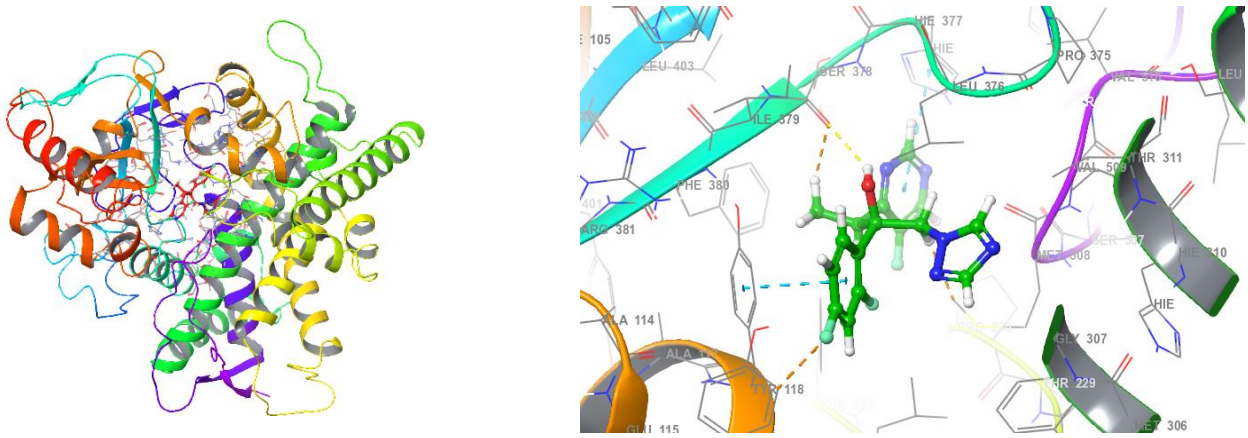

A. B.

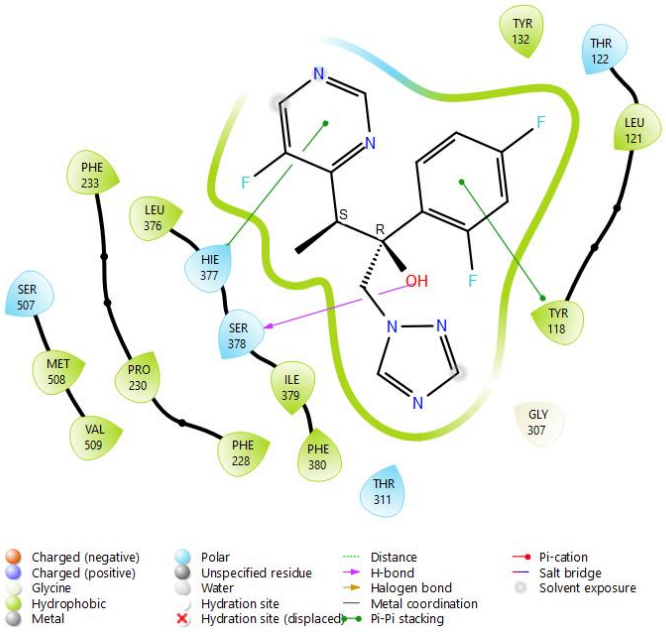

C.

A. 3D visualization, B: 3D zoomed visualization C. 2D visualization of the molecular docking interaction of voriconazole against *C. albicans* Lanosterol 14α -demethylase (5v5z)

Aminoalkyl and Oxazine of 2-Naphthol Derivatives: Synthesis, *In vitro* Antimicrobial and *In Silico* Studies

Gizachew Motbaynor[1,2], Daniel Bisrat[1], Kaleab Asres[1] and Avijit Mazumder[3]

[1]Department of Pharmaceutical Chemistry and Pharmacognosy, School of Pharmacy, College of Health Sciences, Addis Ababa University, P.O. Box 1176, Addis Ababa, Ethiopia;
[2]Department of Pharmacy, College of Health Sciences, Bahir Dar University, Bahir Dar, Ethiopia
[3]Department of Pharmaceutical Technology, Noida Institute of Engineering and Technology, 19 Knowledge Park II, Institutional Area, Greater Noida, 201306, India

ABSTRACT

Antimicrobial resistance of microorganisms, both bacteria and fungi, to available treatments, is a global medical challenge of high priority. One effective strategy to address this challenge involves synthesizing compounds with potential antimicrobial activities. In this study, we synthesized lead compounds from the 2-naphthol framework using a one-pot three-component Mannich-type condensation reaction. The synthesized compounds were purified through column chromatography, and their chemical structures were identified using ^{1}H and ^{13}C, DEPT-90, and DEPT-135 NMR spectral data, as 1-(phenyl(*O-alkylamino*) methyl) naphthalene-2-ol (37) and 2-benzyl-2,3-dihydro-1H-naphtho[1,2-e] [1,3] Oxazine (39). The potential antimicrobial activity of the synthesized compounds was evaluated by the disk diffusion and broth dilution method. At the same time, molecular docking and ADME studies were conducted to investigate their possible mechanism of action and drug-like properties.

From our findings, both synthesized compounds exhibited promising antibacterial activity against most tested bacterial strains at 200 µg/ml, showing zones of inhibitions (ZOIs) ranging from 6.0 mm to 15.5 mm. The positive standard ciprofloxacin demonstrated ZOIs between 11.5 mm and 20.5 mm.

Both compounds 37 and 39 exhibited moderate antifungal activity against most tested fungal species. In the molecular docking analysis, compounds 37 and 39 demonstrated significant binding energy within the binding pocket of *E. coli DNA gyrase* B and *C. albicans* lanosterol 4α-demethylase. The ADMET prediction displayed both synthesized compounds exhibit favorable pharmacokinetics and drug-like characteristics, making them suitable for oral administration. In addition to the in vitro bioassay activity test, the molecular docking results and ADMET predictions collectively confirm the promising antimicrobial properties of both synthesized compounds. These findings imply that conducting further synthesis and evaluation of 2-naphthol derivatives could benefit the ongoing efforts to develop antimicrobial drugs for combating infectious diseases and microbial resistance.

Keywords: *antimicrobial, antibacterial, antifungal, Mannich base, 2-naphthol, oxazine, aminoalkyl, in silico study, DNA gyrase B, molecular docking, ADMET*

1. INTRODUCTION

Infectious diseases, caused by pathogens like bacteria, viruses, parasites, or fungi present a significant global threat, affecting public health and economies (J. M. van Seventer and N. S. Hochberg, 2017). Despite advancements, diseases like lower respiratory tract infections, HIV/AIDS, tuberculosis, diarrheal diseases, and malaria persist as leading causes of death worldwide, with a pronounced impact in developing countries (I. Abubakar *et al.*, 2015, S. Janowska *et al.*, 2023, I. N. Okeke *et al.*, 2005). The emergence of antibiotic resistance adds urgency to the situation, with multidrug-resistant pathogens posing a severe global health risk (N. Gohil *et al.*, 2018).

Mannich bases are characterized by a group of compounds consisting of an aminoalkyl group in their structures. Mannich bases play crucial roles in their application in pharmaceutical chemistry, particularly in optimizing and enhancing the pharmacokinetic properties of drugs within the human body (A. N. Saab *et al.*, 1990). Additionally, Mannich bases serve as significant pharmacophores or bioactive lead molecules, leading to the synthesis of various potential active ingredients with a core aminoalkyl chain (S. Bala *et al.*, 2014). Clinical examples of Mannich bases with an aminoalkyl chain include fluoxetine, atropine, ranitidine, cocaine, trihexyphenidyl, procyclidine, and biperiden, among others (S. Bala *et al.*, 2014).

Naphthalene, a bicyclic aromatic hydrocarbon, is used as a versatile building block for synthesizing various scaffolds. Extensive research has explored its medicinal properties, including antimicrobial(Y. Rokade and R. Sayyed, 2009), antiviral (I. A. Ali *et al.*, 2005, N. S. Hamad *et al.*, 2010), antidiabetic (N. Mahindroo *et al.*, 2006), anticancer (I. A. Ali *et al.*, 2005), anti-inflammatory (W. V. Murray *et al.*, 1991), antihypertensive (K. Rahn *et al.*, 1974, K. L. Duchin *et al.*, 1980), anticonvulsant effects (R. V. Shingalapur *et al.*, 2010).

In particular, naphthalene-containing medications like bedaquiline, nafitifin, and terbinafine, among others, play a crucial role in managing microbial infections (G. Petranyi *et al.*, 1987). Furthermore, 2-naphthol, a hydroxy analog of naphthalene commonly used as a dye, exhibits excellent antimicrobial properties.

The FDA has approved several drugs containing 2-naphthol with diverse pharmacological activities. Notable examples include nafcillin, an antibiotic belonging to the beta-lactam penicillin class, used for treating infections caused by Gram-positive bacteria (F.-Y. Chang *et al.*, 2003). Rifampicin, another 2-naphthol-based drug, is employed as an antitubercular agent, often in combination with isoniazid, pyrazinamide, and ethambutol (A. Nusrath Unissa *et al.*, 2016). Tolnaftate, a synthetic anti-fungal with a thiocarbamate moiety, inhibits squalene epoxidase—an essential enzyme in ergosterol biosynthesis during the fungi life cycle (N. Ryder *et al.*, 1986). This study aimed to synthesize, *in vitro* antimicrobial, and *in silico* study of aminoalkyl and oxazine 2-naphthol derivatives.

2. MATERIALS AND METHODS

2.1 Materials

2.1.1 Chemicals and Reagents

The following chemicals, reagents, and solvents were used in this study: Benzylamine, O-toluidine, and 2-naphthol (LobaChem PV. LTD., Mumbai, India). Formaldehyde, $ZnCl_2$ (Sigma-Aldrich Co., Stein helm, Germany), ethanol, hexane, ethyl acetate, methanol, and chloroform (LobaChem PV. LTD., Mumbai, India). Williams, England), tetramethyl silane (TMS) deuterated chloroform (CDCl3), Nutrient Agar (NA), Mueller-Hinton Broth (MHB), Sabouraud Dextrose Agar (SDA) and Sabouraud Dextrose Broth (SDB) (HiMedia Laboratories Pvt. Ltd. India), (Sisco Research Laboratories Pvt. Ltd. India). Ciprofloxacin and Griseofulvin were used as a reference drug. All the solvents were of analytical grade. The chemicals and reagents were used without further purification process.

2.1.2 Instruments

Analytical TLC plates (60 F_{254}, 0.2 mm thick, Merck KGaA, Darmstadt, Germany), columnar silica gel (60 F_{254}, 70–240 mesh, Merck KGaA, Darmstadt, Germany), A rotary evaporator (BUCHI Rotavapor™ R-300, Switzerland), A UV-visible spectrophotometer (Evolution 60S), ^{1}H and ^{13}C NMR spectra were recorded at 400 MHz and 100 MHz, respectively, on a Bruker Avance DMX400 FT NMR spectrometer (Bruker, Billerica, Massachusetts, USA.

2.1.3 Test Micro-organisms

2.1.3.1 Bacterial Strains

The *in vitro* antibacterial assays were carried out against the following Gram-positive bacterial strains (GPBSs): *Bacillus pumilus* 82, American type culture collection (ATCC 6633) strains of *B. subtilis,* and *Staphylococcus aureus* ML 267. Gram-negative bacterial strains used were: *Escherichia coli* 3:37C, *E. coli* 7360, *E. coli* 872, *E. coli* CD/99/1, *E. coli* K 88, *E. coli* T 37, *E. coli* ROW 7/12, *E. coli* 5933, *E. coli* HB101, *E. coli* 600, *Salmonella enterica* TD 01, *S. typhi* Ty2, *Shigella boydii* D13629, *S. dysentery* 8, *S. flexneri* Type 6, *S. soneii* 1, and NCTC strains of *Vibrio cholera (Vibrio cholerae* NCTC 4693, *V. cholerae* NCTC 5596, *V. cholerae* NCTC 10732, and *V. cholerae* NCTC 11501). In addition to this, *Pseudomonas aeruginosa* MDR 1*, *S. aureus* MDR 1*, and *S. aureus* MDR 2* resistant bacterial strains were employed.

2.1.3.2 Fungal Strain

Antifungal activity testing was carried out against the following fungal pathogens: *Aspergillus niger* ATCC 6275, *Candida albicans* ATCC 10231, *Penicillium funiclosum* NCTC 287and *P. notatum* ATCC 11625.

2.2 Methods

2.2.1 Synthesis of 2-naphthol Derivatives

Compound 37 and compound 39 were synthesized using the general one-pot three-component reaction principles outlined in Scheme 2, following the published method by (B. Priya *et al.*, 2016).

2.2.1.1 Synthesis of Aminoalkyl Derivative (37)

Compound **37** was synthesized by reacting benzaldehyde (2 mmol), 2-naphthol (2 mmol), and O-toluidine (2 mmol) in ethanol with a $ZnCl_2$ catalyst (10 mol%). Initially, benzaldehyde and $ZnCl_2$ were prepared in a 25 mL Erlenmeyer flask. O-toluidine was added to this mixture. Meanwhile, 2-naphthol was prepared in ethanol in a separate flask. The benzaldehyde-$ZnCl_2$-O-toluidine solution was then gradually added dropwise to the 2-naphthol solution. The reaction mixture was refluxed at 120 °C with continuous stirring for 10 hours.

TLC was used to monitor the reaction progress, with a mobile phase of hexane: ethyl acetate (5:1). After completion, the mixture was cooled to room temperature and partitioned with distilled water and ethyl acetate (3 x 20 ml). The ethyl acetate fraction was purified using silica gel column chromatography, eluting with a hexane: ethyl acetate ratio of 1:1, resulting in a white crystal substance (compound 37).

2.2.1.2 Synthesis of the 1,3-oxazine derivative of 2-naphthol (39)

In a 25 mL Erlenmeyer flask, 10 mol% of $ZnCl_2$ was initially added to 37% aqueous formaldehyde (10 mmol).

Benzylamine (5 mmol) was gradually added to the formaldehyde-$ZnCl_2$ solution with continuous stirring. Simultaneously, a solution of 2-naphthol (5 mmol) in EtOH was prepared in a separate flask. The formaldehyde-benzylamine solution was then gradually added to the 2-naphthol solution. The reaction mixture was then refluxed at 120 °C for 7 hrs with continuous stirring. The reaction progress was monitored by TLC using a solvent system of hexane-EtOAc (5:1). After completion, the reaction mixture was cooled to room temp, and subjected to extraction with distilled water (3 x 20 ml) and EtOAc, respectively.

The EtOAc layer was subjected to silica gel column chromatography, yielding two fractions by elution with hexane (Fr. 1) and hexane-EtOAc (2:1; Fr. 2). After removing the solvent from Fr. 2, a white solid crystal was obtained, and identified as the 1,3-oxazine derivative of 2-naphthol (compound 39).

2.2.2 Structural Elucidation

The structures of the compound were determined using ^{1}H and ^{13}C nuclear magnetic resonance (NMR) at 400 MHz and 100 MHz, respectively, recorded at room temperature in $CDCl_3$.Scanning ranges were 0-20 ppm for ^{1}H NMR and 0-205 ppm for ^{13}C NMR.

Tetramethylsilane (TMS) served as an internal standard. Results were reported in δ (ppm) for chemical shifts and Hz for coupling constants (J). ^{1}H NMR signal multiplicities were denoted as singlet (s), doublet (d), doublet of doublets (dd), triplet (t), or multiple (m).

2.2.3 *In vitro* Antimicrobial Activity Assay

2.2.3.1 Determination of Zones of Inhibition

The *in vitro* antibacterial susceptibility test was carried out using the disc diffusion method based on the CLSI protocol (CLSI, 2012) by determining zones of inhibition produced by the test samples and comparing them with the standard drug. Two sets of dilutions of 200 µg/ml, a test sample, and ciprofloxacin dissolved in 1% DMSO were prepared in sterile McCartney bottles. Bacteria cell suspensions were adjusted to 0.5 McFarland turbidity standards to prepare 1×10^{8} bacterial/ml inoculum. Each final suspension of 5×10^{5} CFU/ml bacteria was inoculated on Mueller-Hinton agar plates, and the plates were then allowed to dry for 5 minutes.

Sterile filter paper discs (Whatman no. 1) of 6-mm diameter was impregnated in a stock solution (200 µg/ml) of test samples and placed on the surface of inoculated Mueller-Hinton agar plates, marked as quadrant at the back of the Petri dishes. A ciprofloxacin 200 µg disk was used as the positive control, and a 1% DMSO-soaked filter paper disk was used as the negative control. The Plates were incubated for 24 h at 37°C. After incubation, the zones of inhibition were recorded as the diameter of the growth-free zones measured in mm. The antifungal potential of the test sample at (1500 µg/ml) was screened by disc diffusion method (as described for the determination of antibacterial activity) against the fungal pathogens on Saborauds dextrose media. The Petri dishes were incubated at room temperature for 3 days and the diameter of the zone of inhibition was measured in mm. Griseofulvin was used as a reference standard.

2.2.3.2 Determinations of MICs

The MICs of the samples were determined using the broth microdilution method described by (A. Schumacher *et al.*, 2018). Nutrient agar and Saboraud's dextrose agar were used for bacterial and fungal growth, respectively. In addition, Muller-Hinton broth (MHB) and Saborauds dextrose broth (SDB) were used for suspension. Serial dilutions of test compounds were carried out to obtain concentrations ranging from 3.125 µg/ml to 800 µg/ml and 50 to 2000 µg/ml in the 96 well plates containing 100 µl Muller-Hinton broth (MHB) and Saborauds dextrose broth for antibacterial and antifungal activity tests, respectively by dissolving the test samples in 1% DMSO. Wells were inoculated with a diluted bacterial and fungal suspension standardized to final concentration loads of 5 x 10^{5} CFU/ml and 0.5-2.5 $\times 10^{4}$ CFU/ml for bacteria and fungi, respectively. Then, bacterial strains were incubated at 37 °C for 24 hours and 3 days for fungus. A well plate containing nutrient broth only and nutrients with microbes was incubated at the same temperature and time, serving as sterility and growth control respectively.

Then a color-giving agent, 40 μL of [3-(4,5-dimethylthiazol-2-yl)-2,5-diphenyltetrazolium bromide] was added into the well plates and incubated at 37 ℃ for bacteria and 25 ℃ for fungi for 30 min. The test experiments were prepared in triplicates. The lowest concentrations at which disappearing of purple color was recorded as the MIC value of the synthesized compounds

2.2.4 *In silico* Studies

2.2.4.1 Molecular Docking Study

Molecular docking analysis was conducted to assess how the synthesized compounds bind within the active sites of the target protein, utilizing the Glide module (Schrodinger Suites 2023.1), following the methodology outlined in the publication by (P. Sp *et al.,* 2022).

Molecular docking comprises four key processes: Protein Preparation, Ligand Preparation, Receptor Grid Generation, and Ligand Docking.

2.2.4.1.1 Protein Preparation

The target proteins (DNA gyrase B, protein data bank (PDB code: 4Z2E), and lanosterol 14α-demethylase, PDB code: 5V5Z) were retrieved in PDB format from the protein database (www.rcsb.org). The proteins were prepared and refined using the Protein Preparation Wizard module in Maestro's Schrödinger Suite. This involved adding hydrogen to heavy atoms, correcting missing side chains, assigning bonding orders, and addressing ionization and tautomer states. Water molecules were removed, and atom-confined energy minimization was conducted using the optimum potential for liquid simulations (OPLS_4) force fields.

The energy minimization process concluded when the root mean square deviation (RMSD) of the heavy atoms exceeded 0.3 Å (standard)(F. Sapundzhi *et al.*, 2023, M. Mechelke and M. Habeck, 2010).

2.2.4.1.2 Ligand Preparation

All synthesized compounds were drawn using ChemDraw 2019 version 1 in structural data format (SDF). Subsequently, the ligands were prepared using the Ligprep wizard in Maestro, a component of the Schrödinger Suite. The process included 2D-to-3D conversion, tautomeric state generation, and adjustment of ring configurations at a physiological pH of 7.0 +/- 2.0, accomplished through Epik2.2. Additionally, energy minimization was conducted using the OPLS-4 force field, resulting in the generation of two and three potential stereoisomers for compounds 37 and 39, respectively.

2.2.4.1.3 Receptor Grid Generation

The docking pocket was established through a grid array using the Glide protocol for generating the receptor grids. The grid boxes were computed in x, y and z coordinates within a specified region centering on the co-crystallized ligand, with the docked ligand restricted to a length of 6.0 Å (T. Qidwai, 2016).

2.2.4.1.4 Glide Extra Precision (XP) Ligand Docking

Molecular docking analysis was performed by utilizing standard parameters, specifically the Glide protocol, employing an extra-precision (XP) docking module. The final score was determined by assessing the placement of the docked ligand within the receptor's active site. The interpretation of docking results took into account factors such as the docking score, gliding energy, the count of hydrogen bonds, and pi interactions. The ligand with the lowest Glide docking score was considered the most favorable.

2.2.4.2 Pharmacokinetics and Drug-likeness Properties

The molecular structures of compounds 37 and 39 were examined using the Qikprop within Schrödinger Suite 2023 version 1 to assess whether each synthesized compound adheres to

Lipinski's rule of five. ADMET descriptor algorithms of the Qikprop prediction protocol were employed to analyze the pharmacokinetic properties of the synthesized compounds. The outcome of these analyses offers insights into the drug-likeness and oral bioavailability of the synthesized compounds.

3. RESULT AND DISCUSSION

3.1 Synthesis of 2-naphthol Derivatives

The growing interest in 1-aminoalkyl-2-naphthol derivatives is attributed to their diverse biological activities and their role in preparing other bioactive compounds, including aminoalkyl naphthols and oxazines. Specifically, the synthesis involves a one-pot multicomponent Mannich-type reaction.

3.1.1 Synthesis of Aminoalkyl Derivative of 2-naphthol (37)

Compound 37 was synthesized through a Mannich-type reaction in a one-pot condensation involving 2-naphthol, benzaldehyde, and O-toluidine in the presence of a Lewis acid ($ZnCl_2$) catalyst. The reaction mechanism is comprised of multiple steps.

Step 1: The carbonyl oxygen of benzaldehyde undergoes an acid-base reaction with the Lewis acid $ZnCl_2$. This forms a strong coordination bond, enhancing the electrophilicity of the carbonyl carbon and activating the carbonyl carbon for increased reactivity in chemical reactions.

Step 2: Imine formation through a nucleophilic addition reaction where O-toluidine reacts with the carbonyl group of benzaldehyde.

Step 3: The electrophilic aromatic substitution reaction involves 2-naphthol reacting with an imine to produce the 1-aminoalkyl derivative of 2-naphthol (the reaction mechanism is depicted in the scheme below).

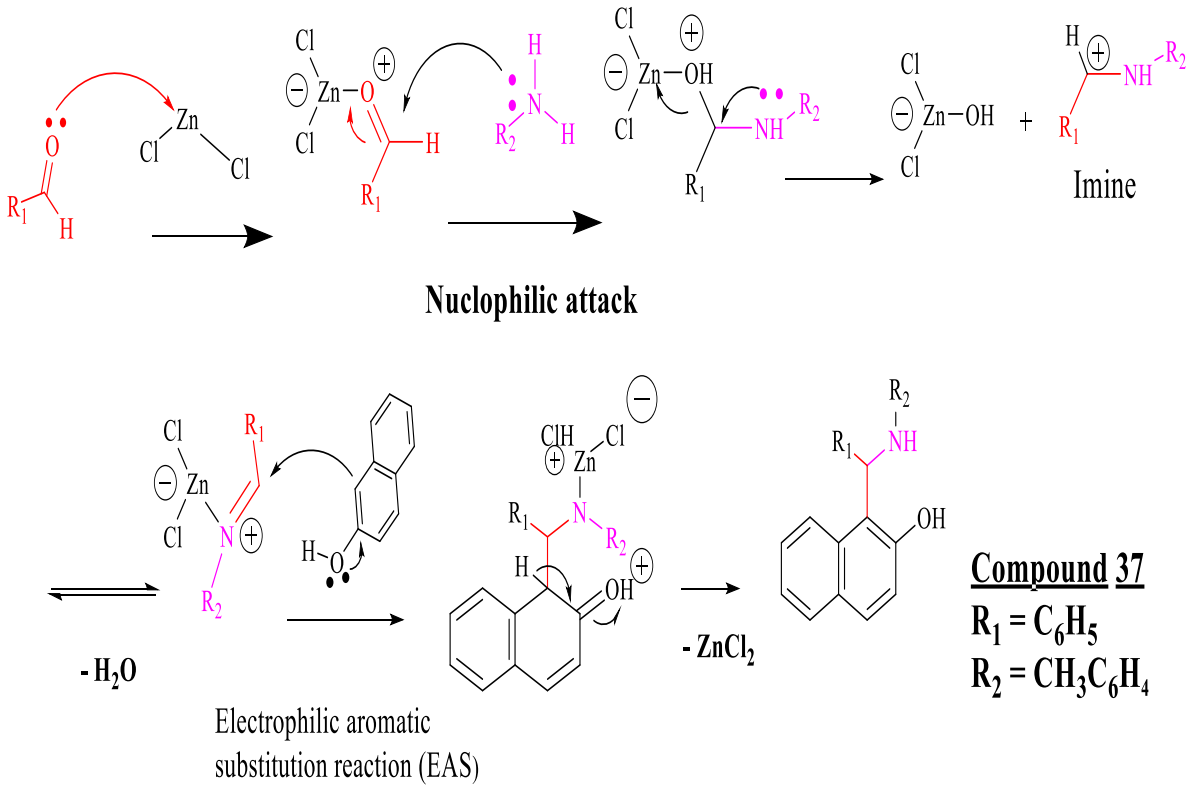

Scheme 1: The proposed reaction mechanism for the synthesis of 1-(phenyl(ortho-tolylamino) methyl) naphthalene-2-ol (37)

3.1.2 Synthesis of 1,3-oxazine Derivative of 2-naphthol (39)

Compound 39 was synthesized through a one-pot condensation reaction that involved 2-naphthol (5 mmol), formaldehyde (10 mmol), and benzylamine (5 mmol) in the presence of a $ZnCl_2$ catalyst. The synthesis process followed a mechanism similar to that described for compound 37. Subsequently, the intermediate aminoalkyl-2-naphthol derivative (38) was subjected to heating with an excess of formaldehyde in absolute ethanol, leading to ring closure and the formation of 1,3-oxazine derivatives of 2-naphthol.

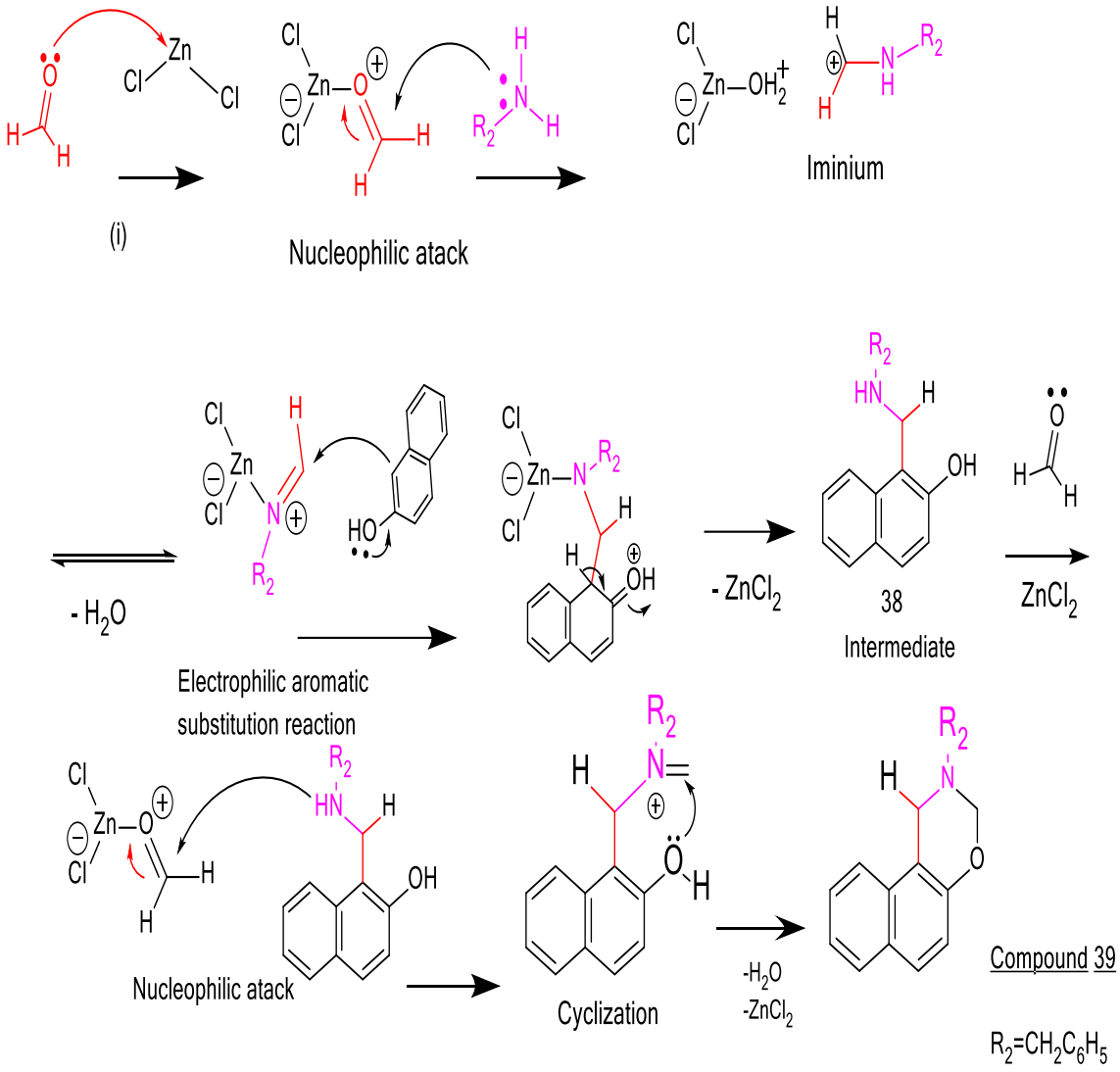

Scheme 2: The proposed reaction mechanism for the synthesis of 2-benzyl-2,3-dihydro-1H-naphtho[1,2-e] [1,3] oxazine (39)

3.2 Structural Elucidation

The structural elucidation of the synthesized compounds (37) and (39) was achieved by utilizing ^{1}H, ^{13}C, DEPT-90, and DEPT-135 NMR spectral data.

3.2.1 Structural Elucidation of Compound (37)

Compound 37 was successfully synthesized via a three-component condensation reaction of benzaldehyde, O-toluidine, and 2-naphthol in the presence of a $ZnCl_2$ catalyst, yielding white crystals (0.88 mmol, 44.3% w/w). The compound exhibited an Rf value of 0.5 on TLC when hexane/EtOAc (1:1) was used as the mobile phase

The ^{1}H-NMR spectrum of compound (**37**) revealed a broad singlet signal at δ11.41, indicative of a chelated aromatic hydroxyl (1H, brs, Ar-OH). Additionally, a singlet at δ4.07 (s, 1H, Ar2-N) suggested the presence of a benzylic methine, confirming the formation of an alkylamino group. This was further supported by a signal at δ62.32 in the ^{13}C-NMR spectrum. In the ^{1}H-NMR spectrum, a singlet signal resonating at δ6.25 was indicative of the existence of a secondary amine group (1H, R_2 NH), supporting the formation of a secondary alkylamino group. The presence of a monosubstituted benzyl group originating from benzaldehyde was also noted.

The structural analysis of compound (**37)** was also consistent with the ^{13}C-NMR, DEPT-90, and DEPT-135 spectral data, indicating the presence of 24 carbon atoms, including sixteen methines (one sp^3 and fifteen sp^2 methines), one methyl carbon, and seven quaternary carbons. The chemical shifts of all protons and carbons in the ^{1}H and ^{13}C-NMR spectra of compound 37 are summarized in Table 1.

Table 1: ^{1}H and ^{13}C NMR data of compound 37

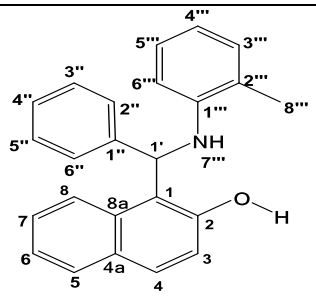

Compound 37

Position	^{13}C NMR δC (ppm)	^{1}H NMR δH (ppm)
1	113.85	
2	156.36	
3	114.49	7.15 (d, J = 8.7 Hz, 1H, C-H 3)
4	129.26	
4a	130.46	7.87 – 7.73 (3H, m, C-H 3, 5, 8)
5	130.12	7.54 – 7.47 (2H, m, C-H 6, 7)
6	123.01	
7	127.71	
8	125.09	
8a	131.67	
2-OH	-------	11.41 (1H, brs, Ar-OH)
1'	62.32	4.07 (s, 1H, Ar2-NH)
7'''-NH	------	6.25 (s, 1H, C-NH -Ar)
1'''	144.91	
2 '''	121.51	
3 '''	129.19	7.15 (d, J = 8.7 Hz, 1H, C-H 3''')
4'''	121.65	6.88 (td, 1H, J = 7.4, 1.2 Hz, C-H 4''')
5'''	128.74	6.98 (1H, td, J = 7.7, 1.7 Hz, C-H 5''')
6'''	120.13	6.72 (1H, dd, J = 8.1, 1.3 Hz, C-H 6''')

1"	141.27	
2"	128.16	7.46 – 7.28 (m, 5H, C-H 2", 3", 4", 5", 6")
3"	129.61	
4"	126.98	
5"	129.61	
6"	128.16	
8"'	18.00	2.24 (3H, s, Ar-CH_3)

3.2.2 Structural Elucidation of Compound (39)

Compound 39 was obtained in the form of white crystals (3.52 mmol, 70.5% w/w yield), and its Rf value on TLC using hexane/EtOAc (2:1) as the mobile phase was 0.6. The ^{1}H-NMR spectrum of compound 39 revealed two important methylene signals at δ4.97 (s, 2H, O–CH_2 –N, C-H 3) and δ4.34 (s, 2H, -Ar–CH_2 –N, C-H 1), confirming the formation of a tri-substituted 1,3-oxazine group. This was further supported by signals at δ82.21 and δ47.42 in the ^{13}C-NMR spectrum. Additionally, benzyl methylene adjacent to the amine group was suggested by a singlet signal at δ4.00 (s, 2H, -Ar-CH_2 -N, H-**7'**). The presence of a mono-substituted benzyl group originating from benzylamine was also observed.

In the ^{13}C-NMR spectrum together with DEPT-90 and DEPT-135, compound (**39)** displayed nineteen signals corresponding to nineteen carbon atoms, including eleven sp^2 methines, three sp^3 methylene carbons, and five quaternary carbon atoms. The complete assignment of all protons and carbons can be found in Table 2.

Table 2**:** ^{1}H and ^{13}C NMR data of compound (**39**)

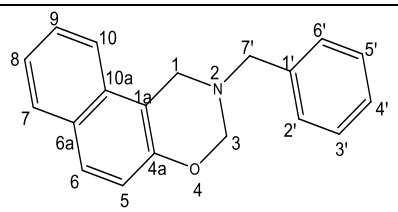

Compound 39

Position	^{13}C NMR δC (ppm)	^{1}H NMR δH (ppm)
1	47.42	4.34 (s, 2H, -Ar-CH_2-N)
1a	111.84	
3	82.21	4.97 (s, 2H, O-CH_2-N)
4a	151.90	
5	118.4	7.69 (d, *J* = 8.9 Hz, 1H, 5)
6	128.18	7.11 (dd, *J* = 8.9, 0.9 Hz, 1H, 6)
6a	132.09	
7	128.78	7.55 (dt, *J* = 8.4, 1.1 Hz, 1H, 7)
8	123.62	7.50 – 7.28 (m, 2H, 8, 9)
9	126.63	
10	121.24	7.80 (dd, *J* = 8.9, 1.3 1H, 10)
10a	129.14	
1'	138.42	
2' and 6'	129.14	7.50 – 7.28 (m, 5H, 2'-6')
3' and 5'	128.64	
4'	127.56	
7'	56.25	4.00 (s, 2H, -Ar-CH_2-N)

3.3 Antimicrobial activity

3.3.1 Antibacterial Activity

Using disk diffusion and broth dilution methods, we assessed the in vitro antibacterial activity of 1-(phenyl(o-tolylamino) methyl) naphthalene-2-ol (**37**) and 2-benzyl-2,3-dihydro-1H-naphtho[1,2-e][1,3]oxazine (**39**) as described (R. M. Humphries *et al.*, 2018).

Table 3 presents the ZOI and MIC values for compounds 37 and 39 against three Gram-positive bacteria (*B. pumilus, B. subtilis*, and *S. aureus*) and eighteen Gram-negative bacteria, including eight strains of *E. coli*, two strains of *Salmonella*, four strains of *Shigella*, four strains of *V. cholera*, and five multi-drug resistant strains.

Our findings revealed that both compounds exhibited variable but comparable inhibitory activities against the majority of tested bacterial strains, with MIC values ranging from 25 µg/ml to 200 µg/ml. The overall inhibitory effectiveness of compounds 37 and 39 against the tested Gram-negative bacteria is particularly notable, with compound 37 demonstrating the lowest MIC value of 25 µg/ml against all tested strains of *E. coli.*

Despite the extra lipopolysaccharide layer forming a hydrophobic permeability barrier in Gram-negative bacteria, which typically contributes to antibiotic resistance, both compounds **(37)** and (**39**) showed strong antibacterial activity against Gram-negative bacteria like *E. coli* and *V. cholera*, with a MIC value of 50 µg/ml. And, their activity against *Salmonella* and *Shigella* species was relatively weak, with MICs ranging from 100-200 µg/ml. However, Gram-positive *Bacilli* (*B. pumilus* and *B. subtilis*) displayed high resistance to both compounds, evident by a zone of inhibition (ZOI) of 6.0 mm at a concentration of 200 µg/ml. Furthermore, compound (**37)** exhibited inhibitory activity against multi-drug-resistant; *S. aureus* (*S. aureus MDR 1** and *S. aureus MDR 2*)* in a pattern similar to that of susceptible strains.

These findings suggest that both compounds (**37)** and (**39)** could possess significant potential in combating the Gram-negative bacteria as well as multi-drug resistance bacterial strains.

Table 3**:** ZOIs at (200 µg/ml) and MICs of the synthesized compounds against 26 bacterial strains.

Bacterial strains	Zone of inhibition (200 µg/ml) [a]			MIC (µg/ml) [b]	
	Compound			Compound	
	37	39	Cipr	37	39
Bacillus pumilus 82	6.0	6.0	19.0	ND	ND
B. subtilis ATCC 6633	6.0	6.0	18.0	ND	ND
Escherichia coli 3:37C	15.5	14.5	16.5	25	50
E. coli 872	14.5	14.0	16.0	25	50
E. coli CD/99/1	14.5	14.0	17.0	25	50
E. coli K88	15.0	13.5	17.0	25	50
E. coli LT37	14.5	13.5	16.0	25	50
E. coli NCTC 5933	14.0	13.0	16.0	25	50
E. coli NCTC 7360	14.5	13.5	17.0	25	50
E. coli ROW 7/12	15.0	14.0	16.5	25	50
E. coli HB101	13.0	12.0	14.0	50	200
E. coli C600	12.5	11.5	13.5	50	200
Salmonella enterica TD 01	13.5	13.5	19.0	100	100
S. typhi Ty2	13.5	13.5	16.0	100	200
Shigella boydii D 13629	12.0	12.0	20.0	200	200
S. dysentery 8	11.5	11.5	20.0	200	200
S. flexneri Type 6	12.0	12.0	20.5	200	200
S. soneii 1	13.0	13.0	19.5	200	200
Staphylococcus aureus ML 267	13.5	13.5	18.0	50	50
Vibrio cholerae NCTC 10732	14.5	14.5	19.0	50	50
V. cholera NCTC 11501	14.5	14.5	18.5	50	50
V. cholerae NCTC 4693	14.0	14.0	17.5	50	50
V. cholerae NCTC 5596	14.5	14.5	18.5	50	50
*Pseudomonas aeruginosa MDR 1**	10.5	10.5	12.5	100	100
*S. aureus MDR 1**	10.5	10.0	11.5	50	200
*S. aureus MDR 2**	11.5	11.5	12.0	50	200

[a] Zones of inhibition measured including 6 mm diameter of the disc, b- triplicate, Cip.ro – Ciprofloxacin; Gris – Griseofulvin; ND– Not determined

4.3.2 **Antifungal activity**

Table 4 presents the results of antifungal activity studies for compounds 37 and 39 against four fungal strains (*A. niger*, *C. albicans*, *P. funiculosum*, and *P. notatum*). Our study revealed a notable sensitivity of the tested fungal strains to both compounds, with MIC values ranging from 800 to 1500 µg/ml.

Among the tested fungal strains, *C. albicans, A. niger, and P. notatum* demonstrated the highest susceptibility to both compounds 37 and 39, exhibiting a ZOI of 13.0 mm, 12.0 mm, and 12.5 mm, respectively, and a consistent MIC of 800 µg/ml each. However, *P. funiculosum* displayed weaker sensitivity (MIC = 1500 µg/ml) compared to the other tested fungal strains. *funiculosum* NCTC 287 showed weak sensitivity (MIC = 1500 µg/ml) compared to the other one.

Table 4**:** ZOIs at (1500 µg/ml) and MICs of the synthesized compounds against bacterial strains.

Fungal strains	ZoI (1500 µg/ml) [a]			MIC µg/ml	
	Compound			Compound	
	37	39	Gris	37	39
Aspergillus niger ATCC 6275	13.0	13.0	14.0	800	800
Candida albicans ATCC 10231	12.0	12.0	15.0	800	800
Penicillium funiculosum NCTC 287	10.0	11.0	13.0	1500	1500
P. notatum ATCC 11625	12.5	12.5	13.0	800	800

[a] *Zones of inhibition measured including 6 mm diameter of the disc; Gris – Griseofulvin*

3.4 In silico Studies of the Synthesized Compounds

3.4.1 Molecular Docking Study

In pharmaceutical research, the utilization of structure-based drug design through molecular docking stands as an advanced and crucial technique. This approach, as outlined by Shoichet et al., focuses on accurately predicting the binding interactions between receptor and ligand molecules objectively to identify potential lead compounds (B. K. Shoichet *et al.*, 2002).

In this study, our specific choice of *E. coli* DNA gyrase B and C. albicans lanosterol 14α-demethylase as a potential target for molecular docking was based on an assessment of the structural features of the synthesized compounds and preliminary docking analysis.

Similarly, the well-known inhibitors ciprofloxacin and voriconazole were docked to validate the docking protocol against DNA gyrase B of *E. coli* and lanosterol 14α-demethylase of *C. albicans* respectively. The docking scores for the synthesized compounds and the standards are presented in Table 5, where a more negative score indicates a stronger binding between the ligand and its target.

DNA gyrase B enzyme plays a crucial role in introducing negative supercoils and relieving topological strain in an ATP-dependent manner during DNA replication (K. Drlica and X. Zhao, 1997).

Interestingly, compounds **(37)** and (**39)** demonstrated effective docking interaction with the binding pockets of *E. coli* DNA gyrase B (PDB: 4z2e) with docking scores of -8.092 and -7.754 kcal/mol, respectively. In comparison, ciprofloxacin exhibited a docking score of -13.37 kcal/mol. The corresponding results are graphically depicted in Figures 6 and 7 and summarized in Table 5.

Table 5: Docking score, hydrogen bond, and hydrophobic interactions of compounds **(37)** and (**39**) against the binding pocket of bacterial DNA gyrase B (4z2e) and fungal 14α-demethylase (5v5z)

PDB code	**Compound**	**Docking score kcal/mol**	**Interacting residue of the target**		
			RIHB	Residue	Types of interaction
4z2e	37	-8.092	DA; H_2	DG; H_1, DT; E_{15}, DA; F_5 (2x)	4 PPI
	39	-7.754	----------	Glu 475, DA; F_5, DG; H_1,	Sb[a], PcI[b], 2 PPI[c]
	Ciprofloxacin	-13.37		GLU 475, Mg; H_{102}, DA; F_4, DG; H_1	4 Sb, 4 PPI
5v5z	37	-7.792	-------	Hydrophobic interaction	……..
	39	-8.995	SER 378	TYR 118, HIE 377, PHE 380	1PPI, 2PcI
	Voriconazole	-8.476	SER 378	TYR 118, HIE 377	2PPI

RIHB; residue involved in a hydrogen bond, [salt] bridge, [b]Pi cation interaction, [c]Pi pi interaction, D-DNA, (A-Adenine, G- Guanine, T- Thiamnie), (H, E, F) represents the regens regions interactions takes place

Compound **(37)** demonstrated effective binding to DNA gyrase B. It formed a hydrogen bond with DA; H2 and engaged in four distinct π-to-π interactions with DG; H1, DT; E1, DA; F5 (Figure 6).

Compound (**39**) also displayed strong binding interactions with various residues of DNA gyrase B, forming salt bridges with GLU 475 and participating in π-to-π interactions with DG; H1. Additionally, it engaged in π interactions with the cation and formed π-to-π interactions with the DA; F5 residue of DNA gyrase B (**Figure 1**). Notably, both synthesized compounds displayed a strong binding affinity with *E. coli* DNA gyrase B, comparable to ciprofloxacin. This suggests that both compounds (**37)** and (**39)** could potentially serve as lead molecules for further optimization.

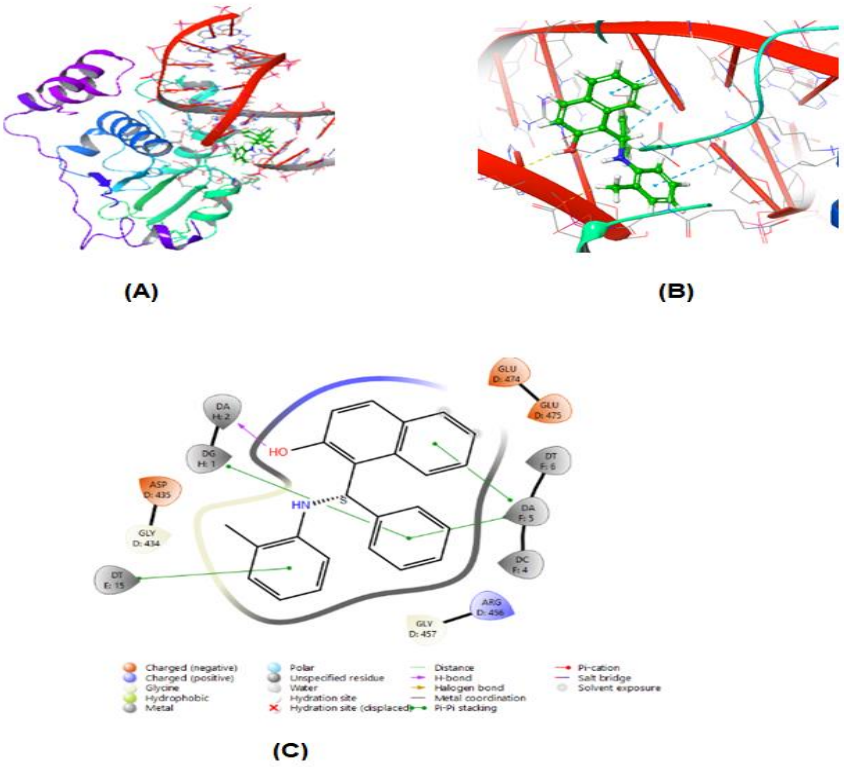

Figure 1: (A): 3D model, (B): 3D model zoomed, and (C): 2D presentation of binding interaction of compound **3**7 with the residues of *E. coli* DNA gyrase B

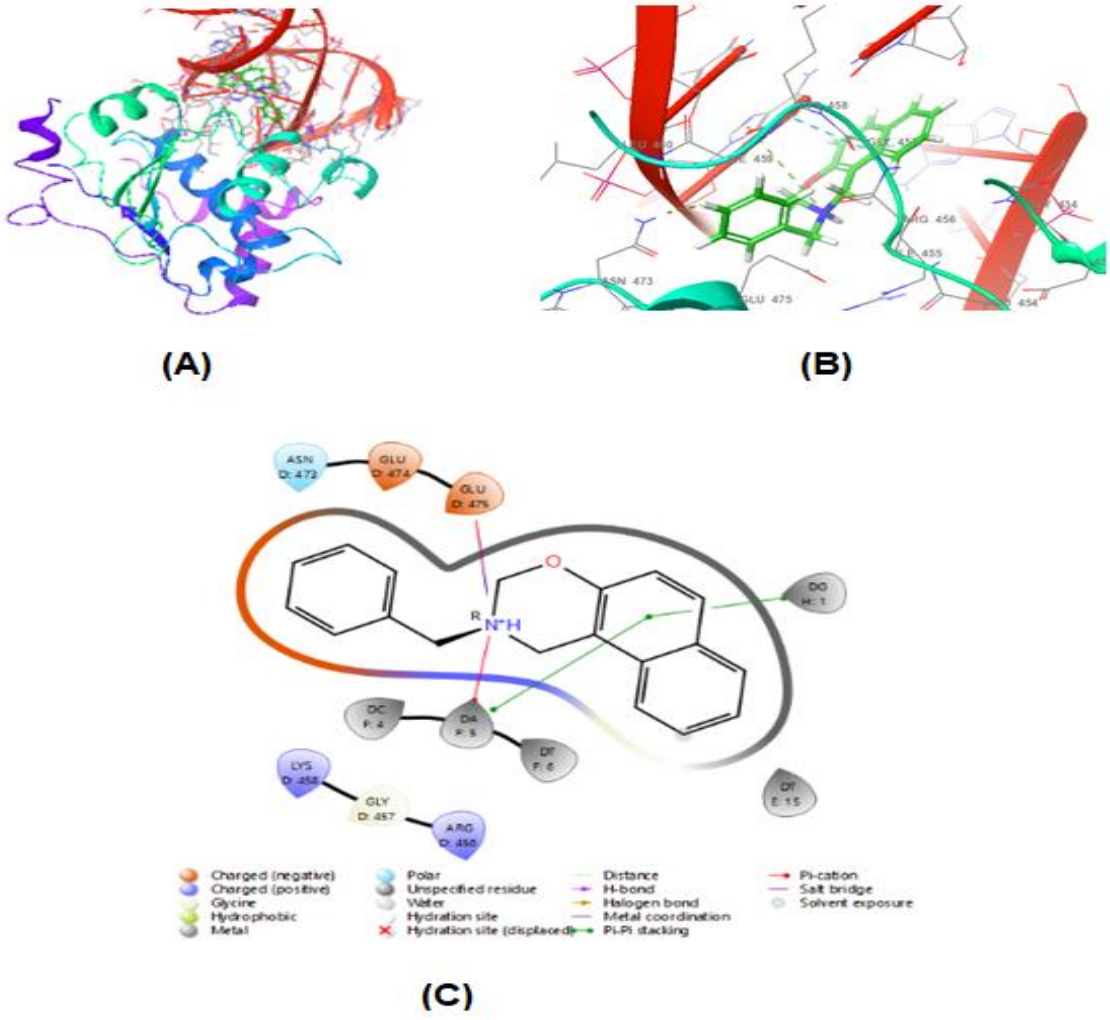

Figure 2: (A): 3D model, (B): 3D zoomed model (C): 2D binding interactions of compound 39 against the residues of *E. coli* DNA gyrase B

We selected 14α-demethylase as a prospective target for molecular docking involving compounds (**37)** and (**39)**, based on preliminary docking tests. Both compounds were subjected to docking in the active site of *C. albicans* 14α-demethylase (PDB: 5v5z) and compared against clinical standards voriconazole. The findings are presented in Table 5 and depicted in Figures 3 and 4.

Interestingly, compound (**39**) demonstrated strong binding affinity to *C. albicans* 14α-demethylase, with a molecular docking score of -8.995 kcal/mol, surpassing the interaction

observed with the reference molecule, voriconazole (-8.476 kcal/mol). Compound 39 formed a hydrogen bond with the SER 378 amino residue of *C. albicans* 14α-demethylase (Figure 4). On the other hand, compound (**37)** exhibited a docking score of -7.792 kcal/mol, primarily engaging in hydrophobic interactions within the binding pockets of *C. albicans* Lanosterol 14α-demethylase (Figure 8). Overall, the molecular docking results from this study suggest that these synthesized ligands may possess potent antimicrobial activities and could be considered as candidates for further exploration as antimicrobial agents.

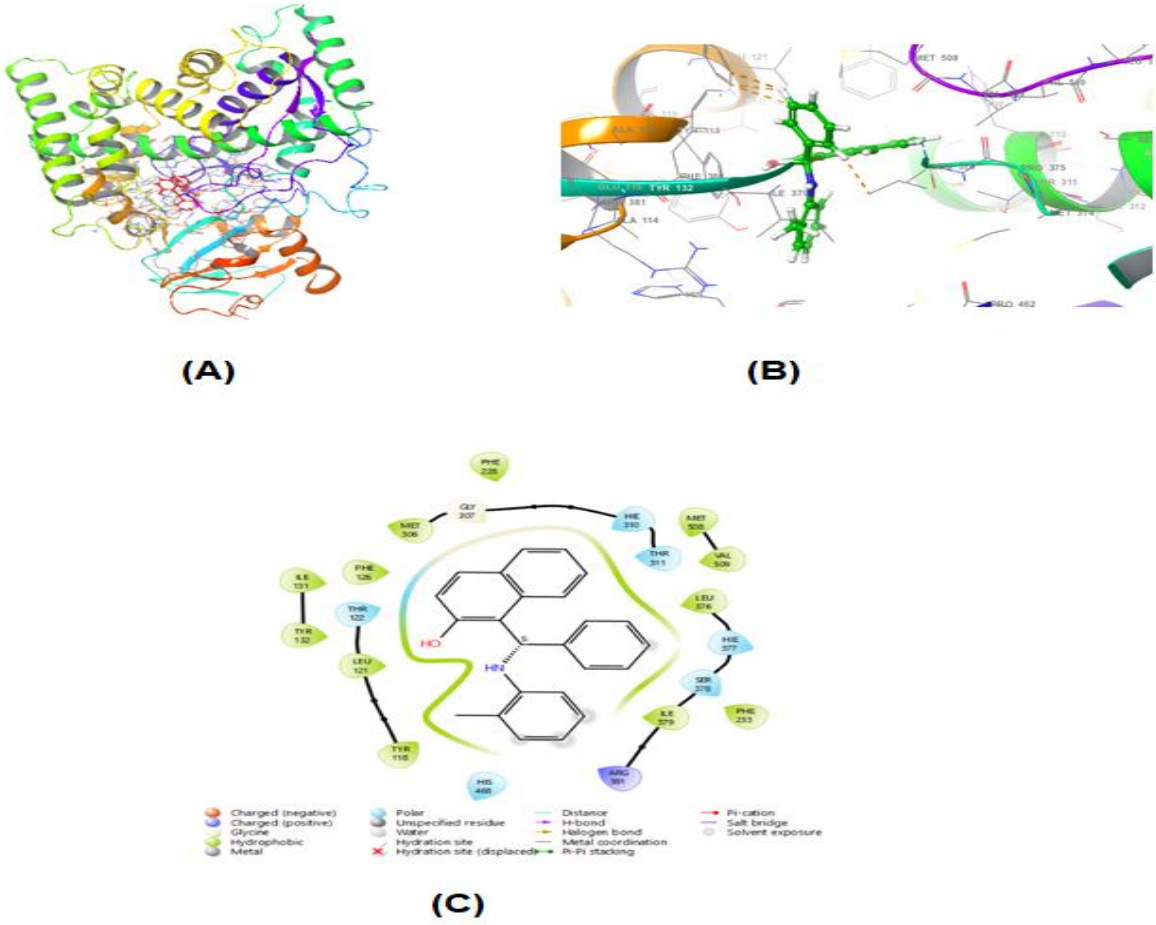

Figure 3: (A): 3D representation, (B): 3D zoomed view, (C): 2D model of compound 37 docking interactions against the residue of *C. albicans* lanosterol 14α -demethylase (5v5z)

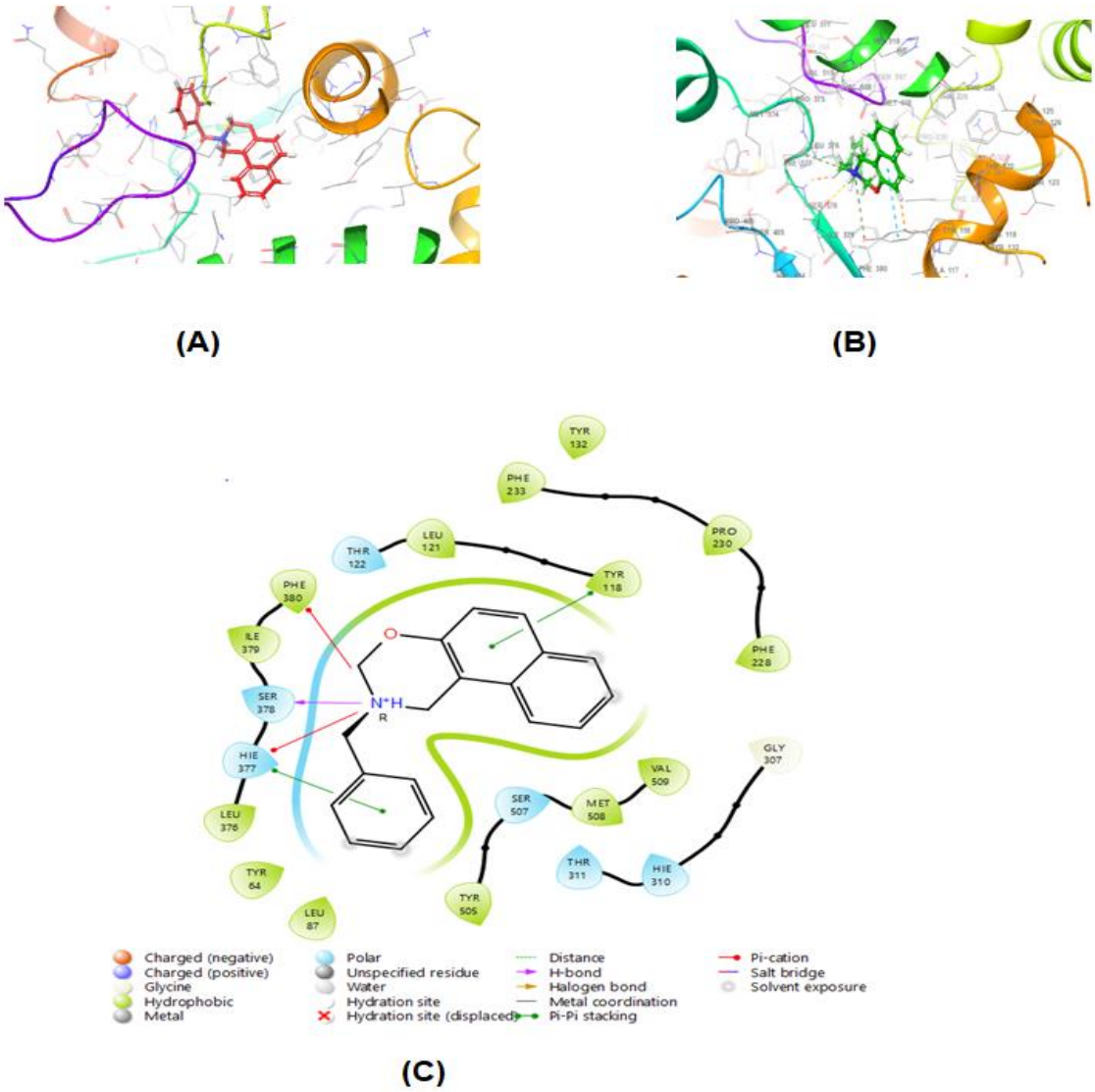

Figure 4: (A): 3D model, (B): 3D zoomed view, (C): 2D model of compound 39 docking interactions against the residue of *C. albicans* lanosterol 14α -demethylase (5v5z

3.4.2 ADMET Predictions of the Synthesized Compounds

Utilization of virtual screening software for predicting pharmacokinetic and physicochemical characteristics is very crucial for the design and optimization of bioactive compounds (T. Qidwai, 2016). The QikProp software, a component of the Schrodinger module, was employed to predict the pharmacokinetic and physicochemical characteristics of compounds (**37)** and (**39)** within the

biological system. Drug-likeness and oral bioavailability of the compounds were predicted and compared following Lipinski's rule of five (C. A. Lipinski *et al.*, 1997).

The ADMET analysis revealed that 2-benzyl-2,3-dihydro-1H-naphtho[1,2-e][1,3]oxazine (39) complies with all parameters of Lipinski's rule. However, 1-(phenyl(*o*-tolylamino) methyl) naphthalene-2-ol (**37**) violates Lipinski's rule due to the partitioning of octanol to water (logP) falling above the normal range (Table 4).

The pharmacokinetic (ADMET) properties of compounds (**37**) and (**39)** were predicted against various parameters, including apparent Caco-2 permeability (colon carcinoma cell), the rule of 5 (number of Lipinski rule violations), blood-brain barrier permeability, water solubility (QPlogS), and QplogHERG (IC50 prediction for blocking HERGK+ - human ether-a-go-go gene). The summary of these predictions is presented in Table 4.

Both compounds fell within the recommended range for most parameters, except for the IC_{50} for blocking HERG-K+ channels (QPlogHERG), which was below -5 for both the synthesized compounds. Notably, Table 4 indicates that both compounds (**37)** and (**39)** exhibit excellent absorption in human intestinal tissue, enhanced permeability in Caco2 cell lines, and a high likelihood of crossing the blood-brain barrier.

Table 6: Calculations of electronic parameters of drug-likeness or oral bioavailability of the synthesized compounds using Qikprop

S. N	Descriptors	Predicted values		Reference		Recommended value
		37	39	Cpr	Vori	
1.	Molecular weight	339.436	275.349	331.346	349.315	<500
2.	HB donor	2.000	0.000	1.000	1.000	≤ 5
3.	HB acceptor	2.000	2.750	6.000	6.250	≤ 10
4.	PlogP o/w	5.479*	3.788,	0.280	3.000	≤ 5
5.	PlogS (Aquas solubility)	-5.333	-3.074,	-3.790	-3.705	-6.5/ 0.5
6.	logKhsa (albumin binding)	0.855	0.410	0.043	-0.117	-1.5/1.5
7.	%HOA	100	100	48.000	100	>80 % good, < 25% poor
8.	PlogHERG	-6.313*	-6.418*	-3.407	-5.000	> -5
9.	PlogBB, brain/blood	0.103	0.830	-0.722	-0.402	-3/1.2
10	QPPCaco-2	2403	6774	12	1229	<25 poor, >500 great

*PlogBB brain/blood partition coefficient, %HOA percent of human oral absorption, Cpr Ciprofloxacin, Vori Voriconazole, *Indicates deviation from the recommended value*

The rapidly increasing resistance of microorganisms, both bacteria, and fungi, to available treatments, is a global medical challenge of high priority (WHO, 2021). The emergence of multidrug-resistant organisms, notably *S. aureus,* and *E. coli* is a pressing issue demanding attention.

Addressing this challenge requires the development of antimicrobials with distinct modes of action to counteract multidrug resistance.

Research has indicated that positions one and two in the 2-naphthol heterocyclic ring are crucial targets for various reactions, leading to the synthesis of biologically active compounds. In response, we designed and synthesized aminoalkyl and 1,3-oxazine 2-naphthol derivatives with potential biological activity.

In our study, the synthesized compounds (**37)** and (**39**) exhibited promising antimicrobial activities against several tested bacterial and fungal strains. Our findings align with previous reports on molecules derived from 2-naphthol scaffolds, showing strong antimicrobial activity (MIC=32-256 µg/ml) (G. Şahin *et al.*, 2002). Additionally, a study by Jasim and Mustafa highlighted the significant efficacy of 2-naphthol derivatives against *E. coli*, *S. typhi*, and *S. dysentery*, with MIC values of (1.4, 1.95, and 1.85) µg/ml, respectively (S. F. F. Jasim and Y. F. Mustafa, 2022). Despite the additional lipopolysaccharide layer forming a hydrophobic permeability barrier in Gram-negative bacteria such as E. coli and V. cholera, which typically restricts the diffusion of antibiotics (A. H. Delcour, 2009), it is interesting that both E. coli and V. cholera exhibited greater susceptibility to compounds (**37)** and (**39)**, with a MIC value of (25-50) µg/ml. This observation is in line with a prior study by Göksu et al., where 5,6-dimethoxynaphthalene-2-carboxylic acid 25a and 5-bromo-6-methoxynaphthalene-2-carboxylic acid derived from the 2-naphthol scaffold demonstrated significant activity against Gram-negative bacterial strains (S. Göksu *et al.*, 2005). Furthermore, a notable finding in our study is that most multi-drug-resistant strains including *E. coli, and S. aureus* exhibited high susceptibility to compound (**37)** and *MDR Pseudomonas aeruginosa* to both the synthesized compounds. This suggests a significant potential for compounds (**37)** and (**39)** in combating multi-drug-resistant microbes.

In the molecular docking analysis, both synthesized compounds demonstrated strong binding affinity within the active site of the bacterial DNA gyrase B enzyme, a potential target for various antibacterial drugs. Similarly, both compounds exhibited favorable interactions within the active site of 14α-demethylase in C. albicans. However, it is crucial to experimentally validate the strong binding nature of compounds (**37)** and (**39**).

Furthermore, in the ADMET analysis, both synthesized compounds displayed favorable pharmacokinetics and drug-like characteristics, suggesting their suitability for oral administration. In summary, the results from the in vitro bioassay activity test, molecular docking analysis, and ADMET predictions collectively affirm the promising antimicrobial properties of both synthesized compounds. These findings highlight the potential benefits of further synthesis and evaluation of 2-naphthol derivatives in the ongoing efforts to develop antimicrobial drugs for combating infectious diseases and microbial resistance.

4. CONCLUSION

Antimicrobial resistance of microorganisms, both bacteria, and fungi, to available treatments, is a global medical challenge of high priority. One effective strategy to address this challenge involves synthesizing compounds with antimicrobial properties. In this study, Aminoalkyl and Oxazine of 2-naphthol derivatives were successfully synthesized using a 2-naphthol framework through a Mannich-type condensation reaction. The synthesized compounds showed promising antibacterial and antifungal activity. The molecular docking result reveals that both the synthesized compounds displayed better interaction with the target protein. ADMET analysis indicates both compounds comply with all parameters of Lipinski's rule, except a violation of (logP) value by compound 37. Overall, aminoalkyl and oxazine derivatives of 2-naphthol hold great potential as lead compounds in the development of novel antimicrobial drugs to tackle the growing threat of infectious diseases and antimicrobial resistance. These results also suggest the need for further investigation to synthesize additional 2-naphthol derivatives to evaluate their antimicrobial potential.

5. **REFERENCES**

Abubakar, I., Tillmann, T. & Banerjee, A. 2015. Global, regional, and national age-sex specific all-cause and cause-specific mortality for 240 causes of death, 1990-2013: a systematic analysis for the Global Burden of Disease Study 2013. *Lancet,* **385 (**9963**):** 117-171.

Ali, I. A., Al-Masoudi, I. A., Saeed, B., Al-Masoudi, N. A. & La Colla, P. 2005. Amino acid derivatives, part 2: Synthesis, antiviral, and antitumor activity of simple protected amino acids functionalized at N-terminus with naphthalene side chain. *Heteroatom Chemistry,* **16 (**2**):** 148-155.

Bala, S., Sharma, N., Kajal, A. & Kamboj, S. 2014. Mannich bases: an important pharmacophore in present scenario. **2014:** 191072.

Chang, F.-Y., Peacock Jr, J. E., Musher, D. M., Triplett, P., MacDonald, B. B., Mylotte, J. M., O'Donnell, A., Wagener, M. M. & Victor, L. Y. 2003. Staphylococcus aureus bacteremia: recurrence and the impact of antibiotic treatment in a prospective multicenter study. *Medicine,* **82 (**5**):** 333-339.

CLSI (2012). Methods for dilution antimicrobial susceptibility tests for Bacteria that grow aerobically; aproved standard-Ninth Edition. CLSI document M07-A9.

Delcour, A. H. 2009. Outer membrane permeability and antibiotic resistance. *Biochim Biophys Acta,* **1794 (**5**):** 808-816.

Drlica, K. & Zhao, X. 1997. DNA gyrase, topoisomerase IV, and the 4-quinolones. *Microbiology and molecular biology reviews,* **61 (**3**):** 377-392.

Duchin, K. L., Vukovich, R. A., Dennick, L. G., Groel, J. T. & Willard, D. A. 1980. Effects of nadolol β-blockade on blood pressure in hypertension. *Clinical Pharmacology & Therapeutics,* **27 (**1**):** 57-63.

Gohil, N., Ramírez-García, R., Panchasara, H., Patel, S., Bhattacharjee, G. & Singh, V. 2018. Book review: quorum sensing vs. quorum quenching: a battle with no end in sight. Frontiers Media SA.

Göksu, S., UĞUZ, M. T., Özdemir, H. & Seçen, H. 2005. A concise synthesis and the antibacterial activity of 5, 6-dimethoxynaphthalene-2-carboxylic acid. *Turkish Journal of Chemistry,* **29 (**2**):** 199-205.

Hamad, N. S., Al-Haidery, N. H., Al-Masoudi, I. A., Sabri, M., Sabri, L. & Al-Masoudi, N. A. 2010. Amino acid derivatives, part 4: synthesis and anti-HIV activity of new naphthalene derivatives. *Archiv der Pharmazie,* **343 (**7**):** 397-403.

Humphries, R. M., Ambler, J., Mitchell, S. L., Castanheira, M., Dingle, T., Hindler, J. A., Koeth, L. & Sei, K. 2018. CLSI Methods Development and Standardization Working Group Best Practices for Evaluation of Antimicrobial Susceptibility Tests. *Journal of Clinical Microbiology,* **56 (**4**):** 10.1128/jcm.01934-01917.

Janowska, S., Andrzejczuk, S., Gawryś, P. & Wujec, M. 2023. Synthesis and Antimicrobial Activity of New Mannich Bases with Piperazine Moiety. *Molecules* [Online], 28.

Jasim, S. F. F. & Mustafa, Y. F. 2022. Synthesis, ADME Study, and Antimicrobial Evaluation of Novel Naphthalene-Based Derivatives. *Journal of Medicinal and Chemical Sciences,* **5 (**5**):** 793-807.

Lipinski, C. A., Lombardo, F., Dominy, B. W. & Feeney, P. J. 1997. Experimental and computational approaches to estimate solubility and permeability in drug discovery and development settings. *Advanced Drug Delivery Reviews,* **23 (**1**):** 3-25.

Mahindroo, N., Wang, C.-C., Liao, C.-C., Huang, C.-F., Lu, I.-L., Lien, T.-W., Peng, Y.-H., Huang, W.-J., Lin, Y.-T. & Hsu, M.-C. 2006. Indol-1-yl acetic acids as peroxisome proliferator-activated receptor agonists: design, synthesis, structural biology, and molecular docking studies. *J Med Chem,* **49 (**3**):** 1212-1216.

Mechelke, M. & Habeck, M. 2010. Robust probabilistic superposition and comparison of protein structures. *BMC Bioinformatics,* **11 (**1**):** 363.

Murray, W. V., Wachter, M. P., Kasper, A. M., Argentieri, D. C., Capetola, R. J. & Ritchie, D. M. 1991. Novel 6-oxo-6-naphthylhexanoic acid derivatives with anti-inflammatory and 5-lipoxygenase inhibitory activity. *Eur J Med Chem,* **26 (**2**):** 159-166.

Nusrath Unissa, A., Hanna, L. E. & Swaminathan, S. 2016. A Note on Derivatives of Isoniazid, Rifampicin, and Pyrazinamide Showing Activity Against Resistant Mycobacterium tuberculosis. *Chem Biol Drug Des,* **87 (**4**):** 537-550.

Okeke, I. N., Laxminarayan, R., Bhutta, Z. A., Duse, A. G., Jenkins, P., O'Brien, T. F., Pablos-Mendez, A. & Klugman, K. P. 2005. Antimicrobial resistance in developing countries. Part I: recent trends and current status. *Lancet Infect Dis,* **5 (**8**):** 481-493.

Petranyi, G., Meingassner, J. G. & Mieth, H. 1987. Antifungal activity of the allylamine derivative terbinafine in vitro. *Antimicrob Agents Chemother,* **31 (**9**):** 1365-1368.

Priya, B., Cherkadu, V., Kalavagunta, P., Ravirala, N. & Shivananju, N. 2016. Zinc Chloride Catalyzed, Dipolar Aprotic Solvent-Mediated, One-Pot Synthesis of 2-[(Benzo[d]thiazol-2-ylamino)(phenyl)methyl]phenols. *Synlett,* **27 (**20)**:** 2795-2798.

Qidwai, T. 2016. QSAR modeling, docking and ADMET studies for exploration of potential anti-malarial compounds against Plasmodium falciparum. *In Silico Pharmacol,* **5 (**1)**:** 6.

Rahn, K., Hawlina, A., Kersting, F. & Planz, G. 1974. Studies on the antihypertensive action of the optical isomers of propranolol in man. *Naunyn-Schmiedeberg's archives of pharmacology,* **286:** 319-323.

Rokade, Y. & Sayyed, R. 2009. Naphthalene derivatives: A new range of antimicrobials with high therapeutic value. *Rasayan J. Chem,* **2 (**4)**:** 972-980.

Ryder, N., Frank, I. & Dupont, M. 1986. Ergosterol biosynthesis inhibition by the thiocarbamate antifungal agents tolnaftate and tolciclate. *Antimicrob Agents Chemother,* **29 (**5)**:** 858-860.

Saab, A. N., Sloan, K. B., Beall, H. D. & Villanueva, R. 1990. Effect of Aminomethyl (N-Mannich Base) Derivatization on the Ability of S6Acetyloxymethyl-S-Mercaptopurine Prodrug to Deliver 6-Mercaptopurine through Hairless Mouse Skin. *Journal of Pharmaceutical Sciences,* **79 (**12)**:** 1099-1104.

Şahin, G., Palaska, E., Ekizoğlu, M. & Özalp, M. 2002. Synthesis and antimicrobial activity of some 1, 3, 4-oxadiazole derivatives. *Il Farmaco,* **57 (**7)**:** 539-542.

Sapundzhi, F., Popstoilov, M. & Lazarova, M. RMSD Calculations for Comparing Protein Three-Dimensional Structures. *In:* Georgiev, I., Datcheva, M., Georgiev, K. & Nikolov, G., eds.

Numerical Methods and Applications, 2023// 2023 Cham. Springer Nature Switzerland, 279-288.

Schumacher, A., Vranken, T., Malhotra, A., Arts, J. & Habibovic, P. 2018. In vitro antimicrobial susceptibility testing methods: agar dilution to 3D tissue-engineered models. *European Journal of Clinical Microbiology & Infectious Diseases,* **37:** 187-208.

Shingalapur, R. V., Hosamani, K. M., Keri, R. S. & Hugar, M. H. 2010. Derivatives of benzimidazole pharmacophore: Synthesis, anticonvulsant, antidiabetic and DNA cleavage studies. *Eur J Med Chem,* **45 (**5**):** 1753-1759.

Shoichet, B. K., McGovern, S. L., Wei, B. & Irwin, J. J. 2002. Lead discovery using molecular docking. *Current Opinion in Chemical Biology,* **6 (**4**):** 439-446.

Sp, P., R, A. S. K. & Ks, J. 2022. Insights from the molecular docking analysis of compounds from Vitex negundoi with targets from Klebsiella pneumoniai causing urinary tract infection. *Bioinformation,* **18 (**11**):** 1062-1068.

van Seventer, J. M. & Hochberg, N. S. 2017. Principles of Infectious Diseases: Transmission, Diagnosis, Prevention, and Control. *International encyclopedia of public health***:** 22-39.

WHO (2021). Global antimicrobial resistance and use surveillance system (GLASS) report 2021. Geneva, WHO.